UNIVERSIDADE FEDERAL DE SÃO CARLOS

CENTRO DE CIÊNCIAS BIOLÓGICAS E DA SAÚDE

DEPARTAMENTO DE FISIOTERAPIA

Andriette Camilo Turi

ESTUDO SOBRE O COMPORTAMENTO E A ADAPTAÇÃO MUSCULAR EM MODELO DE OCLUSÃO DA CARÓTIDA COMUM EM GERBILOS

São Carlos

2015

UNIVERSIDADE FEDERAL DE SÃO CARLOS

CENTRO DE CIÊNCIAS BIOLÓGICAS E DA SAÚDE

DEPARTAMENTO DE FISIOTERAPIA

Dissertação para exame de Defesa de Mestrado

ESTUDO SOBRE O COMPORTAMENTO E A ADAPTAÇÃO MUSCULAR EM MODELO DE OCLUSÃO DA CARÓTIDA COMUM EM GERBILOS

ANDRIETTE CAMILO TURI

Orientador: Prof. Dr. Thiago Luiz de Russo

Apoio Financeiro: Bolsista de Mestrado pela Fundação de Amparo à Pesquisa do Estado de São Paulo (FAPESP).

São Carlos

2015

Ficha catalográfica elaborada pelo DePT da Biblioteca Comunitária da UFSCar

T938ec

Turi, Andriette Camilo.
Estudo sobre o comportamento e a adaptação muscular em modelo de oclusão da carótida comum em gerbilos / Andriette Camilo Turi. -- São Carlos : UFSCar, 2015.
107 f.

Dissertação (Mestrado) -- Universidade Federal de São Carlos, 2015.

1. Fisioterapia. 2. Acidente vascular encefálico. 3. Isquemia. 4. Músculo esquelético. I. Título.

CDD: 615.82 (20ª)

UNIVERSIDADE FEDERAL DE SÃO CARLOS

Centro de Ciências Biológicas e da Saúde
Programa de Pós-Graduação em Fisioterapia

Folha de Aprovação

Assinaturas dos membros da comissão examinadora que avaliou e aprovou a Defesa de Dissertação de Mestrado da candidata Andriette Camilo Turi, realizada em 27/02/2015:

Prof. Dr. Thiago Luiz de Russo
UFSCar

Profa. Dra. Anna Carolyna Lepesteur Gianlorenço
UFSCar

Profa. Dra. Rosana Macher Teodori
UNIMEP

AGRADECIMENTOS

Agradeço primeiramente a minha família e ao meu namorado que sempre me apoiam nos caminhos que escolho seguir. À FAPESP pelo apoio financeiro a esta pesquisa e ao meu orientador Thiago Luiz de Russo que me deu um desafio a cumprir e com este, pude aprender infinitamente.

Às alunas de Iniciação Científica, Rafa e Bruna, imprescindíveis na realização deste projeto, sem a ajuda de vocês teria sido impossível. A Clara, Fer e Teresa, pela ajuda e pela companhia nos longos dias de Western blot e demais análises.

A todas as meninas do laboratório: Gabi, Má, Carol, Lu, Clara e Fer pela amizade, pelas dicas, conversas, risadas e desabafos.

Ao professor Fernando pelo ensino e pela conversa que tivemos.

Ao professor João e a Kelly, que nos ensinaram partes essenciais do procedimento experimental, tornando este projeto possível.

À Rafa que se dispôs a nos ajudar no momento que precisamos.

Ao Edilson, Rodrigo, Sandra, Débora, Lucia e muitos outros amigos que fiz nesse período e as amigas que já tenho (Pati, Lara, Ana, Tamara, Carol, Aline e outras) que me proporcionaram momentos leves para que eu pudesse respirar e continuar a caminhar.

Aos professores da banca de qualificação e defesa por lerem meu projeto com paciência e atenção, pelos comentários pertinentes e por me ajudarem a enxergar o que eu já não via.

Ao Nico, Dita e Judi que sempre me deixam feliz.

RESUMO

Dentre as disfunções decorrentes do acidente vascular encefálico (AVE), as sensório-motoras são as mais prevalentes e as mais incapacitantes, com destaque para a fraqueza muscular. De etiologia complexa e indefinida, esta fraqueza tem sido relacionada a alterações musculares, como a atrofia. O modelo de oclusão da artéria carótida comum (ACC) em gerbilos vem sendo descrito como eficiente em induzir lesões neuronais em áreas motoras e no hipocampo. Contudo, não há informação disponível sobre qual a adaptação muscular em decorrência deste modelo. **OBJETIVO:** Verificar a efetividade de um modelo de indução de AVE isquêmico pela oclusão unilateral da ACC, seguida por reperfusão, sobre as alterações musculares ao longo de 7, 15 e 21 dias, em gerbilos. Para tal, a quantificação da área de secção transversa das fibras musculares e quantificação do conteúdo proteico de Fbxo40, um modulador da hipertrofia muscular, em músculos paréticos (P) e não paréticos (NP) foram relacionados a dados obtidos no teste de campo aberto e Rota Rod. **MATERIAIS E MÉTODOS:** Setenta gerbilos machos adultos (*Meriones unguiculatus*), 2-3 meses, foram submetidos à oclusão unilateral da artéria carótida comum por 10 minutos, com fio de sutura, seguida de reperfusão. Os comportamentos exploratório e motor foram avaliados pelo teste de campo aberto e Rota Rod, respectivamente, no dia anterior à lesão e 6, 13 e 20 dias após o procedimento cirúrgico. Um grupo sham para o procedimento cirúrgico foi realizado. Os animais foram eutanasiados no 7º, 14º ou 21º dia. Análises morfométricas (área de secção transversa da fibra muscular) dos músculos tibial anterior e sóleo foram realizadas. A quantificação do conteúdo proteico da enzima de atrofia Fbxo40 foi analisada pela técnica Western Blot e cortes histológicos das regiões do hipocampo, córtex motor e estriado foram realizados. Para a estatística, os dados foram submetidos a testes de homogeneidade e normalidade. Se detectado que os dados eram paramétricos, o teste Anova *one-way* foi utilizado. Caso houvesse diferença, o teste de Tukey foi aplicado para localizá-las. Se não paramétricos, o teste Kruskal-Wallis seguido de Mann-Whitney foi realizado. Um nível de significância de 5% foi considerado. **RESULTADOS:** Não houve diferença no número de atravessamentos avaliado pelo teste de campo aberto, bem como no tempo de permanência no aparato Rota Rod na comparação entre os grupos experimentais ($p>0.05$). A expressão proteica de Fbxo40, o peso muscular e a área de secção transversa das fibras musculares dos músculos tibial anterior e sóleo, de ambas as patas pélvicas, não diferiram entre os grupos experimentais ($p>0.05$). **CONCLUSÃO:** O modelo de indução de AVE em gerbilos, com 10 minutos de oclusão da artéria carótida comum com reperfusão, não foi capaz de produzir alterações funcionais, comportamentais ou musculares em gerbilos.

Palavras-chave: AVE, Fisioterapia, modelo de isquemia, músculo esquelético.

ABSTRACT

Among the disorders resulting from cerebrovascular accident (CVA), the sensorimotor are the most prevalent and the most disabling, especially muscle weakness. Complex and unknown etiology, this weakness has been related to muscle disorders, such as atrophy. The common carotid artery occlusion model (ACC) in gerbils has been described as effective in inducing neuronal damage in the hippocampus and motor areas. However, no information is available about which muscle adaptation due to this model. To assess the effectiveness of an ischemic stroke induction model by unilateral CCA occlusion followed by reperfusion of the muscle changes over 7, 15 and 21 days in gerbils. To this end, the quantification of the cross-sectional area of muscle fibers and quantification of protein content Fbxo40, a modulator of muscle hypertrophy in paretic muscles (P) and not paretic (NP) were related to data obtained in open field test and Rota Rod. **MATERIALS AND METHODS:** Seventy adult male gerbils (Meriones unguiculatus), 2-3 months, underwent unilateral occlusion of the common carotid artery for 10 minutes, with suture, followed by reperfusion. The exploratory and motor behaviors were evaluated by open field tests and Rota Rod, respectively, the day before the injury and 6, 13 and 20 days after surgery. A sham group for the surgical procedure was performed. The animals were killed on the 7th, 14th or 21st day. Morphometric analysis (cross-sectional area of muscle fibers) of the tibialis anterior and soleus muscles were performed. The quantification of the protein content of the Fbxo40 atrophy enzyme was analyzed by Western blot and histological sections of the regions of the hippocampus, motor cortex and striatum were performed. Statistical data were subjected to homogeneity and normality tests. If detected that the data were parametric, the one-way ANOVA test was used. If there is a difference, the Tukey test was used to locate them. Nonparametric, the Kruskal-Wallis test followed by Mann-Whitney test was performed. A 5% significance level was considered. **RESULTS:** There was no difference in the number of crossings evaluated by field tests, as well as the residence time in the apparatus Rota Rod in the comparison between the experimental groups ($p > 0.05$). Protein expression of Fbxo40, muscle weight and cross-sectional area of muscle fibers of the tibialis anterior and soleus muscles of both legs pelvic did not differ between the experimental groups ($p > 0.05$). **CONCLUSION:** The induction stroke model in gerbils with 10 minutes of occlusion of the common carotid artery with reperfusion, was unable to produce functional or behavioral changes in gerbils muscle.

Keywords: stroke, Physiotherapy, model of ischemia, skeletal muscle.

LISTA DE FIGURAS

FIGURA 1	Comparação dos grupos experimentais nos dias pré-operatório (Dia-1), 6º 13º e 20º dia pós-operatório (D6, D13 e D20, respectivamente) no teste de campo aberto (A) e Rota Rod (B).	27
FIGURA 2	Expressão da proteína Fbxo40 para o músculo Tibial Anterior da pata não parética (TA NP) em A, Tibial Anterior da pata parética (TA P) em B, Sóleo da pata não parética (SOL NP) em C e Sóleo da pata parética (SOL P) em D.	29
FIGURA 3	Imagens digitais de cortes histológicos coronais de encéfalos de gerbilos.	30

LISTA DE TABELAS

TABELA 1	Peso corporal e dos músculos tibial anterior e sóleo.	28
TABELA 2	Área de secção transversa dos músculos tibial anterior e sóleo.	29

SUMÁRIO

APRESENTAÇÃO 9

CONTEXTUALIZAÇÃO 10

REVISÃO BIBLIOGRÁFICA 11
A fraqueza muscular decorrente do AVE 12
Modelos experimentais para a investigação do AVE 13
Vias de atrofia muscular 14

INTRODUÇÃO 18

OBJETIVOS 21
Objetivos Gerais 21
Objetivos Específicos 21

METODOLOGIA 22
Animais 22
Grupos experimentais 22
Procedimento cirúrgico 23
Testes comportamentais 23
Campo aberto 23
Rota Rod 24
Eutanásia e processamento dos encéfalos 24
Avaliação dos músculos 25
Western blot 25
Avaliação estatística 26

RESULTADOS 27
Testes comportamentais 27
Peso corporal, peso muscular e área de secção transversa da fibra muscular 28
Western blot 29
Histologia dos encéfalos 30

DISCUSSÃO 31

CONCLUSÃO 37

REFERÊNCIAS BIBLIOGRÁFICAS 38

PRODUÇÃO NO PERÍODO 43

ANEXOS 45

APRESENTAÇÃO

Esta dissertação de mestrado segue as recomendações do Programa de Pós-Graduação em Fisioterapia da UFSCar. Inicialmente será feita uma breve contextualização do problema, depois o manuscrito inédito produzido neste período, o qual foi submetido ao Brazilian Journal of Physical Therapy e, por fim, a produção da candidata durante o mestrado.

CONTEXTUALIZAÇÃO

Com altos índices de mortalidade e internação, o acidente vascular encefálico (AVE) tem se configurado como um dos principais problemas de saúde pública no mundo. Suas sequelas sensório-motoras, em especial a fraqueza, afetam diretamente a funcionalidade do indivíduo e sua qualidade de vida, sendo ainda um desafio para a equipe de reabilitação atuar de forma a otimizar suas capacidades. Portanto, o desenvolvimento de estudos que foquem esta população, trazendo evidências sobre como o AVE atua sobre os demais sistemas corporais, é necessário para traçar estratégias nos diferentes níveis de atenção à saúde.

Há vários anos, nosso laboratório vem desenvolvendo estudos com ênfase na avaliação e intervenção da Fisioterapia em indivíduos pós-AVE. Apesar de desafiadores, estudos clínicos com seres humanos apresentam inúmeras limitações para o entendimento dos processos de incapacidade e respostas periféricas em decorrência da lesão do sistema nervoso central. Neste sentido, a implementação de modelos animais que possam, ao menos em parte, mimetizar a condição de indivíduos acometidos pelo AVE, são importantes para aprofundar o entendimento dos mecanismos adaptativos frente à lesão.

O presente estudo propôs-se a verificar a efetividade de um modelo de indução de AVE isquêmico pela oclusão unilateral da artéria carótida comum (ACC), seguida por reperfusão do tecido encefálico, sobre as alterações musculares ao longo do tempo. Análises moleculares, morfológicas e comportamentais foram empregadas na tentativa de criar uma linha de base para intervenções futuras. Assim, a hipótese inicial do presente estudo foi que a oclusão da ACC em gerbilos poderia causar alterações moleculares, como o aumento do conteúdo proteico de Fbxo40, uma enzima relacionada à degradação de fatores hipertróficos, portanto, refletindo em atrofia muscular e déficits funcionais.

REVISÃO BIBLIOGRÁFICA

O aumento significativo da incidência de doenças crônicas não transmissíveis, dentre elas o AVE, vem acompanhando o envelhecimento da população mundial (MINISTÉRIO DA SAÚDE, 2005; NATIONAL INSTITUTES OF HEALTH, 2007; JORGE *et al*., 2008; GARRITANO *et al*., 2012). Atualmente, o AVE é considerado a segunda maior causa de mortes no mundo (LAVADOS *et al*., 2007; FEIGIN *et al*., 2009; JOHNSTON *et al*., 2009) e a principal causa de incapacidade em adultos sobreviventes (GRESHAM *et al*., 1975; GRESHAM *et al.,* 1979; WILLIAMS *et al*., 1999; PAK & PATTEN, 2008).

Nas últimas décadas, países pobres e em desenvolvimento apresentaram índices epidêmicos de AVE, ultrapassando pela primeira vez na história os países desenvolvidos (FEIGIN *et al*., 2009). Na América Latina, o Brasil lidera os índices de mortalidade, com cerca de 100 mil mortes devido ao AVE por ano (LOTUFO, 2005; DATASUS, 2012). Em 2011, houve o registro de 180 mil internações decorrentes desta afecção neurológica, que geraram gastos altíssimos ao Sistema Único de Saúde (SUS) brasileiro (R$ 197,9 milhões), caracterizando o AVE como um dos principais problemas de saúde pública no país (DATASUS, 2012).

Já estão consolidados na literatura que os sintomas após o AVE dependem de sua etiologia, localização e severidade inicial, sendo o AVE classificado como isquêmico ou hemorrágico. A forma isquêmica é a mais comum, representando cerca de 85% dos casos, e é causada pela oclusão de uma artéria, geralmente causada por trombos ou êmbolos (AMERICAN HEART ASSOCIATION, 2009; PENTÓN-ROL *et al*., 2011).

Em meio aos mais variados tipos de disfunções decorrentes de um AVE, como as neuropsiquiátricas, visuais, de memória, de atenção ou de linguagem, as disfunções sensório-motoras são as mais prevalentes na prática da equipe de reabilitação, pois afetam diretamente a funcionalidade do indivíduo e sua qualidade de vida (WALTON, 2003).

A fraqueza muscular decorrente do AVE

Dentre as disfunções sensório-motoras mais comuns pós-AVE destaca-se a fraqueza, a qual possui etiologia complexa e variada, sendo oriunda de alterações morfofuncionais dos sistemas nervoso central (SNC) e também do músculo esquelético.

A literatura tem demonstrado que danos aos tratos motores descendentes, após a isquemia cerebral, podem ser refletidos em prejuízos sobre os componentes neurais de geração de força, como por exemplo, alterando o padrão de ativação muscular (GRACIES, 2005; PRADO-MEDEIROS *et al*., 2012), diminuindo a ativação da musculatura agonista do movimento (PATTEN *et al*., 2004) e aumentando a atividade antagonista (SILVA-COUTO *et al.,* 2014). A espasticidade também é outro fator importante que pode contribuir para a paresia e a incapacidade pós-AVE (SHEEAN & MCGUIRE, 2009).

Embora muito tenha sido descrito sobre as alterações neurais, há uma carência de estudos visando às adaptações do sistema muscular decorrentes do AVE. Assume-se que o drive neural alterado chegando ao tecido muscular, aliado à diminuição da atividade que ocorre em sujeitos pós-AVE, pode acarretar em transformações do tecido músculo esquelético, como mudança no tipo de fibra (SNOW *et al.,* 2012), aumento de tecido conjuntivo (RAMSAY *et al.,* 2011) e redução da área de secção transversa das fibras e, portanto, comprometendo a geração de força (SILVA-COUTO *et al*., 2014).

Além disso, ainda é controverso na literatura se há atrofia em músculos paréticos pós-AVE. Estudos em seres humanos diferem seus resultados, variando desde ausência de atrofia muscular no membro parético (SUNNERHAGEN *et al.,* 1999), até diferenças significativas entre lado parético e não parético (RYAN *et al.,* 2002; METOKI *et al.,* 2003) e entre indivíduos hemiparéticos e controles saudáveis (SILVA-COUTO *et al.,* 2014). Fatores como diferentes graus de espasticidade e fraqueza aliados a variabilidade de idades, intervalos pós-AVE e comorbidades existentes atrapalham a homogeneidade dos grupos (SNOW *et al.,* 2012), dificultando a generalização das conclusões.

Modelos experimentais para a investigação do AVE

Diante destas dificuldades, os estudos com animais mostram-se importantes para controlar as variáveis que podem interferir na interpretação dos resultados. Além disso, evita problemas éticos como a obtenção de biópsias. Neste sentido, um modelo de indução de AVE isquêmico em gerbilos (*Meriones unguiculatus*), vem sendo amplamente utilizado por sua facilidade, reprodutibilidade e eficácia em promover isquemia cerebral. Tratam-se dos únicos animais que possuem o círculo arterial de Willis incompleto, ou seja, ausência da artéria comunicante posterior que possibilitaria a anastomose entre as artérias carótidas e vertebrais (O´NEILL & CLEMENS, 2000).

Tais características permitem que poucos minutos de oclusão da artéria carótida comum com fio de sutura (10 min), seguido por breve reperfusão, sejam suficientes para promover danos cerebrais irreversíveis e consecutiva perda de função neuronal em áreas cerebrais, como o córtex motor, hipocampo e corpo estriado (LIPTON, 1999; DE ARAÚJO *et al.*, 2012), levando à diminuição da habilidade motora e déficits de equilíbrio (DE ARAÚJO *et al.*, 2008). Contudo, atualmente não há nenhuma informação disponível sobre a adaptação muscular destes animais.

Em ratos, o uso de diferentes modelos de indução do AVE perpetua a controvérsia. Snow e colaboradores (2012) mostraram, com um modelo de AVE hemorrágico em ratos, atrofia de fibras tipo IIx e hipertrofia de fibras tipo I no músculo tibial anterior, após 2 semanas. Nenhuma alteração foi observada no músculo sóleo. Outro estudo (CHOE *et al.*, 2004) observou atrofia muscular em músculos gastrocnêmios, em patas paréticas e não paréticas, 7 dias após isquemia da artéria cerebral média.

De forma geral, a maioria dos estudos com animais foca-se na mensuração da área de secção transversa da fibra muscular e na tipagem de fibras musculares. Pouca ou nenhuma atenção é dada para os mecanismos moleculares de adaptação. O estudo de vias moleculares de regulação de massa muscular ajuda a identificar potenciais alvos terapêuticos para o tratamento de músculos paréticos, como genes de atrofia, de hipertrofia e de regulação de massa e, permite ainda, criar uma linha de base para intervenções terapêuticas futuras.

Vias de atrofia muscular

O equilíbrio entre síntese e degradação de proteínas que ocorre dentro das fibras musculares reflete um mecanismo altamente controlado de regulação da massa muscular (SCHIAFFINO *et al*., 2013). No momento em que há o aumento da degradação e a redução da síntese proteica ocorre atrofia muscular.

Amplamente estudada em modelos de atrofia como imobilização, desnervação, microgravidade e desnutrição, a via ubiquitina-proteossomo (BODINE *et al.,* 2001; GOMES *et al.,* 2001) vem sendo considerada como a principal via de degradação no tecido muscular (BONALDO & SANDRI, 2013). Com papel chave, as ubiquitina-ligases 3, ou simplesmente E3, são capazes de conjugar ubiquitinas às proteínas musculares alvo e, assim, marcá-las para que sejam degradadas no proteossomo (BONALDO & SANDRI, 2013; SCHIAFFINO *et al*., 2013).

Sabe-se que existem cerca de 650 tipos de ubiquitinas ligases (LEE & GOLDBERG, 2011), o que confere seletividade à determinação do local de ação de cada uma delas (BONALDO & SANDRI, 2013). Poucas foram reconhecidas como músculo-específicas, destacando-se recentemente, Fbxo40 (SHI *et al.,* 2011). Esta E3 ligase desempenha importante papel na regulação dos sinais anabólicos. Sabe-se que a hipertrofia muscular é um processo altamente controlado, em que a via IGF-I/IRS1/IP3K/Akt/mTOR possui papel chave no aumento da síntese proteica. Recentemente foi descoberto que Fbxo40 é capaz de ubiquitinar os substratos para o receptor de insulina I (IRS1), controlando assim a síntese proteica. Este processo ocorre dependente da disponibilidade de IGF-I, sendo um importante mecanismo de controle autócrino da síntese de IGF pelo tecido muscular, regulando assim a hipertrofia (SHI *et al.,* 2011; BONALDO & SANDRI, 2013; SCHIAFFINO *et al*., 2013).

ESTUDO SOBRE O COMPORTAMENTO E A ADAPTAÇÃO MUSCULAR EM MODELO DE OCLUSÃO DA CARÓTIDA COMUM EM GERBILOS

TÍTULO RESUMIDO:

ADAPTAÇÃO MUSCULAR E OCLUSÃO DA CARÓTIDA COMUM

AUTORES: Andriette Camilo Turi[1], Rafaela Firmino de Almeida[2], Bruna Thais Erbereli[3], Fernanda Maria Faturi[4], Rafaela Florindo Pestana Ferrão Batalhote[5], João Eduardo de Araújo[6], Tania de Fátima Salvini[7], Anselmo S. Moriscot[8], Thiago Luiz de Russo[9]

AUTOR DE CORRESPONDÊNCIA: Prof. Dr. Thiago Luiz Russo, Laboratório de Pesquisa em Fisioterapia Neurológica (LaFiN), Departamento de Fisioterapia, Universidade Federal de São Carlos (UFSCar), Rodovia Washington Luís, km 235, C.P. 676 – CEP: 13565-905. São Carlos, SP, Brasil; Telefone: 00 55 16 33066702 - FAX: 00 55 16 33612081; E-mail: thiagoluizrusso@gmail.com ou russo@ufscar.br

PALAVRAS-CHAVE: AVE, Fisioterapia, modelo de isquemia, músculo esquelético.

KEYWORDS: Stroke, Physical Therapy, ischemia model, skeletal muscle.

[1]Universidade Federal de São Carlos (UFSCar) [2]Universidade Federal de São Carlos (UFSCar) [3]Universidade Federal de São Carlos (UFSCar) [4]Universidade Federal de São Carlos (UFSCar) [5]Universidade de São Paulo (USP SP) [6]Universidade de São Paulo (USP RP) [7]Universidade Federal de São Carlos (UFSCar) [8]Universidade de São Paulo (USP SP) [9]Universidade Federal de São Carlos (UFSCar).

RESUMO

Dentre as disfunções decorrentes do acidente vascular encefálico (AVE), a fraqueza muscular tem sido relacionada a alterações musculares, como a atrofia. O modelo de oclusão da artéria carótida comum (ACC) em gerbilos vem sendo descrito como eficiente em induzir lesões neuronais. Contudo, não há informação disponível sobre qual a adaptação muscular em decorrência deste modelo. Assim, verificamos a efetividade de um modelo de indução de AVE isquêmico sobre as alterações musculares ao longo do tempo. Setenta gerbilos foram submetidos à oclusão unilateral da ACC seguida de reperfusão. O teste de campo aberto e Rota Rod avaliaram o comportamento exploratório e motor. Análises morfométricas dos músculos tibial anterior (TA) e sóleo (SOL), quantificação do conteúdo proteico da enzima de atrofia Fbxo40 pela técnica Western Blot e cortes histológicos das regiões do hipocampo, córtex motor e estriado foram realizados. Para a estatística, dados foram submetidos a testes de homogeneidade e normalidade. Se paramétricos, o teste Anova *one-way* e o teste de Tukey foram aplicados. Se não paramétricos, o teste Kruskal-Wallis seguido de Mann-Whitney foi realizado. Um nível de significância de 5% foi considerado. Não houve diferença no número de atravessamentos e no tempo de permanência no aparato Rota Rod entre os grupos experimentais ($p>0.05$). A expressão proteica de Fbxo40, o peso muscular e a área de secção transversa das fibras musculares dos músculos TA e SOL, não diferiram entre os grupos experimentais ($p>0.05$). Concluímos que o modelo de indução de AVE em gerbilos não foi capaz de produzir alterações comportamentais ou musculares.

ABSTRACT

Among the disorders resulting from cerebrovascular accident, the sensorimotor are the most prevalent and the most disabling, especially muscle weakness. Complex and unknown etiology, this weakness has been related to muscle disorders, such as atrophy. The common carotid artery occlusion model (CCA) in gerbils has been described as effective in inducing neuronal damage in the hippocampus and motor areas. However, no information is available about which muscle adaptation due to this model. To assess the effectiveness of an ischemic stroke induction model by unilateral CCA occlusion followed by reperfusion of the muscle changes over 7, 15 and 21 days in gerbils. To this end, the quantification of the cross-sectional area of muscle fibers and quantification of protein content Fbxo40, a modulator of muscle hypertrophy in paretic muscles (P) and not paretic (NP) were related to data obtained in open field test and Rota Rod. **MATERIALS AND METHODS:** Seventy adult male gerbils (*Meriones unguiculatus*), 2-3 months, underwent unilateral occlusion of the common carotid artery for 10 minutes, with suture, followed by reperfusion. The exploratory and motor behaviors were evaluated by open field test and Rota Rod, respectively, the day before the injury and 6, 13 and 20 days after surgery. A sham group for the surgical procedure was performed. The animals were killed on the 7th, 14th or 21st day. Morphometric analysis (cross-sectional area of muscle fibers) of the tibialis anterior and soleus muscles were performed. The quantification of the protein content of the Fbxo40 atrophy enzyme was analyzed by Western blot and histological sections of the regions of the hippocampus, motor cortex and striatum were performed. Statistical data were subjected to homogeneity and normality tests. If detected that the data were parametric, the one-way ANOVA test was used. If there is a difference, the Tukey test was used to locate them. Nonparametric, the Kruskal-Wallis test followed by Mann-Whitney test was performed. A 5% significance level was considered. **RESULTS:** There was no difference in the number of crossings evaluated by open field test, as well as the residence time in the apparatus Rota Rod in the comparison between the experimental groups ($p>0.05$). Protein expression of Fbxo40, muscle weight and cross-sectional area of muscle fibers of the tibialis anterior and soleus muscles of both legs pelvic did not differ between the experimental groups ($p>0.05$). **CONCLUSION:** The induction stroke model in gerbils with 10 minutes of occlusion of the common carotid artery with reperfusion was unable to produce functional or behavioral changes in gerbils muscle.

INTRODUÇÃO

O acidente vascular encefálico (AVE) destaca-se atualmente por ser considerado a segunda maior causa de mortes no mundo (LAVADOS *et al*., 2007; FEIJIN *et al*., 2009; JOHNSTON *et al*., 2009) e a principal causa de incapacidades em adultos sobreviventes (GRESHAM *et al*., 1975; GRESHAM *et al*., 1979; WILLIAMS *et al*., 1999; PAK & PATTEN, 2008). Além disso, o AVE lidera os índices de mortalidade no Brasil, consolidando-se como um problema de saúde pública (LOTUFO, 2005; DATASUS, 2012).

A forma isquêmica, caracterizada pela oclusão de uma artéria por trombos ou êmbolos, é o tipo que mais acomete a população, respondendo por 85% das ocorrências de AVE (AMERICAN HEART ASSOCIATION, 2009; PENTON-ROL *et al*., 2011). Sabe-se que o indivíduo acometido pode apresentar vários sintomas que irão depender do tipo, localização e severidade da lesão inicial. Destacam-se as disfunções sensório-motoras, e dentre elas a paresia, que afeta diretamente a funcionalidade e qualidade de vida do indivíduo (WALTON, 2003).

Na literatura, vários são os achados nos sistemas nervoso central e músculo esquelético que tentam explicar a etiologia desta paresia, como a espasticidade, alterações no drive neural, aumento do tecido conjuntivo intramuscular, redução da área de secção transversa da fibra muscular, entre outros (RAMSAY *et al*., 2011; SNOW *et al*., 2012; SILVA-COUTO *et al*., 2014). Contudo, por apresentar uma etiologia multifatorial, ainda não há consenso na literatura sobre qual a real contribuição destes fatores e, em parte, isso se deve às dificuldades na realização de estudos com humanos de forma controlada. A ampla gama de idades dos sujeitos, intervalos após a lesão, comorbidades coexistentes e as dificuldades na obtenção de biópsias são apenas alguns dos muitos fatores que dificultam a generalização dos resultados (DU *et al*., 2011).

Diante dessas dificuldades, os estudos com modelos experimentais surgem como proposta no que diz respeito ao controle das variáveis. A trombose da artéria cerebral média, a injeção de endotelina-1 e a indução de embolias na artéria carótida interna são as formas de indução de AVE mais frequentemente encontradas na literatura (CASALS *et al*., 2011). Apesar de vastamente utilizadas pela eficácia em causar danos em estruturas corticais e/ou subcorticais, tais métodos apresentam consideráveis desvantagens, como a falta de controle da pressão intracraniana e o fato do método ser

altamente invasivo, com retirada parcial da calota craniana e consequente exposição do tecido encefálico.

Nesse contexto, na década de 60, um modelo de indução de AVE isquêmico em gerbilos destaca-se por sua praticidade e reprodutibilidade. A principal característica destes animais é a ausência da artéria comunicante posterior (ACoP), o que possibilita que poucos minutos de oclusão da artéria carótida comum causem danos cerebrais que levam a alterações funcionais e neurocomportamentais (LIPTON, 1999; O´NEILL & CLEMENS, 2000; DE ARAÚJO *et al*., 2008; DE ARAÚJO *et al*., 2012). Mais recentemente De Araújo e colaboradores (2012) mostraram que 10 minutos de oclusão unilateral da carótida comum, seguida por reperfusão, em gerbilos era suficiente para causar expressiva morte neuronal no córtex motor, hipocampo e corpo estriado. Tal alteração foi acompanhada por déficits comportamentais e funcionais, verificados por testes como o de campo aberto e Rota Rod.

Tendo este modelo bem estabelecido pelos autores supracitados e conhecendo a falta de consenso na literatura sobre as alterações que ocorrem no músculo esquelético após um evento isquêmico encefálico, pode-se reconhecer que estudos direcionados às vias moleculares de regulação de massa muscular poderiam ajudar a identificar possíveis mecanismos de resposta muscular e também alvos para o tratamento farmacológico e não farmacológico de músculos paréticos e, assim, auxiliar no tratamento da fraqueza e na recuperação funcional.

A regulação da massa muscular é altamente controlada pela síntese e degradação de proteínas, sendo que o aumento da degradação não acompanhado pelo aumento da síntese leva a um processo denominado atrofia. A principal via de degradação do tecido muscular é a via ubiquitina-proteossomo, a qual envolve a ação integrada de três classes de enzimas (E1, E2 e E3) para poliubiquitinização de proteínas-alvo e posterior reconhecimento e degradação destas proteínas em aminoácidos através do proteossomo (BODINE *et al*., 2001; GOMES *et al*., 2001; BONALDO & SANDRI, 2013; SCHIAFFINO *et al*., 2013).

As E3, também denominadas enzimas-ligases, assim chamadas por realizarem a ligação das proteínas-alvo com várias unidades de ubiquitina, destacam-se por sua especificidade. Dentre elas está Fbxo40 que desempenha importante papel na regulação dos sinais anabólicos ao adicionar ubiquitinas nos substratos para o receptor de insulina,

na membrana das células, sendo dependente de IGF-1 (BODINE *et al*., 2001; GOMES *et al*., 2001; BONALDO & SANDRI, 2013; SCHIAFFINO *et al*., 2013).

Em vista do que foi exposto, é possível hipotetizar que a oclusão da artéria carótida comum (ACC) ao causar danos encefálicos pode gerar alterações moleculares e morfofuncionais em gerbilos. Portanto, este estudo tem como objetivo verificar a efetividade de um modelo de indução de AVE isquêmico pela oclusão unilateral da ACC, seguida por reperfusão sobre as alterações musculares ao longo de 7, 15 e 21 dias, em gerbilos. Para tal, a quantificação da área de secção transversa das fibras musculares e quantificação do conteúdo proteico de Fbxo40 em músculos paréticos (P) e não paréticos (NP) foram relacionadas aos testes de campo aberto e Rota Rod.

OBJETIVOS

Objetivos Gerais

Verificar a efetividade de um modelo de indução de AVE isquêmico pela oclusão unilateral da artéria carótida comum, seguida por reperfusão sobre as alterações musculares ao longo de 7, 15 e 21 dias, em gerbilos.

Objetivos Específicos

- Quantificar a área de secção transversa das fibras musculares em músculos paréticos e não paréticos;
- Quantificar o conteúdo proteico de Fbxo40 em músculos paréticos e não paréticos;
- Analisar de modo qualitativo os cortes histológicos da região do hipocampo, corpo estriado e córtex motor;
- Correlacionar os achados morfológicos e moleculares com a funcionalidade.

METODOLOGIA

O presente projeto foi aprovado e realizado segundo as normas do Comitê de Ética no Uso de Animais da Universidade Federal de São Carlos (Protocolo Nº 042/2013), em anexo.

Animais

Foram usados 70 gerbilos machos (*Meriones unguiculatus*), de dois a três meses, pesando de 50 a 80 g, provenientes de um único criadouro particular. Antes dos experimentos, os animais foram separados em grupos de quatro animais por gaiolas coletivas (41 x 34 x 16 cm) e permaneceram durante duas semanas no biotério do Departamento de Fisioterapia para controle de possíveis doenças. Os animais foram mantidos em gabinete com temperatura (23 ± 1º C) e luminosidade (ciclo claro/escuro de 12 horas) controladas e com acesso a comida e água *ad libitum*.

Grupos experimentais

Os animais foram divididos em 7 grupos experimentais, sendo avaliados 10 animais por grupo:

Grupos AVE 7, 15 e 21 dias: animais submetidos ao procedimento cirúrgico, o qual ocluiu a artéria carótida comum direita por 10 minutos. Foram submetidos aos testes de funcionalidade no dia anterior à cirurgia (-1) e 6, 13 ou 20 dias pós-lesão. Foram eutanasiados após 7, 15 ou 21 dias do início do experimento, respectivamente.

Grupos SHAM 7, 15 e 21 dias: animais submetidos ao procedimento cirúrgico, entretanto, sem oclusão da artéria carótida comum. Foram submetidos aos testes de funcionalidade no dia anterior à cirurgia (-1) e 6, 13 ou 20 dias de pós-cirúrgico. Foram eutanasiados após 7, 15 ou 21 dias do início do experimento, respectivamente.

Grupo Controle: animais não submetidos ao procedimento cirúrgico, utilizados para parâmetros comparativos. Foram submetidos aos testes de funcionalidade no dia -1, 6, 13 ou 20 e eutanasiados após 21 dias do início do experimento.

Procedimento cirúrgico

Os animais foram submetidos a um procedimento cirúrgico amplamente utilizado por sua eficácia em produzir uma lesão isquêmica unilateral encefálica (BLOCK, 1999; LIPTON, 1999; LEE *et al*., 2003). Eles foram anestesiados com quetamina e xilasina administrado via intraperitoneal, seguida da tricotomia e incisão ventral no pescoço. Os tecidos subcutâneo e muscular foram afastados para promover a exposição da artéria carótida comum ipsilateral ao hemisfério lesionado. Através de um fio de sutura, a artéria carótida comum direita foi tensionada obtendo a interrupção do fluxo sanguíneo, verificada de forma visual, por 10 minutos enquanto a região foi hidratada com cloreto de sódio (0,9%). Após o término do tempo pré-determinado, a oclusão foi interrompida e o local suturado. Durante o procedimento cirúrgico, a temperatura do animal foi mantida em torno de 37 ± 0,5º C com aquecedores até o gerbilo retomar a consciência.

Testes comportamentais

Os comportamentos exploratório e motor foram avaliados por dois testes: Campo aberto e Rota Rod (RR), respectivamente.

Campo aberto

O teste de campo aberto consistiu de uma área quadrada fechada de 50 cm de diâmetro, dividida em 25 quadrantes de 10x10 cm, elevada 50 cm do chão e acoplada a uma câmera filmadora. Os animais foram individualmente colocados no centro da gaiola de teste e 15 minutos de sessão foram gravados um dia antes da cirurgia e 6, 13 e 20 dias após a cirurgia (grupos AVE e Sham). O grupo controle foi avaliado no mesmo período que os demais grupos. O número de atravessamentos (i.e. número de seções do

chão percorridas) foi avaliado, como previamente descrito por De Araújo (2012). Este teste permite avaliar o comportamento exploratório dos animais. No modelo de indução isquêmica, a lesão na região hipocampal leva a hiperatividade com consequente aumento do número de atravessamentos pelos animais (KUROIWA *et al*., 1991; COULBOURNE *et al*., 1998; LAIDLEY *et al*., 2005).

Rota Rod

Imediatamente após o teste de campo aberto todos os animais foram colocados no aparato Rota Rod (EFF 412 model, Insight LTDA, Brazil), o qual possui uma superfície cilíndrica que se move ao redor de um eixo com uma aceleração de 5,5 rpm. Em três tentativas, os animais deviam se equilibrar no cilindro em movimento e o teste era interrompido a qualquer momento logo após a queda do animal. O sistema estava acoplado a uma câmera filmadora e fornecia a medida de tempo de permanência no aparato. O animal devia permanecer por pelo menos 3 segundos com as quatro patas apoiadas sobre o cilindro para a tentativa ser considerada válida. Para a análise estatística, a média dos valores de tempo referentes as três tentativas foi realizada. Este teste é amplamente utilizado para avaliar o comportamento motor (coordenação motora e equilíbrio) em experimentos com lesões cerebrais globais ou focais em ratos ou camundongos (DE ARAÚJO *et al*., 2012; DING *et al*., 2004; YAN *et al*., 2007).

Eutanásia e processamento dos encéfalos

Após a conclusão dos procedimentos experimentais, os animais receberam uma overdose de anestésico. A seguir, os animais foram decapitados, os encéfalos removidos, identificados e acondicionados individualmente em coletores com solução de formalina 10%. Foram realizados cortes histológicos (10 µm) na região do córtex motor primário, hipocampo e corpo estriado em micrótomo, estes cortes foram corados pelo método de Nissl (Cresil) para visualização e análise qualitativa dos neurônios.

Avaliação dos músculos

Os músculos tibial anterior e sóleo de ambas as patas pélvicas foram dissecados e removidos. Eles foram divididos em duas porções a partir do ventre muscular, uma proximal e outra distal. A porção distal foi fixada e congelada em isopentano pré-resfriado em nitrogênio líquido e foi utilizada para análise histológica e morfométrica. A porção proximal foi congelada em nitrogênio líquido e utilizada para a análise proteica. Todos os músculos foram armazenados em freezer a –86°C.

Para as análises morfométricas e morfológicas foram realizados cortes histológicos seriados (10 μm), na porção média do músculo, em micrótomo criostato a -25ºC. Estes cortes foram corados com azul de toluidina (TB) para análise de morfologia geral e também para as medidas de área de secção transversa das fibras musculares. Cem fibras musculares foram escolhidas aleatoriamente, de cada músculo, e foram mensuradas a partir da imagem obtida da região central do ventre muscular.

Western Blot

Cem miligramas de tecido foram homogeneizados em um tampão de lise (Ripa buffer: 10 mM Tris-HCl, pH 7,4; 150 mM NaCl; 1% Nonideto P-40; 1% deoxicolato de sódio; 0,1% SDS; 10% glicerol) com inibidores de proteases (10 mM sodiopirofosfato; 10 mM NaF; 1 mM SoV_4; 2 mM PMSF; 10 μg/ml de inibidores de leupeptina, tripsina, aprotinina e antipaina). As amostras foram agitadas durante 30 min a 4ºC e depois centrifugadas por 30 min também a 4ºC. As proteínas totais foram quantificadas por espectofotômetro pelo método de Bradford a 550 nm e comparadas a uma curva de concentração de BCA. Quantidades iguais de proteína foram separadas em um gel SDS-PAGE a 12%. Um padrão pré-corado foi usado para averiguar o peso molecular das proteínas (Kalidoscope Prestained Standards, Bio-Rad). Posteriormente, as proteínas foram transferidas para uma membrana de nitrocelulose por eletroforese. Estas membranas foram avaliadas com *red ponceau* para confirmação da qualidade da corrida e a presença das proteínas. Para incubação dos anticorpos, as membranas passaram pelos seguintes passos: 3 banhos de 10 min cada de TBST; 1 banho de 1 h em 5% de leite em pó dissolvido em TBST; incubação *overnight* a 4ºC com o anticorpo primário dissolvido em 1 ml de TBST. O anticorpo primário foi de Fbxo40. A α-tubulina (1:500

– Sigma) foi usada como controle endógeno. Após incubação, as membranas foram lavadas 3 vezes de 10 min cada em TBST e passaram por incubação com o anticorpo secundário (IgG, hosearadish peroxidase linked whole antibody; 1:7000 em 0,1% de leite em pó em TBST). Por fim, as membranas foram lavadas 3 vezes em TBST e foi adicionado reagente ECL Western blotting para detecção de sinal com fotodocumentador IMP Chemi Doc (Bio-Rad).

A análise densitométrica das bandas foi realizada usando o software de imagem GeneTools v3.06 software (Syngene, Cambridge, UK). Os sinais foram normalizados pela α-Tubulina.

Avaliação estatística

Os dados foram submetidos a testes de homogeneidade (Levene) e normalidade (Shapiro-Wilk). Se detectado que os dados eram paramétricos, o teste Anova *one-way*, seguido do Tukey, foi utilizado para detectar a presença de diferença entre os grupos. Se não paramétricos, o teste Kruskal-Wallis seguido de Mann-Whitney foi realizado. Um nível de significância de 5% foi considerado.

RESULTADOS

Testes comportamentais

Os grupos Controle, Sham 21 dias e AVE 21 dias são apresentados como dados representativos dos demais grupos experimentais. Não houve diferença entre o número de atravessamentos no teste campo aberto e o tempo de permanência no Rota Rod nos diferentes grupos experimentais (p>0.05) como demonstrado na **Figura 1**.

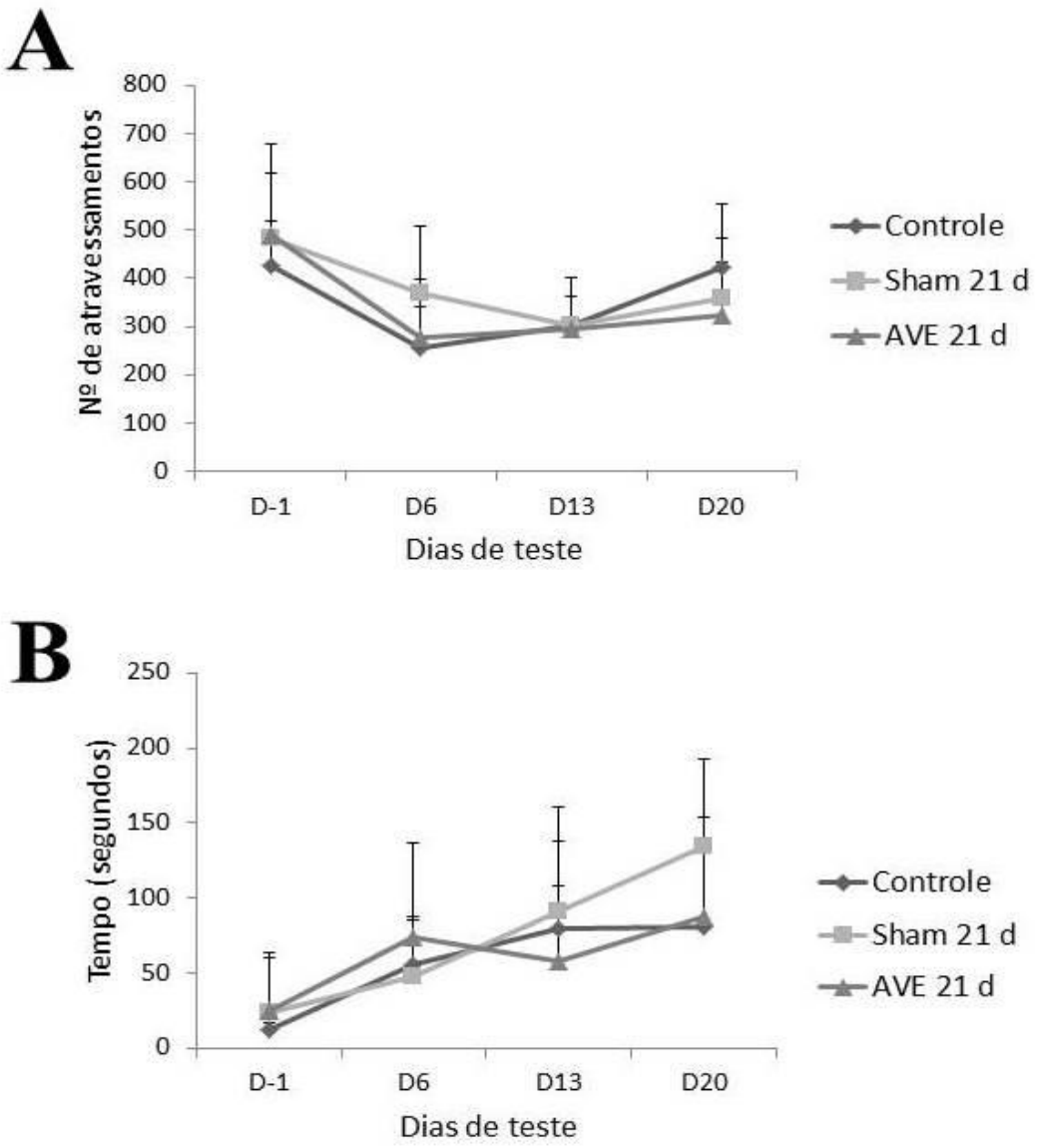

FIGURA 1. Comparação dos grupos experimentais nos dias pré-operatório (Dia-1), 6º 13º e 20º dia pós-operatório (D6, D13 e D20, respectivamente) no teste de campo aberto (A) e Rota Rod (B). Não houve diferença em nenhum dos períodos avaliados (p>0.05) para ambos os testes.

Peso corporal, peso muscular e área de secção transversa da fibra muscular

No dia da eutanásia dos animais e previamente aos procedimentos de retirada dos músculos e do encéfalo, os animais foram anestesiados e pesados em balança de precisão a fim de obtermos os dados relativos ao peso corporal. Após análise estatística destes dados, constatou-se diferença no peso corporal dos animais pertencentes ao grupo AVE 15d comparado a AVE 7d, Sham 21d e Controle ($p<0.05$). Assim, as medidas dos pesos musculares passaram pelo procedimento de normalização previamente a análise estatística.

Não houve redução no peso do músculo tibial anterior e sóleo de ambas as patas pélvicas dos animais de todos os grupos ($p>0.05$), os valores médios seguidos pelo desvio padrão estão representados na **Tabela 1** a seguir. Tal achado corrobora com os dados da área de secção transversa da fibra muscular, onde também não houve diferença entre os grupos, **Tabela 2**.

TABELA 1. Peso corporal e dos músculos tibial anterior e sóleo.

GRUPOS	PESO CORPORAL	% TA NP	% TA P	% SOL NP	% SOL P
Controle	61.50 ± 4.52*	0.31 ± 0.02	0.31 ± 0.03	0.055 ± 0.005	0.053 ± 0.008
Sham 7d	59.88 ± 3.55	0.32 ± 0.01	0.31 ± 0.03	0.054 ± 0.005	0.054 ± 0.006
Sham 15d	60.50 ± 4.52	0.32 ± 0.05	0.31 ± 0.04	0.050 ± 0.004	0.053 ± 0.007
Sham 21d	59.37 ± 7.22*	0.33 ± 0.02	0.29 ± 0.02	0.053 ± 0.003	0.055 ± 0.006
AVE 7d	53.30 ± 5.88*	0.46 ± 0.43	0.32 ± 0.03	0.061 ± 0.009	0.058 ± 0.008
AVE 15d	62.00 ± 5.47	0.30 ± 0.02	0.31 ± 0.03	0.056 ± 0.006	0.052 ± 0.008
AVE 21d	58.70 ± 3.59	0.28 ± 0.03	0.28 ± 0.03	0.054 ± 0.008	0.052 ± 0.006

Valores de média e desvio padrão relativos aos pesos corporal e muscular dos animais. %TA NP: porcentagem do peso corporal do músculo tibial anterior da pata não parética. %TA P: porcentagem do peso corporal do músculo tibial anterior da pata parética. % SOL NP: porcentagem do peso corporal do músculo sóleo da pata não parética. %SOL P: porcentagem do peso corporal do sóleo da pata parética. *$p<0.05$ na comparação de AVE 15d com os grupos AVE 7d, Sham 21d e Controle.

TABELA 2. Área de secção transversa dos músculos tibial anterior e sóleo.

	SOL NP	SOL P	TA NP	TA P
Controle	1298.07 ± 137.957	1235.15 ± 295.406	808.21 ± 118.228	971.53 ± 123.400
Sham 7d	1309.42 ±151.672	1217.12 ± 289.046	1018.83 ± 298.393	1080.67 ±190.782
AVE 7d	1249.94 ± 289.182	1430.00 ± 255.366	1206.74 ± 225.435	1259.90 ± 217.259
Sham 15d	1429.50 ± 166.997	1463.57 ± 265.803	1070.04 ± 270.264	1134.32 ± 159.601
AVE 15d	1475.95 ± 268.185	1317.86 ± 297.853	1127.02 ± 249.077	1088.65 ± 213.845
Sham 21d	1396.62 ± 493.962	1312.58 ± 205.660	1076.84 ± 215.776	1232.51 ± 222.013
AVE 21d	1525.86 ± 290.196	1364.82 ± 207.185	1103.12 ± 165.693	1208.83 ± 245.903

Valores de média e desvio padrão referente a área de secção transversa dos músculos. TA NP: tibial anterior da pata não parética. TA P: tibial anterior da pata parética. SOL NP: sóleo da pata não parética. SOL P: sóleo da pata parética. Não houve diferença nos valores de área de secção transversa entre os grupos (p>0.05).

Western blot

A análise do conteúdo proteico de Fbxo40, não revelou diferença de expressão entre os diferentes grupos experimentais **(Figura 2)**, bem como na comparação entre os músculos e os lados parético e não parético de cada grupo (dados não apresentados).

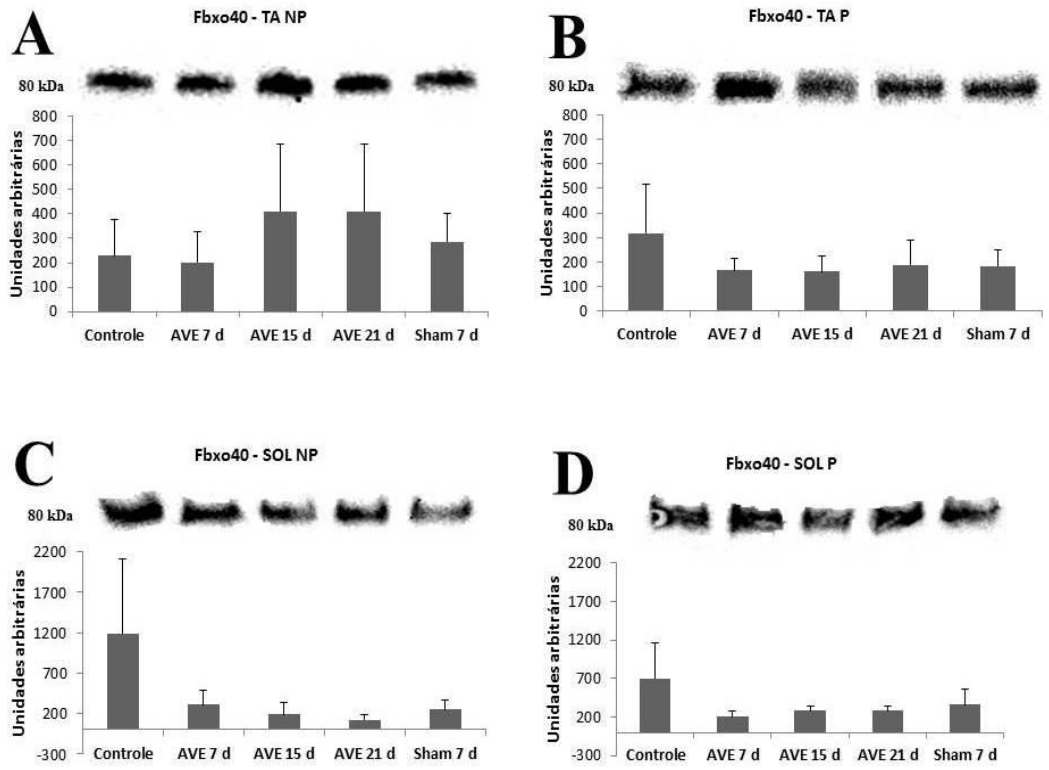

FIGURA 2. Expressão da proteína Fbxo40 para o músculo Tibial Anterior da pata não parética (TA NP) em A, Tibial Anterior da pata parética (TA P) em B, Sóleo da pata não parética (SOL NP) em C e Sóleo da pata parética (SOL P) em D. Não houve diferença entre os grupos (p>0.05).

Histologia dos encéfalos

Fotomicrografias representativas de cortes histológicos dos encéfalos dos animais submetidos à oclusão da ACC são apresentados na **Figura 3.** Não foi detectada morte neuronal ou outros achados indicativos de lesão nestes animais.

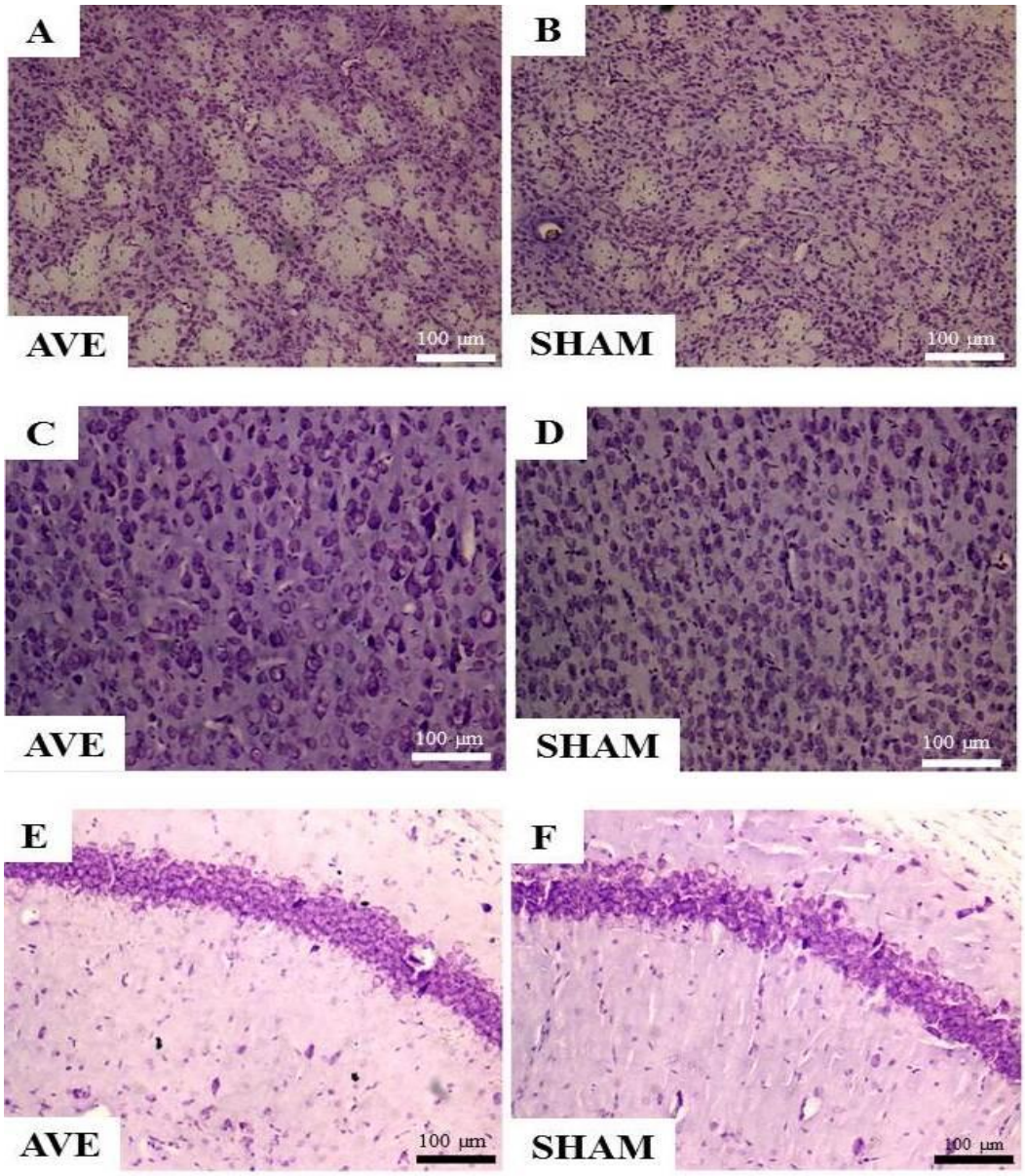

FIGURA 3. Imagens digitais de cortes histológicos coronais de encéfalos de gerbilos. As imagens ilustram os corpos celulares de neurônios ou células da glia corados pelo método de Nissl (Cresil). As imagens à esquerda representam um gerbilo submetido a oclusão da ACC (AVE), as imagens à direita representam um gerbilo do grupo Sham, ambos eutanasiados no 5º dia P.O. Em A e B, temos neurônios do corpo estriado, em C e D neurônios piramidais corados na 6ª camada cortical do córtex motor primário (M1) e em E e F neurônio do Corno de Amon 1 (CA1) no hipocampo. Nota-se a grande quantidade de corpos celulares corados no animal AVE.

DISCUSSÃO

A proposta inicial de nosso trabalho foi a de caracterizar e entender os mecanismos envolvidos nas alterações que ocorrem no músculo esquelético após a oclusão da ACC em modelo experimental. Este tipo de procedimento é descrito na literatura como capaz de causar dano encefálico por isquemia (JANAC *et al*., 2006; DE ARAÚJO *et al*., 2012). Atualmente, é um desafio para os pesquisadores a realização de estudos com AVE em humanos por inúmeros fatores, dentre eles: ampla gama de idades e intervalos após a lesão dos indivíduos, variabilidade no grau de espasticidade e fraqueza, comorbidades coexistentes, pouca praticidade no controle dos níveis de atividade física geral dos participantes, dificuldade na obtenção de biópsias e o fato destas não representarem a totalidade muscular, impossibilidade ética de avaliação da recuperação espontânea na ausência de terapias reabilitadoras e médicas apropriadas, além da plasticidade ser facilmente influenciada por alterações naturais do envelhecimento e desuso (DU *et al*., 2011).

Apesar dos modelos com animais permitirem o controle das variáveis e possibilitarem que análises difíceis de serem realizadas em humanos sejam feitas, ainda permanece a busca de um modelo experimental de isquemia encefálica que se aproxime da mesma condição em humanos, ou seja, um modelo com alta relevância clínica e reprodutibilidade, de fácil execução experimental e sem efeitos colaterais não relacionados a isquemia (DU *et al*., 2011).

Os modelos experimentais mais frequentemente encontrados para indução de isquemia, como oclusão da artéria cerebral média, a injeção de endotelina-1 e indução de embolias na artéria carótida interna, apesar de efetivos para a indução de lesões encefálicas, dependem da retirada parcial da calota craniana com afastamento das meninges, o que expõe o tecido encefálico deixando-o vulnerável a infecções e alterando a pressão intracraniana. Frente a essas desvantagens, o modelo com gerbilos, mesmo sendo animais de pequeno porte, sensíveis a hipotermia e com limitadas habilidades para execução de testes comportamentais, ainda é vantajoso, segundo a literatura, por ser de fácil execução, breve e reproduzível, além de minimamente invasivo e com baixa demanda de equipamentos (DU *et al*., 2011).

Como demonstrado por De Araújo e colaboradores (2012), apenas 10 minutos de oclusão da ACC esquerda, seguida de reperfusão, permitiu a constatação de 41% de

morte neuronal no hipocampo, 70% no corpo estriado e 69% no córtex motor quando avaliados no 6º dia pós-operatório. Não apenas este, mas outros vários estudos (KITAGAWA *et al*., 1996; LAIDLEY *et al*., 2005; DE ARAÚJO *et al*., 2008) corroboraram com tais achados histológicos evidenciando marcante perda celular em diferentes áreas encefálicas após poucos minutos de oclusão uni ou bilateral permitindo ou não a reperfusão e isso pôde auxiliar na consolidação deste modelo.

Embasados na literatura e considerando a facilidade, reprodutibilidade e eficácia de tal modelo, nos dispusemos a estudar as alterações musculares após isquemia unilateral realizada com fio de sutura na ACC direita por 10 minutos seguida de reperfusão em gerbilos. Contudo, nossos resultados não concordaram com a literatura. Achados histológicos não evidenciaram lesões na região hipocampal, do corpo estriado ou do córtex motor, além disso, os testes de funcionalidade e a análise da expressão proteica da proteína Fbxo40 corroboraram com a ausência de achados histológicos, não evidenciando diferenças entre os grupos Sham e os grupos submetidos a oclusão em qualquer um dos tempos analisados (7, 15 e 21 dias após a lesão). O peso dos músculos TA e SOL assim como os dados da área de secção transversa das fibras musculares concordaram com os achados anteriores.

Algumas hipóteses foram levantadas para explicar os resultados encontrados. Inicialmente, a grande variabilidade anatômica entre os gerbilos. Du e colaboradores (2011) após analisarem minuciosamente as características do Círculo de Willis de 413 gerbilos encontraram quatro padrões distintos para a artéria comunicante posterior, com proporções semelhantes, sendo o tipo I descrito como a presença completa desta artéria, o tipo II, ausência da mesma, tipo III com o ramo esquerdo ausente e tipo IV com o ramo direito ausente. Os mesmos autores relatam que a artéria comunicante anterior também possui grande variabilidade nestes animais, tendo também sido classificada em quatro subtipos. Laidley e colaboradores (2005) compararam animais advindos de Charles River (CR) e High Oak (HO), duas regiões distintas do Canadá e concluíram que os gerbilos de CR, possuíam maior variabilidade anatômica da artéria comunicante posterior. Esta artéria apresentou três situações anatômicas distintas: ausência e presença uni ou bilateral.

Deste modo, a presença de uma ACoP funcional, considerada como sendo aquelas com diâmetro superior a 50 µm (LAIDLEY *et al*., 2005) e que portanto é capaz

de reestabelecer rapidamente o fluxo sanguíneo cerebral, parece amenizar o dano do tecido neural e acelerar a recuperação do desempenho dos testes funcionais (KITAGAWA *et al*., 1996; DU *et al*., 2011; LAIDLEY *et al*., 2005). Por exemplo, gerbilos de CR, com maior ocorrência de ACoP, exibem 24% menos de morte neuronal no hipocampo comparado ao grupo HO. Tais achados evidenciam que origens distintas dos animais podem influenciar os resultados e, portanto, dificultar a reprodutibilidade dos estudos.

Em nosso estudo, menos de 10% dos animais apresentaram sinais clínicos de isquemia (dados não apresentados), sendo a ptose palpebral unilateral o sinal mais frequente. Tal fato parece indicar que nosso grupo de animais possuía ampla variabilidade anatômica e, diferentemente do que mostrou Laidley e outros (KITAGAWA *et al*., 1996; JANAC *et al*., 2006; DE ARAÚJO *et al*., 2012), nossos animais não apresentam sinais histológicos, somado ao fato de que o desempenho no teste campo aberto e Rota Rod não foi diferente em animais submetidos ou não a isquemia. A avaliação de aspectos éticos e da viabilidade de estudos com gerbilos deve ser feita pelos pesquisadores para trabalhos futuros, pois apenas uma pequena parte dos animais poderia entrar neste critério, sendo necessária uma grande mortandade.

Em relação ao comportamento motor destes animais, estudos prévios afirmam que um sinal clássico após a isquemia é justamente o aumento agudo na locomoção (hiperlocomoção) que persiste por pelo menos um dia sendo oriundo de lesões hipocampais (COULBOURNE *et al*., 1998; DING *et al*., 2004; LAIDLEY *et al*., 2005). Fato que ocorreu até as primeiras 16 horas para gerbilos de CR ou manteve-se até o 10º dia em gerbilos de HO no estudo de Laidley e colaboradores (2005) após a oclusão da ACC. Além disso, achados morfológicos indicam que o pico de morte neuronal nesta região deve ocorrer em torno de 4 dias após oclusão da ACC (DE ARAÚJO *et al*., 2012).

Em outro estudo, Janac e colaboradores (2006) também submeteram animais ao teste de campo aberto após 5, 10 ou 15 minutos de oclusão bilateral em vários períodos após a cirurgia. Apenas os animais submetidos 15 minutos de oclusão bilateral apresentaram diferença na atividade locomotora comparado ao controle no 7º dia P.O. O grupo submetido a 5 minutos de oclusão bilateral apresentou diferença apenas na avaliação realizada 24 horas após o procedimento cirúrgico, enquanto o grupo

submetido a 10 minutos de oclusão apresentou diferença na atividade locomotora somente até o 4º dia P.O. Somado a isso, todos os grupos, inclusive os animais submetidos a oclusão por 15 minutos já haviam retornado a valores basais quando foram avaliados no 14º, 21º e 28º dias. Tais achados evidenciam que lesões neurais não necessariamente refletem déficits funcionais ao longo do tempo neste modelo de isquemia.

É necessário esclarecer que um estudo piloto, desenvolvido por nosso grupo, em que os gerbilos tiveram a oclusão da ACC por 10 min, também falhou em observar alterações motoras e comportamentais 1 e 4 dias após o procedimento (dados não apresentados). A escolha dos tempos para a avaliação motora e comportamental do presente estudo, ou seja, 6, 13 e 20 dias após a oclusão da ACC ocorreu por acreditar-se que as adaptações musculares frente a isquemia poderiam acontecer mais tardiamente, semelhante ao que ocorre na prática clínica, e portanto modificariam as respostas motoras no teste Rota Rod, além de que o comportamento exploratório, observado pelo teste de campo aberto, permitiria verificar a efetividade do modelo de lesão e verificar sua recuperação ao longo do tempo.

Algumas ressalvas devem ser realizadas para a interpretação dos resultados obtidos neste trabalho. Primeiro, apesar de não terem sido observadas alterações morfológicas, não é possível verificar se alterações mais tênues do sistema nervoso central ocorreram em decorrência à oclusão da ACC, como por exemplo, a depressão metabólica de neurônios, alterações da pressão intracraniana, mudanças da excitabilidade cortical ou a ativação de vias moleculares da plasticidade neural. Contudo, mesmo se tivessem ocorrido, tais modificações não foram suficientes para gerar mudanças motoras, comportamentais ou morfológicas do tecido muscular. Mesmo análises bastante sensíveis como a mensuração do conteúdo proteico de proteínas ligadas a degradação muscular não foram capazes de detectar qualquer alteração nos grupos submetidos à oclusão.

Tal análise dedicou-se a mensuração da expressão proteica de Fbxo40. O *knockdown* de Fbxo40 induz a hipertrofia das miofibras, sendo assim, descobriu-se recentemente que esta é uma importante E3 cuja função é adicionar ubiquitinas nos substratos para o receptor de insulina (IRS1). Quando isso acontece, a cascata de sinalização para síntese proteica através da via IRS1/PI3k/Akt é rapidamente desligada

e, a menos que o músculo seja capaz de sintetizar novo IGF-1, a fim de manter a sinalização para síntese proteica, o sinal anabólico é interrompido. Somado a isso, parece que a proteína Fbxo40 age num circuito curto, onde a ubiquitinação de IRS1 impede a inibição do fator de transcrição FOXO por meio de Akt, permitindo que E3 ligases importantes para o desenvolvimento de atrofia, como MAFbx e MuRF-1, sejam ativadas (GLASS, 2005; SHI *et al*., 2011; SATOH *et al*., 2011). Como sabemos, MAFbx e MuRF-1 são ativados previamente a redução da área de secção transversa e assim, nossos dados da expressão proteica de Fbxo40 juntamente com os achados da área de secção transversa da fibra muscular nos indicam que uma das principais vias de atrofia muscular não foi ativada, confirmando que este não é um modelo adequado para estudos deste tecido.

Não podemos deixar de considerar uma hipótese alternativa para a ausência de diferença na expressão proteica de Fbxo40 entre os grupos AVC e Sham. Em um estudo, Satoh e colaboradores (2011) avaliaram a expressão de uma proteína chamada Galectica-3, importante na proliferação celular e regulação apoptótica, sendo um relevante marcador de micróglia ativa, após oclusão bilateral das ACC em gerbilos por 5 minutos. Eles detectaram que, na avaliação realizada em 24 e 48 horas após a isquemia não era possível detectar a expressão da proteína, às 72 horas após o insulto, a expressão era levemente aparente, às 96 horas foi quando ocorreu o pico de expressão e duas semanas mais tarde não era possível observar nada novamente. Isso nos leva a pensar que a detecção da expressão de algumas proteínas é passível de ser detectada num intervalo curto e específico de tempo, fato que pode ser perdido caso a expressão proteica seja avaliada em recortes de tempo anteriores ou posteriores ao pico de expressão. Isso pode ter ocorrido em nosso estudo, visto que a extração muscular e processamento dos tecidos para análise molecular ocorreu no mínimo 7 dias após o procedimento de oclusão.

Este trabalho experimental gera uma série de recomendações para estudos futuros com este modelo. Para garantir a reprodutibilidade do experimento é necessário que a origem dos animais seja relatada. Uma análise anatômica detalhada da presença das artérias que compõe o círculo de Willis deve ser realizada para caracterizar o perfil de irrigação sanguínea dos encéfalos pré-oclusão, usando técnicas de imagem por contraste, ou pós-oclusão, com o estudo anatômico e histológico dos encéfalos. Outro fator importante a ser considerado é em relação ao tempo de oclusão da ACC para gerar

lesões, que deve variar de acordo com a origem dos animais e também de acordo com as gerações. Uma rigorosa descrição dos procedimentos de oclusão arterial e também do controle da temperatura dos animais deve ser realizado para garantir sua reprodutibilidade. É relatado na literatura que a indução de hipotermia após isquemia poder ser benéfica ao exercer efeito protetor no sistema nervoso central de animais, como evidenciado no estudo de Coulborne & Corbett (1994) e Satoh (2011). No estudo de Coubourne & Corbett, a hipotermia resultou em menor morte neuronal na região CA1 do hipocampo. Para Satoh e colaboradores não foi diferente, a expressão molecular de galectina-2 foi praticamente inibida pela hipotermia, demonstrando que baixas temperaturas corporais previnem danos neuronais graves.

Até o momento, em estudo de revisão em fase de andamento em nosso laboratório, podemos constatar que os estudos de isquemia encefálica realizados com gerbilos da Mongólia carecem de técnicas que comprovem a eficácia do procedimento de indução de isquemia em tempo real. Enquanto os modelos realizados a partir da oclusão da artéria cerebral média ou por injeção de endotelina-1 usam técnicas objetivas para comprovação da interrupção do fluxo sanguíneo como o uso de Laser Doppler em momentos pré, durante e após a isquemia, os estudos com gerbilos não possuem uma avaliação em tempo real durante a execução do procedimento de oclusão com ou sem reperfusão, ficando a comprovação da lesão, na maioria das vezes, a cargo de uma avaliação de sinais clínicos realizada pelo próprio pesquisador e/ou ainda a cargo de danos histológicos evidenciados no SNC somente após o processamento dos tecidos.

Por fim, este modelo de oclusão em gerbilos, com as características apresentadas neste estudo, parece não ser adequado para o estudo do tecido muscular, pois suas alterações não são persistentes ao longo do tempo e, portanto, limita a resposta adaptativa muscular. Deste modo, apesar de ser dito pela literatura como um modelo de isquemia encefálica simples, inúmeros cuidados devem ser tomados com o modelo a fim de garantir sua reprodutibilidade e eficácia, Tais problemas experimentais impactam a pesquisa da área de neuroreabilitação pós-AVE, pois há dificuldade em se estabelecer modelos de isquemia do sistema nervoso central de forma semelhante como acontece em seres humanos.

CONCLUSÃO

O modelo de indução de AVE em gerbilos a partir de 10 minutos de oclusão da artéria carótida comum direita com reperfusão não foi capaz de produzir alterações histológicas, comportamentais e no sistema músculo esquelético de gerbilos.

REFERÊNCIAS BIBLIOGRÁFICAS

AMERICAN HEART ASSOCIATION STATISTICS COMMITTEE AND STROKE STATISTICS SUBCOMMITTEE, HEART DISEASE AND STROKE STATISTICS – UPDATE, **Circulation,** v.119, p.e21–e181, 2009.

BLOCK, F. Global ischemia and behavioural deficits. **Progress Neurobiol**, v.58, n.3, p.279-295, 1999.

BODINE, S.C.; LATRES, E.; BAUMHUETER, S.; LAI, V.K.M.; NUNEZ, L.; CLARKE, B.A. et al. Identification of ubiquitin ligases required for skeletal muscle atrophy. **Science**, v.294, p.1704-1708, 2001.

BONALDO, P.; SANDRI, M. Cellular and molecular mechanisms of muscle atrophy. **Disease Models & Mechanisms**, v.6, p.25-39, 2013.

CASALS, J.B.; PIERI, N.C.G.; FEITOSA, M.L.T.; ERCOLIN, A.C.M.; ROBALLO, K.C.S.; BARRETO, R.S.N.; BRESSAN, F.F.; MARTINS, D.S.; MIGLINO, M.A.; AMBROSIO, C.E. The use of animal models for stroke research: a review. **Comparative Medicine**, v.61, n.4, p. 305-313, 2011.

CHOE, M.A.; AN, G.J.; LEE, Y.K.; IM, J.H.; CHOI-KWON, S.; HEITKEMPER, M. Effect of inactivity and undernutrition after acute ischemic stroke in a rat hindlimb muscle model. Nurs Res, v.53, n.5, p.283-92, 2004.

COLBOURNE, F.; CORBETT, D. Delayed and prolonged post-ischemic hypothermia is neuroprotective in the gerbil. Brain Research, v.654, p.265-272, 1994.

COULBOURNE, F.; AUER, R.N.; SUTHERLAND, G.R. Characterization of postischemic behavioral déficits in gerbils with and without hypothermic neuroprotection. **Brain Res**, v.803; p. 69-78, 1998.

DATASUS. Site no Ministério da Saúde. AVC: governo alerta para principal causa de mortes. Acesso em 06/04/2013 (http://portalsaude.saude.gov.br/portalsaude/noticia/7904/162/avc:-governo-alerta-para-%3Cbr%3Eprincipal-causa-de-mortes.html).

DE ARAÚJO, F.L.B.; BERTOLINO, G.; FUNAYAMA, C.A.R.; COIMBRA, N.C.; DE ARAÚJO, J.E. Influence of treadmill training on motor performance and organization of exploratory behavior in Meriones unguiculatus with unilateral ischemic stroke: Histological correlates in hippocampal CA1 region and the neostriatum. **Neuroscience Letters,** v.431, p.179-183, 2008.

DE ARAÚJO, F.L.B.; BERTOLINO, G.; GONÇALVES, R.B.; MARINI, L.C.; COIMBRA, N.C.; DE ARAÚJO, J.E. Neuropathology and behavioral impairments after three types of global ischemia surgery in Meriones unguiculatus: Evidence in motor cortex, hippocampal CA1 region and the neostriatum. **J Neurol Sci**, v.15, p.73-8, 2012.

DING, Y.; LI, J.; LAI, Q.; RAFOUOLS, J.A.; LUAN, X.; CLARK, J. et al. Motor balance and coordination training enhances functional outcome in rat with transient middle cerebral artery occlusion. **Neuroscience,** v.123, p.667–74, 2004.

DU, X.Y.; ZHU, X.D.; DONG, G.; LU, J.; WANG, Y; ZENG, L.; ZHAO, T.Y.; YE, H.H.; LI, R.S.; BAI, J.Y.; CHEN, Z.W. Characteristics of circle of Willis variations in the Mongolian gerbil and a newly established ischemia-prone gerbil group. **ILAR e-Journal**, v.52, e1-e7, 2011.

EGERMAN, M.A.; GLASS D.J. Signaling pathways controlling skeletal muscle mass. **Crit Rev Biochem Mol Biol**, v.49 (1), p. 59-69, 2014.

FEIGIN, V.L.; LAWES, C.M.M.; BENNETT, D.A.; BARKER-COLLO, S.L.B.; PARAG, V. Worldwide stroke incidence and early case fatality reported in 56 population-based studies: a systematic review. **Lancet Neurol**, v.8, p.355–69, 2009.

GARRITANO, C.R.; LUZ, P.M.; PIRES, M.L.E.; BARBOSA, M.T.S.; BATISTA, K.M. Analysis of the Mortality Trend due to Cerebrovascular Accident in Brazil in the XXI Century. **Arq Bras Cardiol**., v.98, n.6, p.519-527, 2012.

GLASS, D.J. Skeletal muscle hyppertrophy and atrophy signaling pathways. **The International Journal of Biochemistry & Cell Biology**, v. 37, p. 1974-1984, 2005.

GOMES, M.D.; LECKER, S.H.; JAGOE, R.T.; NAVON, A.; GOLDBERG, A.L. Atrogin-1, a muscle specific F-box protein highly expressed during muscle atrophy. **Proc Natl Acad Sci**, v.98, p.14440–14445, 2001.

GRACIES, J.M. Pathophysiology of spastic paresis I: Paresis and soft tissue changes. **Muscle Nerve**, v.31, n.5, 535–551, 2005.

GRESHAM, G.E.; FITZPATRICK, T.E.; WOLF, P.A.; MCNAMARA, P.M.; KANNEL, W.B.; DAWBER, T.R. Residual disability in survivors of stroke — The Framingham study. **N Engl J Med**; v.293, n.19, p.954–956, 1975.

GRESHAM, G.E.; PHILLIPS, T.F.;GRESHAM, G.E.; PHILLIPS, T.F.; WOLF, P.A.; MCNAMARA, P.M.; KANNEL, W.B.; DAWBER, T.R. Epidemiologic profile of long-term stroke disability: The Framingham study. **Arc Phys Med Rehabil**, v.60, n.11, p.487–491, 1979.

JANAC, B.; RADENOVIC, L.; SELAKOVIC, V;. PROLIC, Z. Time course of motor behavior changes in Mongolian gerbils submitted to diferente durations of cerebral ischemia. **Behavioural Brain Research**, v.187, p. 362-373, 2006.

JOHNSTON, S.C.; MENDIS, S.; MATHERS, C.D. Global variation in stroke burden and mortality: estimates from monitoring, surveillance, and modeling. **Lancet Neurol**, v.8, n.4, p.345-54, 2009.

JORGE, M.H.P.M.; LAURENTI, R.; LIMA-COSTA, M.F.; GOTLIEB, S.L.D.; CHIAVEGATTO FILHO, A.D.P. A mortalidade de idosos no Brasil: a questão das causas mal definidas. **Epidemiol Serv Saúde,** v.17, n.4, p.271-81, 2008.

KITAGAWA, K.; MATSUMOTO, M.; MATSUSHITA, K.; MANDAI, K.; MABUCHI, T.; YANAGIHARA, T.; KAMADA, T. Ischemic tolerance in moderately symptomatic gerbils after unilateral carotid occlusion. **Brain Research**, v. 716, p. 39-46, 1996.

KUROIWA, T.; BONNEKOH, P.; HOSSMANN, K.A. Locomotor hyperactivity and hipocampal CA1 injury after transiente forebrain ischemia of gerbils. **Neurosci Lett**, v.122, p141-144, 1991.

LAIDLEY, D.T.; COLBOURNE F.; CORBETT, D. Increased behavioral and histological variability arising from changes in cerebrovascular anatomy of the Mongolian gerbil. **Current Neurovascular Research**, v.2, n.5, p 401-407, 2005.

LAVADOS, P.M.; HENNIS, A.J.; FERNANDES, J.G.; MEDINA M.T.; LEGETIC, B.; HOPPE, A.; SACKS, C.; JADUE, L.; SALINAS, R. AVC epidemiology, prevention, and management strategies at a regional level: Latin America and the Caribbean. **Lancet Neurol**, v.6, n.4, p.362-72, 2007.

LEE, S.H.; KIM, Y.; KIM, S.S.; LEE, T.H.; LIM, B.V.; CHANG, H.K.; JANG, M.H.; SHIN, M.C.; SHIN, M.S.; KIM, C.J. Treadmill exercise supresses ischemia-induced increment in apoptosis and cell proliferation in hippocampal dentate gyrus of gerbils. **Life Sci**, v.73, p.2455-2465, 2003.

LEE, D.; GOLDBERG, A. Atrogin1/MAFbx: what atrophy, hypertrophy, and cardiac failure have in common. **Circ. Res**, v. 109, p. 123-126, 2011.

LIPTON, P. Ischemic cell death in brain neurons. **Physiol Rev**, v.79, p.1431-1568, 1999.

LOTUFO, P.A. Stroke in Brazil: a neglected disease. **São Paulo Med J**,v.123, n.1, p.3-4, 2005.

METOKI, N.; SATO, Y.; OKUMURA, K.; IWAMOTO, J. Muscular atrophy in the hemiplegic thigh in patients after stroke. **Am J Phys Med Rehabil**, v.82, p.862–865, 2003.

MINISTÉRIO DA SAÚDE. A vigilância, o controle e a prevenção das doenças crônicas não transmissíveis: DCNT no contexto do Sistema Único de Saúde brasileiro / Brasil. Brasília: Organização Pan-Americana da Saúde, 2005.

NATIONAL INSTITUTES OF HEALTH. Why population aging matters: a global perspective. Bethesda (MD): National Institute on Aging, National Institutes of Health, US Department of Health and Human Services, US Department of State, p.1-32, 2007.

O´NEILL, J.M.; CLEMENS, J.A. Rodents Models of global cerebral ischemia. **Preclinical Models of Neurological and Psychiatric Disorders**, suplement 12, u.9.5, 2000.

PAK, S.; PATTEN, C. Strengthening to Promote Functional Recovery Poststroke: An Evidence-Based Review. **Top Stroke Rehabil,** v.15, n.3, p.177–199, 2008.

PATTEN, C.; LEXELL. J.; BROWN, H.E. Weakness and strength training in persons with post stroke hemiplegia: rationale, method, and efficacy. **J Rehab Res Dev**, v.41 (3A), p.293-312, 2004.

PENTÓN-ROL, G.; MARÍN-PRIDA, J.; PARDO-ANDREU, G.; MATÍNEZ-SÁNCHEZ, G., ACOSTA-MEDINA, E.F.; VALDIVIA-ACOSTA, A.; LAGUMERSINDEZ-DENIS, N.; RODRÍGUEZ-JIMÉNEZ, E.; LLÓPIZ-ARZUAGA, A.; LÓPEZ-SAURA, P.A.; GUILLÉN-NIETO, G.; PENTÓN-ARIAS, E. C-

Phycocyanin is neuroprotective against global cerebral ischemia/reperfusion injury in gerbils. **Brain Research Bulletin,** v.86, p.42-52, 2011.

PRADO-MEDEIROS, C.L.; SILVA, M.P.; LESSI, G.C.; ALVES, M.Z.; TANNUS, A.; LINDQUIST, A.N.; SALVINI, T.F. Muscle atrophy and functional deficits of knee extensors and flexors in people with chronic stroke. **Physical Therapy**, v.92, n.3, 2012.

RAMSAY, J.W.; BARRANCE, P.T.; BUCHANAN, T.S.; HIGGINSON, J.S. Paretic muscle atrophy and non-contractile tissue content in individual muscles of the post-stroke lower extremity. **Journal of Biomechanics,** v.44, p.2741–2746, 2011.

RYAN, A.S.; DOBROVOLONY, C.L.; SMITH, G.V; SILVER, K.H., MACKO, R.F. Hemiparetic muscle atrophy and increased intramuscular fat in stroke patients. **Arch Phys Med Rehab.** v.83, p.1703–1707, 2002.

SATOH, K.; NIWA, M; GODA, W.; BINH, N.H.; NAKASHIMA, M.; TAKAMATSU, M.; HARA, A. Galectin-3 expression in delayed neuronal death of hippocampal CA1 following transient forebrain ischemia and its inhibition by hypothermia. **Brain Research**, v. 1382, p. 266-274, 2011.

SCHIAFFINO, S.; DYAR, K.A.; CICILIOT, S.; BLAAUW, B.; SANDRI, M. Mechanisms regulating skeletal muscle growth and atrophy. **The Authors Journal Compilation**, 2013.

SHEEAN, G.; MCGUIRE, J.R. Spastic Hypertonia and Movement Disorders: Pathophysiology, Clinical Presentation, and Quantification. **Amer Acad of Phys Med and Rehab,** v.1, (9), p. 827-833, 2009.

SHI, J.; LUO, L.; EASH, J.; IBEBUNJO, C.; GLASS, D.J. The SCF-Fbxo40 Complex Induces IRS1 Ubiquitination in Skeletal Muscle, Limiting IGF1 Signaling. **Developmental Cell**, v.21, p.835–847, 2011.

SILVA-COUTO, M.A.; PRADO-MEDEIROS, C.L.; OLIVEIRA, A.B.; ALCÂNTARA, C.C.; GUIMARÃES, A.T.; SALVINI, T.F.; MATTIOLI, R.; RUSSO, T.L. Muscle atrophy, voluntary activation disturbances, and low serum concentrations of IGF-1 and IGFBP-3 are associated with weakness in people with chronic stroke. **Physical Therapy**, v.94, n.7, p. 957-967, 2014.

SNOW, L.M.; LOW, W.C.; THOMPSON, L.V. Skeletal muscle plasticity after hemorrhagic stroke in rats: Influence of Spontaneous Physical Activity. Am. J. Phys. Med. Rehabil., v.91, n.11, 2012.

SUNNERHAGEN, K.S.; SVANTERSSON, U.; LONN, L. Upper motor neuron lesions: their effect on muscle performance and appearance in stroke patients with minor motor impairment. **Arch Phys Med Rehab,** v.80, p.155–161, 1999.

WALTON, K. Management of patients with spasticity: a pratical approach. **Pratical Neurology**, v. 3, p. 342-353, 2003.

WILLIAMS, G.R.; JIANG, J.G.; MATCHAR, D.B.; SAMSA, G.P. Incidence and occurrence of total (first-ever and recurrent) stroke. **Stroke**, v.30, n.12, p.2523–2528, 1999.

YAN, X.B.; WANG, S.S.; HOU, H.L.; JI, R.; ZHOU, J.N. Lithium improves the behavioral disorder in rats subjected to transient global cerebral ischemia. **Behav Brain Res,** v.177, p.282–9, 2007.

PRODUÇÃO NO PERÍODO

A bolsista esteve envolvida na preparação de dois manuscritos a serem submetidos neste ano, em ambos ela atua como coautora:

- **Title:** ´´The intermitent stretching induces fibrosis in rat denervated muscle"

Authors: Fernanda Maria Faturi, MS, Rúbia Cristina Franco, Davilene Gigo-Benato, PhD, Andriette Camilo Turi, Marcela de Abreu Silva Couto, MS, Sabrina Peviani Messa, PhD; Thiago Luiz Russo, PhD)

Este estudo encontra-se em fase final de correção das considerações feitas pela revista. Será submetido a revista Muscle & Nerve. Foi observado que o alongamento intermitente realizado a cada 48 horas no músculo sóleo desnervado induz a proliferação de tecido conjuntivo intramuscular pela ativação da via TGF-beta/miostatina **(ANEXO)**.

- **Title:** "Low level laser therapy modulates neurotrophin and matrix metalloproteinase expression in nerves and muscles after axonotmesis in rats"

Authors: Davilene Gigo-Benato, PhD, Andriette Camilo Turi, MS, Carolina Carmona Alcântara, MS, Thaianne Silva Mata, Livia Gaspar Fernandes, Juanita J Anders, PhD, Tania Fátima Salvini, PhD, Alexandre Rodrigues Leite Oliveira, PhD, Fernanda Maria Faturi, PhD, Thiago Luiz Russo, PhD.

Este artigo está sendo trabalhado em conjunto com a Profa. Juanita Anders e investigou o efeito do laser de baixa potência sobre a regeneração neuromuscular pós-axonotmese. De forma geral, este trabalho verificou que o laser, aplicado no nervo esmagado, gera modificações no padrão de atividade de enzimas de remodelamento da matriz e também na expressão de fatores neurotróficos como o BDNF. A bolsista pôde participar ativamente deste projeto auxiliando em todas as suas fases de realização **(ANEXO).**

A aluna também realizou atendimentos voluntários na área de Fisioterapia Neurológica na Unidade Saúde Escola, localizada na Universidade Federal de São Carlos com duração de um ano. Também participa de uma Atividade de Extensão intitulada ‘’Grupo Terapêutico para indivíduos hemiparéticos crônicos’’ que fornece

atendimentos a um grupo de hemiparéticos crônicos, duas vezes por semana, totalizando 4 horas semanais.

Por fim, os resultados parciais do presente projeto deram origem ao resumo descrito abaixo e apresentado na forma de pôster.

- **Título:** Desempenho funcional e adaptação muscular em gerbilos pós-isquemia.
  Evento: 3º Congresso Brasileiro de Fisioterapia Neurofuncional, Belo Horizonte, Minas Gerais.

ANEXOS

UNIVERSIDADE FEDERAL DE SÃO CARLOS
PRÓ-REITORIA DE PESQUISA
Comissão de Ética no Uso de Animais
Via Washington Luis, km. 235 - Caixa Postal 676
Fones: (016) 3351.8025 / 3351.9679
Fax: (016) 3351.8025
CEP 13560-970 - São Carlos - SP - Brasil
ceua@ufscar.br - www.propq.ufscar.br

Parecer da Comissão de Ética no Uso de Animais

nº 042/2013

Protocolo nº. 042/13

A Comissão de Ética no Uso de Animais da Universidade Federal de São Carlos - CEUA/UFSCar **APROVOU** o projeto de pesquisa intitulado *"Adaptações morfológicas e moleculares de músculos esqueléticos paréticos em gerbilos pós-acidente vascular encefálico"*, submetido pela pesquisadora *Andriette Camilo Turi*.

São Carlos, 24 de setembro de 2013.

Azair Liane Matos do Canto de Souza

Profa. Dra. Azair Liane Matos do Canto de Souza

Presidente da Comissão de Ética no Uso de Animais

ANEXOS

A seguir são apresentados os artigos supracitados em fase final de correção.

- **Title:** ´´The intermitent stretching induces fibrosis in rat denervated muscle"

  Authors: Fernanda Maria Faturi, MS, Rúbia Cristina Franco, Davilene Gigo-Benato, PhD, Andriette Camilo Turi, Marcela de Abreu Silva Couto, MS, Sabrina Peviani Messa, PhD; Thiago Luiz Russo, PhD).

- **Title:** "Low level laser therapy modulates neurotrophin and matrix metalloproteinase expression in nerves and muscles after axonotmesis in rats"

  Authors: Davilene Gigo-Benato, PhD, Andriette Camilo Turi, MS, Carolina Carmona Alcântara, MS, Thaianne Silva Mata, Livia Gaspar Fernandes, Juanita J Anders, PhD, Tania Fátima Salvini, PhD, Alexandre Rodrigues Leite Oliveira, PhD, Fernanda Maria Faturi, PhD, Thiago Luiz Russo, PhD.

ANEXOS

Original Article

Title:

The intermittent stretching induces fibrosis in rat denervated muscle

Authors:

Fernanda M. Faturi[1], MS, Rúbia C. Franco[1], Davilene Gigo-Benato[1], PhD, Andriette C. Turi[1], MS, Marcela A. Silva-Couto[1], MS, Sabrina P. Messa[2], PhD, Thiago L. Russo[1], PhD.

[1]Research Laboratory of Neurological Physiotherapy (LaFiN), Department of Physiotherapy (DFisio), Federal University of São Carlos (UFSCar), São Carlos, São Paulo, Brazil; [2]Laboratory of Muscle Plasticity, DFisio, UFSCar, São Carlos, São Paulo, Brazil.

Acknowledgments: This study was supported by FAPESP (Fundação de Amparo à Pesquisa do Estado de São Paulo; process numbers: 2011/07463-0, 2013/14024-9, and 2013/21621-3). Authors thank Joice Arnoni for technical support.

Corresponding author: Prof. Dr. Thiago Luiz Russo, Laboratório de Pesquisa em Fisioterapia Neurológica (LaFiN), Departamento de Fisioterapia, Universidade Federal de São Carlos (UFSCar), Rodovia Washington Luís, km 235, C.P. 676 – CEP: 13565-905. São Carlos, SP, Brazil; Phone: 00 55 16 33066702 - FAX: 00 55 16 33612081; E-mail: thiagoluizrusso@gmail.com ou russo@ufscar.br

Running title: stretching in denervated muscle

ABSTRACT

Introduction: Stretching (St) has been used for treating denervated muscles. However, its effectiveness and safety claims for more studies. **Material and Methods:** Rats were divided into: Denervated (D) muscles evaluated 7 or 15 days after sciatic nerve crush injury, D muscles submitted to St during 7 or 15 days, and Normal. Muscle fiber cross-sectional area, serial sarcomere number, sarcomere length, and connective tissue density were measured. MMP-2, -9, TIMP-1, TGF-β1 and myostatin mRNAs were determined by real time PCR. MMP-2 and -9 activity was evaluated by zymography. Collagen I was localized using immunofluorescence. **Results:** St did not prevent muscle atrophy due to denervation. It increased fibrosis and collagen I deposition on day-15. St also upregulated MMP-9 and TGF-β1 gene expressions at day-7, and myostatin at day-15. **Discussion:** Stretching denervated muscle does not prevent muscle atrophy. In addition it increases fibrosis via temporal modulation of TGF-β1/myostatin and MMP-9 cascades.

Keywords: Physiotherapy, Neurorehabilitation, Skeletal Muscle, Muscle Atrophy, Stretching.

INTRODUCTION

The peripheral nerve injuries (PNI) are considered as a challenge to rehabilitation team. Directly affected by the lack innervation, the skeletal muscle passes by innumerous deleterious changes, such as the muscular atrophy [1-3], the loss of capacity force generation[4], the increase of connective tissue proliferation[5], and consequently the flexibility loss. Other muscular alterations, resulting of denervation, are the shift of myosin heavy chain from type I to II[6-8].

Morphofunctional changes that happen in the denervated muscles are due to the molecular alterations of the muscle trophism regulatory pathways, such as hypertrophy[9, 10] atrophy[1, 9] and mass regulation ones[1, 11], besides the control and remodeling pathways of the extracellular matrix (ECM)[5]. In this sense, the tumoral growth factor beta (TGF-β1)/myostatin pathway has an important role in mediating the mass regulation, as well as the matrix extracellular modifications[12]. During denervation, the TGF-β1 acts stimulating the myostatin. Also known as GDF-8, myostatin is a negative factor of muscular mass control, in other words, increases of myostatin restrict the muscle growth and hypertrophy, and also stimulate rigidity collagens (I and III) on the ECM, thus generating fibrosis[12].

Among the main agents of ECM remodeling, a family of zinc-dependent enzymes, name matrix metalloproteinases (MMPs) stands out, being the MMP-2 and -9 (collagenase - A and -B, respectively) rather common and important to the ECM of skeletal muscle, for collagen turnover, for example, the type IV[13]. These MMPs (-2 and -9) are regulated by enzymes, called TIMP-1 (tissue inhibitor of metalloproteinase-1). Such regulation is essential to the maintenance of structural tissue integrity[14].

Early studies, with animal models, that studied resources used during the neurorehabilitation process showed that there are lacks about the efficiency and the safety of therapeutic resources used in the clinic to the denervated muscle treatment. The study of the resources that stimulate the nerve growth, as well as reduce or prevent the muscular atrophy are still needed. Gigo-Benato *et al*[15] showed that the electrical stimulation seems to impair the neuromuscular recuperation after nerve injury by crush. Furthermore, the electrical stimulation associated to stretching or not does not prevent the muscular atrophy, although it regulates muscular pathways, such as ubiquitin-proteasome, transcription factors (such as the myogenic regulatory factors), myostatin, and also the MMPs[1]. On the other hand, studies that focused in the use of intermittent stretching attenuated the muscular atrophy and the phenotype changes[8]. Therefore, in order to investigate parameters for the success or not of the therapeutic intervention, used by the rehabilitation team, pre-clinic studies are necessary.

Among the main tools used to the denervated muscle treatment, the stretching stands out or is noteworthy. The most common form of stretching used in the clinic and sports is the intermittent stretching. Most of the findings about the effects of the stretching were made in immobilization situation, but in innervated muscles[16-18]. However, the researches in the literature, that investigated the effects of intermittent stretching in the denervated muscle, are still limited. Currently, it does not exist a consensus in the literature about the effectiveness and the security of the intermittent stretching in the treatment of denervated muscle, because the results found are divergent. A possible factor that explains these discrepancies among studies is the diversity of protocols, nerve injury models and time of investigation.

Thus, considering clinically relevant thematic for the neurologic rehabilitation, the present study intends to investigate the effect of intermittent stretching on the muscular

tropism and the ECM regulation in rat denervated muscles. It is possible to hypothesize that the intermittent stretching will modify the contractile (cross sectional area, sarcomere number and size) and no contractile (connective tissue proliferation and type) muscle contents, modulating the TGF-β1/myostatin and MMPs pathways, in the rat denervated muscle.

MATERIAL AND METHODS

Animals

The laboratory animal practice was conducted according to the international standards for animal experimentation following approval by our institution Animal Care and Ethics Committee (029/2011). The animals were kept in their cages on Department of Physical Therapy, UFSCar, divided into boxes (3 animals per cage) and had free access to water and pelleted food. The vivarium was maintained at 23^0 C with controlled lighting (light/ dark cycle of 12 hours).

Experimental groups

The rats were randomly divided in 5 experimental groups (n=9 per group; Fig 1): 1) Normal (N): control animals without peripheral nerve injury and euthanized 15 days after the beginning of the experiment; 2) 7-day denervation (D 7d): animals submitted to injury by crushing of right sciatic nerve and to 3 applications of anesthesia (2, 4 and 6 days post-injury); 3) 7-day denervation and stretching (D+St 7d): animals submitted to injury by crushing of right sciatic nerve and to 3 intermittent stretching sessions with the anesthetized animal (2, 4, and 6 days post-injury). They were euthanized 7 days

after nerve injury; 4) 15-day denervation (D 15d): animals submitted to injury by crushing of right sciatic nerve and to 7 applications of anesthesia (2, 4, 6, 8, 10, 12 and 14 days post-injury), and euthanized 15 days after injury; and 5) 15-day denervation and stretching (D+St 15d): animals submitted to injury by crushing of right sciatic nerve and to 7 intermittent stretching sessions with the anesthetized animals (2, 4, 6, 8, 10, 12 and 14 days post-injury), and euthanized 15 days after injury. For more details of the procedures carried out in the experimental groups see figure 1.

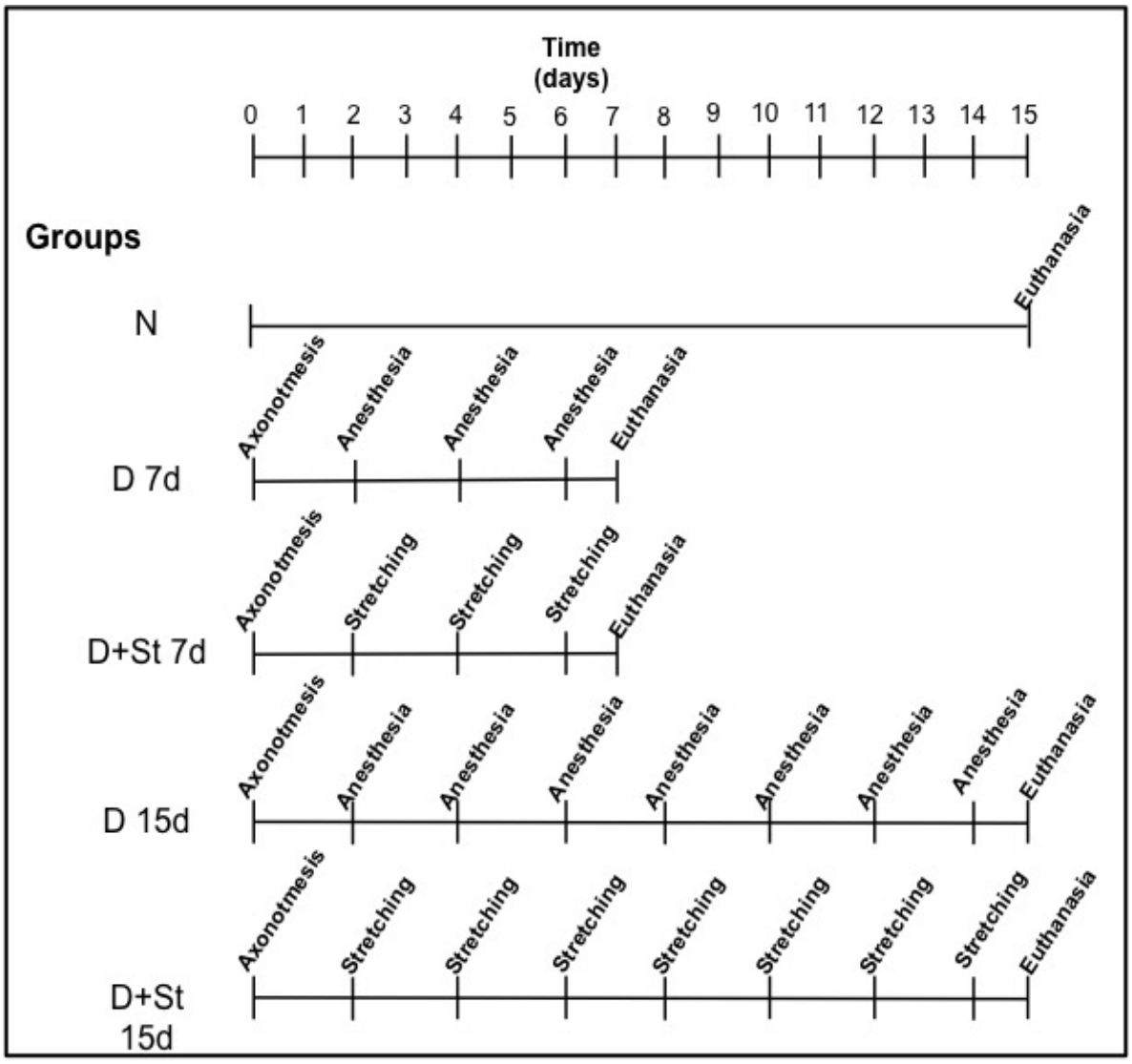

Anesthesia

The animals were anesthetized with an intraperitoneal injection of xylazine (12 mg/Kg) and ketamine (95 mg/Kg) previously to the surgical procedures of sciatic nerve injury, of the muscle removal and of the stretching. The animals of lesion groups (D 7d and D 15d) also received anesthesia to compare with the stretching groups (D+St 7d and D+St 15d). All the animals were euthanized with anesthetic overdose according to the description of the experimental groups and Figure 1.

Surgical procedures for the nerve injury

With the animals anesthetized, the skin was shaved and cleaned with 10% povidone iodine. A 2-cm long incision was made on the skin through a gluteal approach, and the right sciatic nerve was exposed. A non-serrated clamp, exerting a force of 54N, was used for a period of 30 seconds, 10 mm above the bifurcation[19, 20], to achieve good reproducibility of the axonotmetic lesion. The nerves were kept moist with sterile saline solution throughout the surgical intervention. After surgery, animals were housed in single cages and fed rat chow and water ad libitum. For four days, it was added paracetamol 750 mg (13,5 mg/100 ml) to the water for the pain reduction. A single dose of terramycin antibiotic (1 mg/0,1ml) was administered for preventing secondary complications regarding to potential infections. The sciatic injury nerve was regularly used in research for denervation of lower limb, including the soleus muscle[21, 22].

The stretching

The stretching procedures were performed as previously described[23, 24]. The right ankle was held manually in full dorsiflexion. A full dorsiflexion was considered when the paw dorsal portion touched the anterior surface of the tibia. Each session of intermittent

stretching was performed once a day and consisted of 10 series lasting 60 seconds each, with 30 second between them, when the joint were maintained free. The stretching session was performed day other day (each 48 hours; Fig. 1).

Muscle evaluation

Euthanasia of animals was in accordance with previously described (Fig. 1). The right soleus muscle was carefully dissected and removed. A small longitudinal fragment was obtained from all samples for counting the number of sarcomeres and sarcomere length. Then, muscle was divided into two parts at the middle belly. The distal fragment was used for CSA measurements as well as the immunofluorescence assay of collagen I and it was frozen in isopentane, while the proximal fragment was again divided into two parts and used for total RNA and zymography.

Count the number of sarcomeres and sarcomere length

The method used in this study to determine the number and length of sarcomeres along of a single muscle fiber was developed by Williams & Goldspink (1988)[25]. The muscle longitudinal fragment was fixed in the resting position (L length) for 3 h in 2.5% glutaraldehyde and then removed, placed in 30% HNO3 for two days, and subsequently stored in 50% glycerol.

Five individual fibers of each soleus muscle were then teased out from tendon to tendon and mounted and their length was measured using a caliper rule. The number and length of the sarcomeres along 100 μm distance were quantified at different points of the middle region of each single fiber using a projection microscope (Axiolab, Carl Zeiss, Oberkochen, Germany). The total number of sarcomeres in each single muscle fiber was

determined by the correlation between the number of sarcomeres identified along a distance of 300 μm and the total fiber length. The number and the length of sarcomeres in series, over 100 μm, was quantified in each photo using the software (Axiovision 3.0.6 SP4, Carl Zeiss).

Morphological and morphometric analysis

Serial cross-sections (10 μm) were then obtained from the middle belly frozen soleus muscle using a microtome cryostat (HM 505E, Microm, Walldorf, Germany). The sections were stained with the Masson to evaluated the fibers general morphological and the cross-sections. For morphometric evaluation, 100 muscle fibers were randomly measured from photomicrographs obtained of central region of muscle belly second recent methodology[5, 26].

Futhermore, it was evaluated the density connective tissue and identification of possible areas of fibrosis. For analysis of intramuscular connective tissue, a planimetry system was used with scoring points, and the quantification was accomplished by means of a reticulum with total area of 2500 μm^2, containing 56 straight-line intersections. The percent connective tissue density of the connective tissue was calculated by dividing the sum of the number of coincident points in the straight-line intersections in the connective tissue (endomysium and perimysium) by the total number of points. This analysis was realized in 5 areas per slice, including 5 slices per animal, totaling 1400 points per animal.

Immunofluorescence Analysis

The antibodies used for immunofluorescence for collagen I: monoclonal mouse anti-collagen I (1:100 dilution, catalog no. C2456; Sigma-Aldrich, St. Louis, MO, USA) and the secondary antibody was Alexa Fluor 488 goat anti-mouse IgG, IgA, IgM (1:300 dilution, catalog no. A10667; Molecular Probes, Eugene, OR). The sections were fixed with 4% paraformaldehyde (Sigma P6148) in 0.2 M phosphate buffer (PB) for 10 min at room temperature, blocked with 0.1 M glycine in PB for 5 min, and permeabilized in 0.2% Triton X-100-PB for 10 min. Subsequently, the sections were incubated in 1% bovine serum albumin (BSA) for 20 min at room temperature to block nonspecific binding and incubated with respective primary antibody (diluted in 1% BSA) overnight at 4°C. After the slides were washed with 0.1 M PB (3 times for 10 min each), they were incubated with respective secondary antibody (diluted in 1% BSA) for 2 h in a dark room. Slides were washed in 0.1 M PB (3 times for 10 min each) with Hoescht, to mark nuclei, and then mounted with Vectashield mounting medium (catalogue no. H-1200; Vector Laboratories). Negative control sections were not incubated with the primary antibody and experimental results were considered only if these controls did not show immunoreactivity. Analyses were performed by obtaining photomicrographs (20x magnification) of the stained sections using a fluorescence microscope (Axiolab, Carl Zeiss, Jena, Germany) and a digital camera (Sony DSC s75, Tokyo, Japan).

Analysis of the activity of MMPs

The MMPs activity was evaluated by zymography technique. Muscle fragments was processed as previously described[2, 5]. The molecular mass of gelatinase activity of each band was determined by compared to a marker of protein molecular mass (PageRuler

Prestained Protein Ladder; Fermentas Life Sciences, Burlington, Ontário). The bands activity was identified according to their molecular weights (72 kDa: pro-MMP-2; 64 kDa: intermediary-MMP-2; 57 kDa: MMP-2 active; 92 kDa: pro-MMP-9; 81 kDa: MMP-9 ative). Densitometric quantitative analysis of proteins bands in zymography was realized using the software GeneTools v3.06 (Syngene, Cambridge, UK).

Extraction of total RNA

One frozen fragment of each muscle was homogenized, and the total RNA was isolated using the Trizol reagent (Invitrogen, Carlsbad, CA, USA) according to the manufacturer's instructions. The extracted RNA was dissolved in Tris–HCl and ethylene diaminetetracetic acid (TE) pH 7.6. The extracted RNA purity was determined spectrophotometrically at 260 and 280 nm (ratios were between 1.8 and 2.0) and by ethidium bromide staining (Invitrogen). Has also evaluated the quality of the material by electrophoresis of samples (2 μg of total RNA) in denaturing agarose gel formamide (1%), in buffer MOPS (40 mM of morfolinopropanosulfônico acid). Posteriorly, the gel was stained with ethidium bromide.

RT-PCR (**Reverse Transcription-Polymerase Chain Reaction)**

One microgram of total RNA was used to synthesize cDNA. The reaction was performed with different volumes of total RNA (200 U of reverse transcriptase); 0.8 mM dNTPs; 1 mM MgCl2; 0.02 mg/ml primer oligo dT; 4 mM of DTT. Reverse transcription was performed at 70ºC for 10 minutes, followed by incubation at 42ºC for 60 minutes and at 94ºC for 10 minutes. The integrity of RT product (cDNAs) was confirmed through non-denaturing agarose gel, stained with ethidium bromide.

Real time PCR

The PCR amplifications were performed using 10– 80 ng/μl of cDNA added to a reaction containing 25 μl of SYBR Green PCR master mix and 50–900 nM of primers (sense and anti-sense) in a solution with 55 μl of total volume, divided into two tubes (duplicate). The cycling conditions to target genes were performed following each primer standard. Data were analyzed using the comparative cycle threshold (Ct) method and described by the manufacturer. GAPDH was considered as control gene. A blank with no template sample but just water, primers and SYBR green was also performed.

Oligonucleotide Primers

The oligonucleotide primers of PCR in real time GAPDH, MMP-2, MMP-9, TIMP-1, TGF-β1 and myostatin are described below (Table 1):

TABLE 1

Statistics

The data were subjected to homogeneity testing (Levene) and normality (Shapiro-Wilk). In the case of data parametric, the Anova one-way test was used to detect the presence of difference between the groups. In the case of difference, the test of Tukey was applied for locate these differences. A significance level of 5% was considered.

RESULTS

The Masson´staining was used to verify the general skeletal muscle morphology (Fig. 2). Normal groups showed polygonal muscle fibers, with peripheral nuclei and connective tissue around fibers. All denervated groups presented atrophied and rounded muscle fibers (Fig. 2). Furthermore, increased connective tissue was observed in the perimysium of denervated groups compared to N (Fig. 2). This increase is more evident on the D+ST 15d compared to the other denervated groups (Fig. 2).

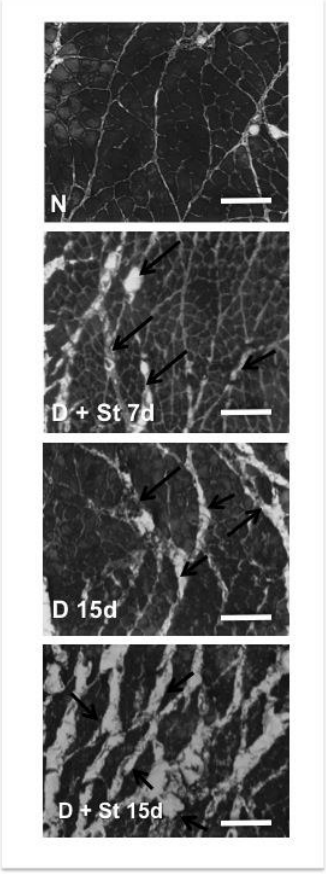

Representative photomicrografies of type I collagen (green) and nuclei (blue) can be observed on Fig. 3. Connective tissue proliferation is followed by increasing of collagen I content, mainly in the endomysium and perimysium of denervated muscles, compared to innervated ones (N; Fig. 3).

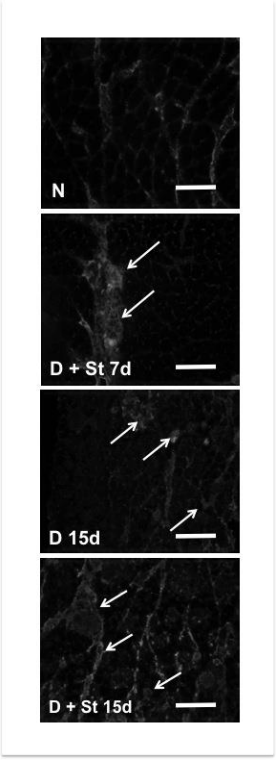

Regarding sarcomere structure, neither the serial number nor the length was altered in denervated groups compared to N ($p>0.05$, Fig. 4A and B). All denervated groups (D7d, D+St7d, D15d e D+St15d) showed muscle atrophy (reduction of muscle fiber cross-sectional area) compared to N ($p<0.05$; Fig. 4C), with no difference amongst denervated groups ($p>0.05$; Fig. 4C). The 4D figure presents the connective tissue density of the experimental groups. There was an increase of density connective tissue in the D7d and D+St7d groups compared to N ($p<0.05$), but with no difference between them ($p>0.05$; Fig. 4D). In addition, D+St 15d showed an increase of connective tissue proliferation compared to D 15d and N ($p<0.05$; Fig. 4D).

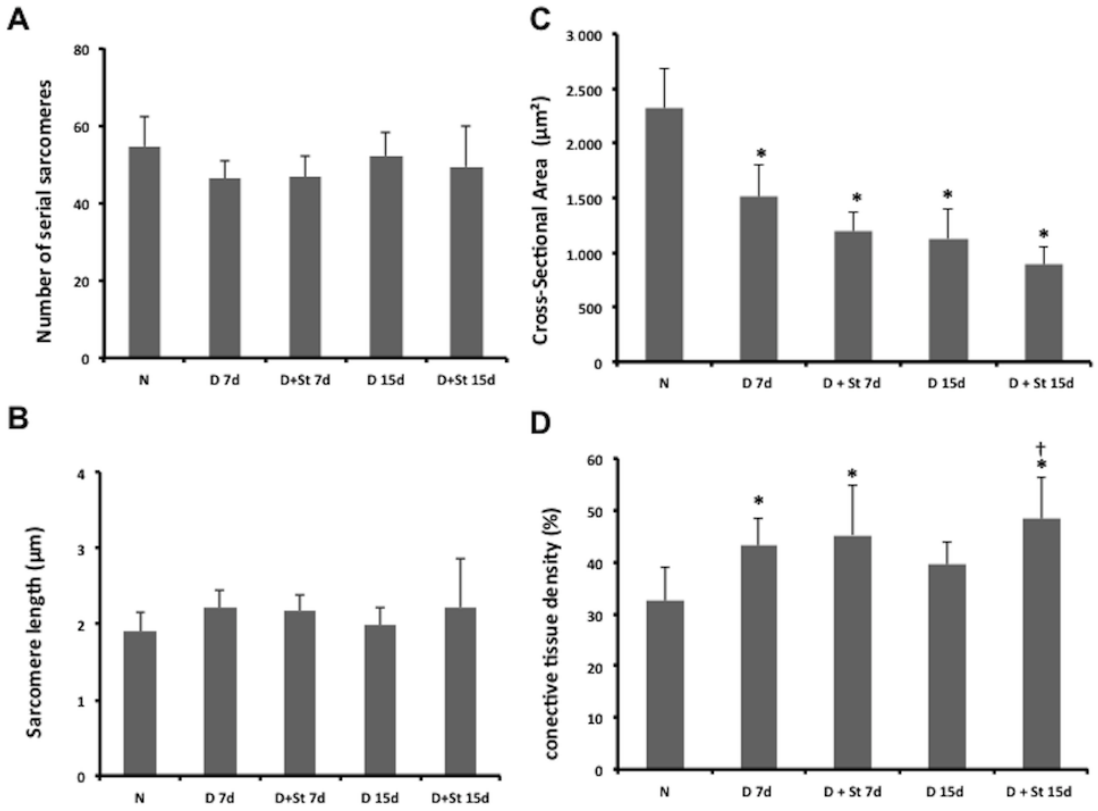

Regarding the gene expression of MMP-2, -9 and TIMP-1, it was observed that: for MMP-2: D 15d presented up-regulation of MMP-2 compared to the others ($p<0.05$; Fig. 5A); for MMP-9: an increase of MMP-9 was observed on D+St 7d compared to the others ($p<0.05$; Fig. 5A); and for TIMP-1: both D 15d and D+St 15d presented an up-regulation of TIMP-1 compared to N ($p=0,05$ and $p=0,04$, respectively; Fig. 5A). About zymography, the MMP-9 activity was not identified in any of the experimental groups (data not showed). On the other hand, 3 well defined bands of MMP-2 were observed (72 KDa – pro-MMP-2; 64 KDa – intermediary MMP-2; and 57 KDa – active MMP-2; Fig. 6B). The densitometric analysis of MMP-2 activity did not show any difference among the bands and also the experimental groups ($p>0.05$; Fig. 5C).

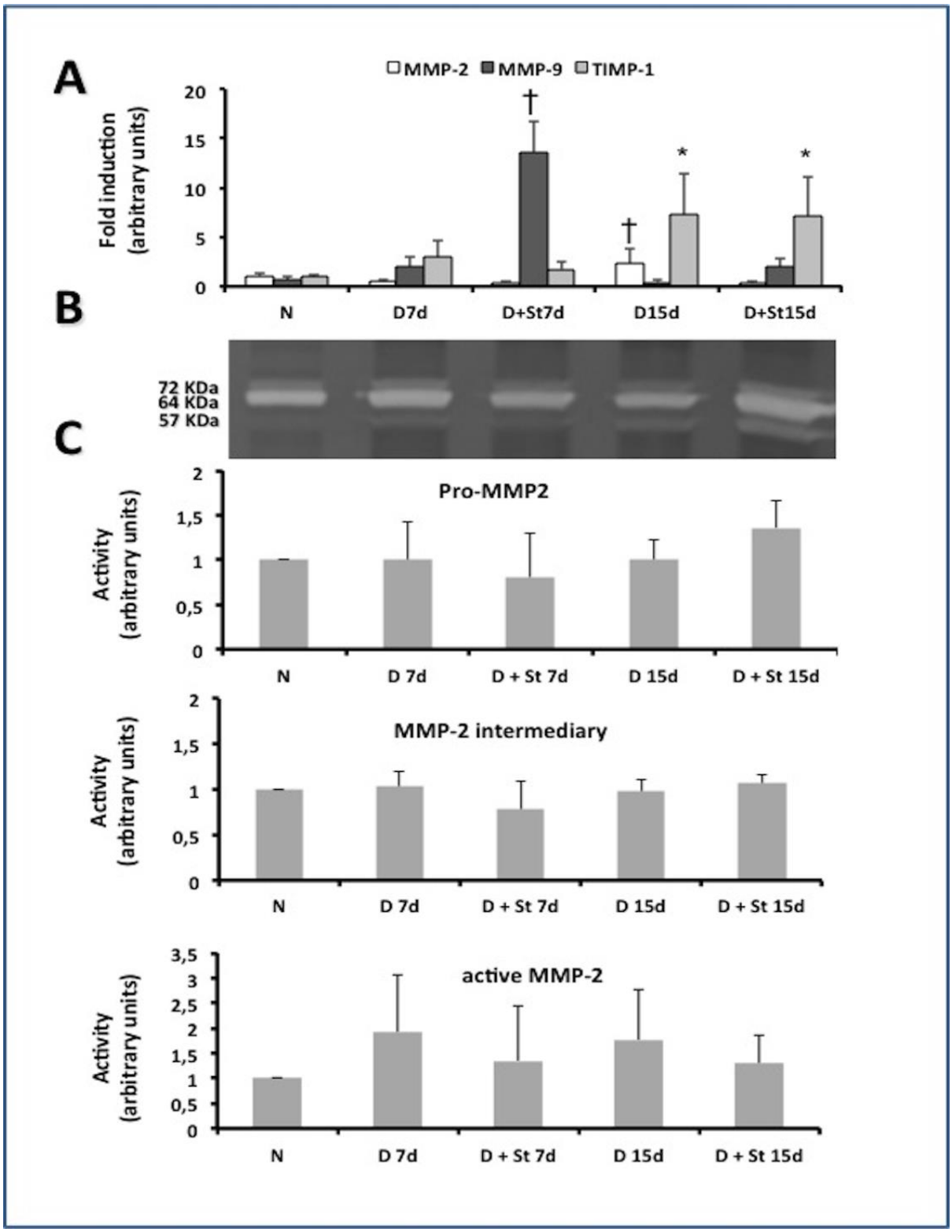
A
MMP-2
MMP-9
TIMP-1
Fold induction (arbitrary units)
20
15
10
5
0
†
†
*
*
N
D7d
D+St7d
D15d
D+St15d
B
72 KDa
64 KDa
57 KDa
C
Pro-MMP2
Activity (arbitrary units)
2
1,5
1
0,5
0
N
D 7d
D + St 7d
D 15d
D + St 15d
MMP-2 intermediary
Activity (arbitrary units)
2
1,5
1
0,5
0
N
D 7d
D + St 7d
D 15d
D + St 15d
active MMP-2
Activity (arbitrary units)
3,5
3
2,5
2
1,5
1
0,5
0
N
D 7d
D + St 7d
D 15d
D + St 15d

An increase of TGF-β1 gene expression was observed on D+St 7d compared to the other experimental groups ($p<0.05$; Fig. 6A). Myostatin was increased on D+St 15d compared to the other groups ($p<0.05$; Fig. 6B).

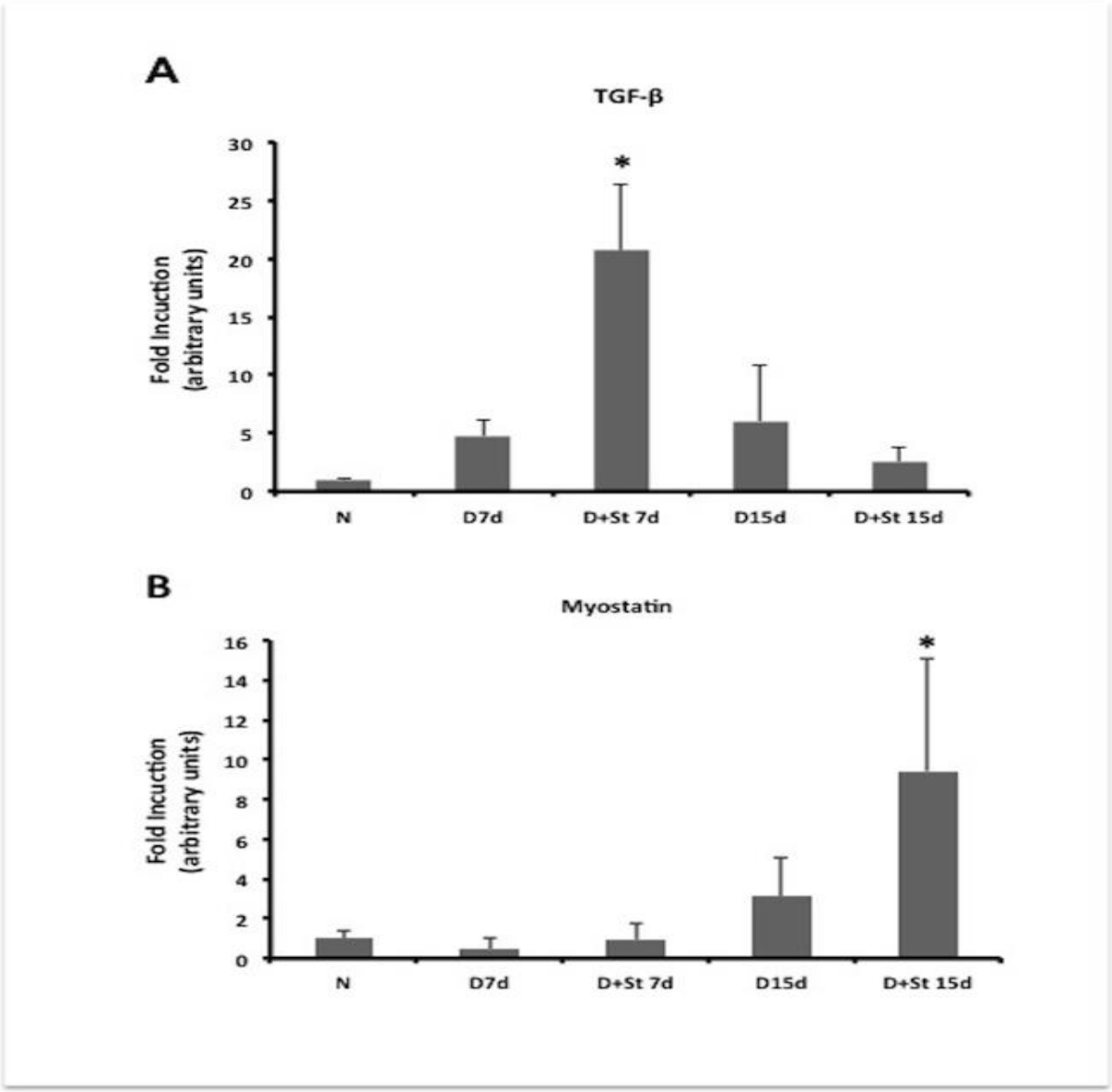

DISCUSSION

The present study showed new evidence about intermittent stretching applied in denervated muscles. It was demonstrated that stretching activated MMP-9, TGF-β1 and myostatin gene expressions, increased the proliferation of connective tissue, but did neither avoid muscle fiber atrophy nor induce sarcomerogesis of denervated soleus muscle of rat. These results showed that more studies should be conducted on this thematic, comparing different protocols of stretching, time of injury and type of muscle to support the safety of this procedure on the clinical practice.

Regarding the intermittent stretching parameters, time of resting between each stretching repetition seems to be relevant to muscle adaptation. For example, Stauber and Williems[27] performed stretching during plantar flexor muscle contractions (eccentric contractions) and varied the time rest between each stretching. A total of 30 stretching repetitions (around 600 ms each) were performed, considering either 40 s or 180 s time rest between each repetition. They observed that short inter-stretch rest time (40 s) damaged muscle fibers, increased inflammatory infiltration inside necrotic muscle fibers. On the other hand, long inter-stretch rest time (180 s) did not cause any histopathologic changes on muscles. In addition, both short and long times decreased muscle tension, compared to control group. The authors discussed that calcium-related pathways could be involved in this problem, but it is also possible to speculate that changes on extracellular matrix, such as, collagen reorganization could contribute to muscle tension decrease.

Agata et al.[28] performed manual intermittent stretching procedures of soleus muscle very similar to the present study. However, they differed regarding the number of stretching repetitions, the stretching time, and also the inter-stretching rest time. For

example, Agata et al.[28] performed 180 stretching repetitions (during 15 min with around 5 seconds of rest between each stretching repetition), 6 times a week, during 2 weeks, while the present study did 10 stretching repetitions of 60 s each and 30 s of time rest, day other day, during 7 or 15 days. While Agata et al.[28] observed that the stretching protocol reduced muscle fiber atrophy (around 42% compared to denervated control groups), via activation of protein synthesis pathways, such as Akt/mTOR/p70S6K or 4E-BP1 cascades, the present results showed an increase of connective tissue proliferation via TGF-β1/myostatin pathway.

Thus, to interpret the present results it is important to consider the previous information[27, 28]. It is possible to hypothesize that inter-stretching rest time is a key parameter to improve or to damage muscles submitted to stretching. Long inter-stretching rest times seem to be more protective to muscle than short ones. The present study considered the amount of 30 s of resting between each stretching repetition (60 s), this represents the relation of 1:2. On the other hand, Agata et al.[28] performed protocols probably with the relation of 5:1 or less (e.g., 5 s of resting and 1s or less of stretching). Other important aspect is related to the number of stretching sessions. Day other day sessions of stretching seems to be less effective than when performed daily[28]. Future studies should consider investigating these aspects in detail to confirm the presented hypotheses.

Previous data[1, 2] of the effects of intermittent stretching on denervated tibialis anterior muscle showed that 4 stretching repetitions of 3,2 min each one, with 10 min rest between each repetition, applied daily during 6 days, increased MMP-2 gene expression and activity, and decreased the expression of genes related to atrophy (atrogin-1 and MuRF-1) and mass regulation (myostatin). However, stretching did not avoid or delay muscle atrophy. No signals of muscle degeneration of reduction of

reinnervation factors were observed. It is possible to note that time rest between stretching can affect differently muscles, according their composition and function, e.g., soleus[28] versus tibialis anterior muscles[1, 29].

It is also important to discuss the different effects between intermittent and short duration static stretching protocols. Sakakima and Yoshida[8] stretched soleus muscle with taping during 40 min, 6 times week, during 1, 2, 3 or 4 weeks. They found that stretching maintained type I muscle fiber cross sectional area until 2 weeks, but did not after 3 or 4 weeks of denervation. It also reduced muscle fiber shift from I to II at 3 weeks of denervation. This data showed that static stretching could delay muscle atrophy and phenotype shift due to denervation.

Data from immobilized muscles submitted to stretch can also help to understand how the longitudinal tension can affect muscle adaptation. Mattiello-Sverzut et al.[30] showed that intermittent stretching (10 repetitions of 15 seconds, with 30 s of resting) applied during 10 consecutive days in post-immobilization soleus muscles increased the proliferation of connective tissue. On the other hand, static stretching (40 min), applied once a week or three times a week, during 3 weeks of immobilization, damaged sarcomere structure[31]. All together it is possible to hypothesize that stretching can affect the sarcomere structure, mainly by disrupting the Z line, and this alteration can trigger connective tissue proliferation, which can be interpreted as a protective mechanism to avoid more damage of immobilized muscles.

Regarding the present data, it is observed that stretching did not induce sarcomerogenesis. Probably the period of two weeks was not enough to observe such modification. Salvini et al.[18] stretched soleus muscles; which were under immobilization for 4 weeks; three times per week during 3 weeks. The protocol of

stretching was similar to the present one, e.g., 10 stretching bouts, each maintained for 1 min, with 30 s rest intervals between bouts of stretching. They found that this amount of stretching was able to increase muscular length and number of serial sarcomeres after 3 weeks[18]. On the other hand, no improvement on collagen organization was observed with this protocol[24].

The proliferation of tissue connective observed in the present study might be related to the up-regulation of genes related to inflammatory process (MMP-9), and ECM remodeling, such as TGF-β1/myostatin pathway. The role of TGF-β1 and myostatin to induce muscle fibrosis were reviewed before (see Burks and Cohn, 2011)[12]. Persistent exposure to the inflammatory response leads to an altered ECM and increased levels of growth factors and cytokines, including TGF-β1, contributing to the formation of fibrotic tissue via transforming myoblasts into fibrotic tissue and inhibiting satellite cell activation and impairing myocyte differentiation. Furthermore, once fibroblasts are within the environment of the injured muscle, they express myostatin and differentiate into myofibroblasts, a process that in turn accelerates the deposition of collagen and connective tissue, ultimately promoting the formation of tissue fibrosis. Furthermore, myostatin inhibits the activation, differentiation, and self-renewal of satellite cells and the expression of the muscle regulatory factors (for review see Burks and Cohn, 2011)[12].

Bouffard et al.[32] provided relevant information about the TGF-β1 regulation due to stretching. They found that tissue stretching attenuated the increase of soluble TGF-β1 and type-1 procollagen following subcutaneous connective tissue injury. They also proposed that brief stretching of tissue beyond the habitual range of motion can decrease fibrotic response, less collagen deposition, and reduce tissue adhesion. On the other hand, Gutierrez and Perr[33] showed that 18 hours of tonic stretch increases TGF-

β1 and α-1 (I) collagen in primary cultures of human fetal intestinal mooth muscle cells. It seems that TGF-β1 can be affected by stretching according to time and in a tissue-specific manner.

MMP-9 is a well-known mediator of the inflammatory response in skeletal muscle and ECM remodeling. It has already been described that collagen IV from basal lamin, and components of dystrophin-glicoprotein complex of muscle membram are target of MMP-9[34]. Furthermore, MMP-9 was implicated to cause the activation of latent TGF-β1 into mature form, thus increasing fibrosis in dystrophic muscles[35]. Li et al.[34, 35] also showed that mdx animals with MMP-9 knockout presented less atrophy, necrotic fibers and inflammation cells. The inhibition of MMP-9 also increases the number of satellite cells, via stimulation of Notch and canonical Wnt signaling in mdx animals[36].

Ozawa et al.[14] investigated the regulation of connective tissue remodeling the early phase of soleus muscle denervation. Using a severe nerve injury (neurotmesis) they found that connective tissue proliferation (fibrosis) and muscle fiber atrophy increased progressively throughout 2 weeks of denevertation. Collagen I and III increased their content in the endomysium and perimysion compared to control. TGF-β1 protein content was increased at 14 days of denervation compared to control. Regarding the MMP family, MMP-2 and TIMP-1 did not present any difference on gene expression due to denervation. The author supported the idea that TGF-β1 might be active in stimulating collagen synthesis as well as inhibiting collagen degradation.

Interpreting our results, TIMP-1 upregulation observed on D15d group probably occurred to regulate MMP-2 expression, and to control the ECM turnover. On the other hand, the increase of TIMP-1 expression on D+St15d is observed in response to the MMP-9 upregulation that occurred at day 7 (D+St7d). In addition, the increase of

MMP-9 expression observed on D+St7d might also be related to activation of TGF-β1 /myostatin cascade on day 7 and 15, respectively.

Briefly, some rational aspects about how stretching could generate fibrosis in denervated muscle is presented here. Stretching probably can disrupt mechanically sarcomere integrity (Anna Raquel), disturb calcium homeostasis (Stauber), and activate inflammatory process, via MMP-9, according to the time rest between each repetition. MMP-9 probably activates TGF-β1/myostatin pathway causing fibrosis (Li 2009).

This study has some few limitations: the mechanical tension applied during stretching was not controlled, trying to mimic the clinical practice. Furthermore, just one type of muscle was investigated and no analysis regarding muscle reinnervation was performed, therefore the results should be generalized neither for different muscles nor for the reinnervation process. Future studies are still necessary to investigate different protocols of stretching in denervated muscles to ensure the safety and effectiveness of this procedure.

In conclusion, intermittent stretching increased connective tissue via activation of MMP-9, TGF-β1 and myostatin gene expressions, with no prevention of muscle fiber atrophy or sarcomeregenesis in denervated muscle of rats.

ABBREVIATIONS

D – Denervated

ECM – Extracellular matrix

MMPs – Matrix Metaloproteinases

N – Normal

PNI – Peripheral nerve injury

St – Stretching

TGF-β1 – Transforming growth factor-beta 1

TIMP – Metaloproteinases inhibiting tissue

REFERENCES

1. Russo, T. L.; Peviani, S. M.; Durigan, J. L.; Gigo-Benato, D.; Delfino, G. B.; Salvini, T. F. Stretching and electrical stimulation reduce the accumulation of MyoD, myostatin and atrogin-1 in denervated rat skeletal muscle, *Journal of muscle research and cell motility*. **2010, *31,*** 45-57.

2. Peviani, S.; Gomes, A.; de Araujo, H. S.; Salvini, T. MMP-2 is not altered by stretching in skeletal muscle, *International journal of sports medicine*. **2009, *30,*** 550-554.

3. Bodine, S. C.; Stitt, T. N.; Gonzalez, M., et al. Akt/mTOR pathway is a crucial regulator of skeletal muscle hypertrophy and can prevent muscle atrophy in vivo, *Nature cell biology*. **2001, *3,*** 1014-1019.

4. Dow, D. E.; Cederna, P. S.; Hassett, C. A.; Kostrominova, T. Y.; Faulkner, J. A.; Dennis, R. G. Number of contractions to maintain mass and force of a denervated rat muscle, *Muscle & nerve*. **2004, *30,*** 77-86.

5. Russo, T. L.; Peviani, S. M.; Durigan, J. L. Q.; Salvini, T. F. Electrical stimulation increases matrix metalloproteinase-2 gene expression but does not change its activity in denervated rat muscle, *Muscle & nerve*. **2008,** ***37,*** 593-600.

6. Lieber, R. L. *Skeletal muscle structure, function, and plasticity*: Lippincott Williams & Wilkins Baltimore, MD:, 2009.

7. Kurose, T.; Asai, Y.; Mori, E.; Daitoku, D.; Kawamata, S. Distribution and change of collagen types I and III and elastin in developing leg muscle in rat, *Hiroshima journal of medical sciences*. **2006,** ***55,*** 85-91.

8. Sakakima, H.; Yoshida, Y. Effects of short duration static stretching on the denervated and reinnervated soleus muscle morphology in the rat, *Archives of physical medicine and rehabilitation*. **2003,** ***84,*** 1339-1342.

9. Bodine, S. C.; Latres, E.; Baumhueter, S., et al. Identification of ubiquitin ligases required for skeletal muscle atrophy, *Science*. **2001,** ***294,*** 1704-1708.

10. Glass, D. J. Molecular mechanisms modulating muscle mass, *Trends in molecular medicine*. **2003,** ***9,*** 344-350.

11. Zhang, D.; Liu, M.; Ding, F.; Gu, X. Expression of myostatin RNA transcript and protein in gastrocnemius muscle of rats after sciatic nerve resection, *Journal of Muscle Research & Cell Motility*. **2006,** ***27,*** 37-44.

12. Burks, T. N.; Cohn, R. D. Role of TGF-beta signaling in inherited and acquired myopathies, *Skeletal muscle*. **2011,** ***1,*** 19.

13. Demestre, M.; Orth, M.; Wells, G.; Gearing, A.; Hughes, R.; Gregson, N. Characterization of matrix metalloproteinases in denervated muscle, *Neuropathology and applied neurobiology*. **2005,** ***31,*** 545-555.

14. Ozawa, J.; Kurose, T.; Kawamata, S.; Kaneguchi, A.; Moriyama, H.; Kito, N. Regulation of connective tissue remodeling in the early phase of denervation in a rat skeletal muscle, *Biomedical Research*. **2013,** ***34,*** 251-258.

15. Gigo- Benato, D.; Russo, T. L.; Geuna, S.; Domingues, N. R. S. R.; Salvini, T. F.; Parizotto, N. A. Electrical stimulation impairs early functional recovery and accentuates skeletal muscle atrophy after sciatic nerve crush injury in rats, *Muscle & nerve*. **2010,** ***41,*** 685-693.

16. Goldspink, G.; Williams, P.; Simpson, H. Gene expression in response to muscle stretch, *Clinical orthopaedics and related research*. **2002,** ***403,*** S146-S152.

17. Goldspink, G. Changes in muscle mass and phenotype and the expression of autocrine and systemic growth factors by muscle in response to stretch and overload, *J Anat*. **1999,** ***194 (Pt 3),*** 323-334.

18. Salvini, T. F.; Coutinho, E. L.; Russo, T. L.; DeLuca, C. One-minute bouts of passive stretching after immobilization increase sarcomerogenesis in rat soleus muscle, *Braz J Morphol Sci*. **2006,** ***23,*** 271-277.

19. Varejão, A. S.; Cabrita, A. M.; Meek, M. F., et al. Functional and morphological assessment of a standardized rat sciatic nerve crush injury with a non-serrated clamp, *Journal of neurotrauma*. **2004,** ***21,*** 1652-1670.

20. Beer, G. M.; Steurer, J.; Meyer, V. E. Standardizing nerve crushes with a non-serrated clamp, *Journal of reconstructive microsurgery*. **2001, *17,*** 531-534.

21. Jungnickel, J.; Haase, K.; Konitzer, J.; Timmer, M.; Grothe, C. Faster nerve regeneration after sciatic nerve injury in mice over-expressing basic fibroblast growth factor, *Journal of neurobiology*. **2006, *66,*** 940-948.

22. Seo, T. B.; Han, I. S.; Yoon, J. H.; Hong, K. E.; Yoon, S. J.; Namgung, U. Involvement of Cdc2 in axonal regeneration enhanced by exercise training in rats, *Med Sci Sports Exerc*. **2006, *38,*** 1267-1276.

23. Peviani, S. M.; Gomes, A. R. S.; Moreira, R. F. C.; Moriscot, A. S.; Salvini, T. F. Short bouts of stretching increase myo-D, myostatin and atrogin-1 in rat soleus muscle, *Muscle & nerve*. **2007, *35,*** 363-370.

24. Coutinho, E. L.; DeLuca, C.; Salvini, T. F.; Vidal, B. C. Bouts of passive stretching after immobilization of the rat soleus muscle increase collagen macromolecular organization and muscle fiber area, *Connective tissue research*. **2006, *47,*** 278-286.

25. Williams, P. E.; Catanese, T.; Lucey, E. G.; Goldspink, G. The importance of stretch and contractile activity in the prevention of connective tissue accumulation in muscle, *J Anat*. **1988, *158,*** 109-114.

26. Russo, T. L.; Peviani, S. M.; Freria, C. M.; Gigo-Benato, D.; Geuna, S.; Salvini, T. F. Electrical stimulation based on chronaxie reduces atrogin-1 and myoD gene expressions in denervated rat muscle, *Muscle & nerve*. **2007, *35,*** 87-97.

27. Stauber, W. T.; Willems, M. E. Prevention of histopathologic changes from 30 repeated stretches of active rat skeletal muscles by long inter-stretch rest times, *European journal of applied physiology*. **2002, *88,*** 94-99.

28. Agata, N.; Sasai, N.; Inoue-Miyazu, M., et al. Repetitive stretch suppresses denervation-induced atrophy of soleus muscle in rats, *Muscle & nerve*. **2009, *39,*** 456-462.

29. Peviani, S. M.; Russo, T. L.; Durigan, J. L., et al. Stretching and electrical stimulation regulate the metalloproteinase-2 in rat denervated skeletal muscle, *Neurological research*. **2010, *32,*** 891-896.

30. Mattiello-Sverzut, A.; Carvalho, L.; Cornachione, A.; Nagashima, M.; Neder, L.; Shimano, A. Morphological effects of electrical stimulation and intermittent muscle stretch after immobilization in soleus muscle. **2006**.

31. Gomes, A. R.; Cornachione, A.; Salvini, T. F.; Mattiello-Sverzut, A. C. Morphological effects of two protocols of passive stretch over the immobilized rat soleus muscle, *Journal of anatomy*. **2007, *210,*** 328-335.

32. Bouffard, N. A.; Cutroneo, K. R.; Badger, G. J., et al. Tissue stretch decreases soluble TGF-beta1 and type-1 procollagen in mouse subcutaneous connective tissue: evidence from ex vivo and in vivo models, *J Cell Physiol*. **2008, *214,*** 389-395.

33. Gutierrez, J.; Perr, H. Mechanical stretch modulates TGF-b1 and a1 (I) collagen expression in fetal human intestinal smooth muscle cells, *American Journal of Physiology-Gastrointestinal and Liver Physiology*. **1999, *40,*** G1074.

34. Li, H.; Mittal, A.; Paul, P. K., et al. Tumor Necrosis Factor-related Weak Inducer of Apoptosis Augments Matrix Metalloproteinase 9 (MMP-9) Production in Skeletal Muscle through the Activation of Nuclear Factor-κB-inducing Kinase and p38 Mitogen-activated Protein Kinase A POTENTIAL ROLE OF MMP-9 IN MYOPATHY, *Journal of Biological Chemistry*. **2009*, 284,*** 4439-4450.

35. Li, H.; Mittal, A.; Makonchuk, D. Y.; Bhatnagar, S.; Kumar, A. Matrix metalloproteinase-9 inhibition ameliorates pathogenesis and improves skeletal muscle regeneration in muscular dystrophy, *Human molecular genetics*. **2009*, 18,*** 2584-2598.

36. Hindi, S. M.; Shin, J.; Ogura, Y.; Li, H.; Kumar, A. Matrix metalloproteinase-9 inhibition improves proliferation and engraftment of myogenic cells in dystrophic muscle of mdx mice, *PloS one*. **2013, *8,*** e72121.

LEGEND

Figure 1. Diagram of the experimental groups. In the upper part of the figure, it is shown a time line and in the middle and lower portion the experimental groups and the procedures performed over time.

Figure 2. Photomicrographs of experimental groups stained with Masson's Trichrome. N: Normal group; D + St 7d: rats denervated and stretched 7 days; D 15d: rats denervated for period of 15 days; and D + St 15d: rats denervated and stretched for period of 15 days. Black arrows show increase of total collagen in the perimysium. Bar: 50 μm.

Figure 3. Representative photomicrographs of Type I collagen and nuclei of experimental groups. N: Normal group; D + St 7d: rats denervated end stretched for period of 7 days; D 15d: rats denervated for period of 15 days; and D + St 15d: rats denervated and stretched for period of 15 days. White arrows show collagen I accumulation in the perimysium. Bar: 50 μm.

Figure 4. Muscle morphometric analyses. (A) number of serial sarcomeres, (B) sarcomeres length, (C) Muscle fiber cross-sectional area and (D) connective tissue density. N: normal group; D 7d and D 15d: denervated groups submitted to crush nerve injury and analyzed 7 or 15 days post-injury, respectively; and D+St 7d and D+St 15d: denervated groups submitted to stretching day other day during 7 or 15 days. *$p<0.05$: compared to N; †$p<0.05$ compared to D 15d.

Figure 5. MMPs and TIMP-1 gene expressions and zymography. N: normal group; D 7d and D 15d: denervated groups submitted to crush nerve injury and analyzed 7 or 15 days post-injury, respectively; and D+St 7d and D+St 15d: denervated groups submitted to stretching day other day during 7 or 15 days. (A) MMP-2, -9 and TIMP-1 mRNA levels are presented. *p<0.05 compared to N; ‡ (B) Representative MMP-2 Graphics associated with the molecular mass of gelatinase activity of each band of the gene expression of MMP-2, -9 and TIMP-1. (C) MMP-2 isoforms activity. N: normal group; D 7d and D 15d: denervated groups submitted to crush nerve injury and analyzed 7 or 15 days post-injury, respectively; and D+St 7d and D+St 15d: denervated groups submitted to stretching day other day during 7 or 15 days. Note an increase of MMP-9 and MMP-2 gene expressions in D+St 7d and D 15d, respectively. Furthermore, TIMP-1 gene expression was increased in both D 15d and D+St 15d.

Figure 6. TGF-β1 and myostatin gene expressions. N: normal group; D 7d and D 15d: denervated groups submitted to crush nerve injury and analyzed 7 or 15 days post-injury, respectively; and D+St 7d and D+St 15d: denervated groups submitted to stretching day other day during 7 or 15 days. *p<0.05 compared to the other groups. Note stretching increased TGF-β1 and myostatin mRNA levels at day-7 and -15, respectively.

ANEXOS

Title:

Low leval laser therapy modulates neurotrophin and matrix metalloproteinase expression in nerves and muscles after axonotmesis in rats.

Authors:

Davilene Gigo-Benato[1,2], PhD, Andriette Camilo Turi[1], MS, Carolina Carmona Alcântara[1], MS, Thaianne Silva Mata[1], Livia Gaspar Fernandes[1], Juanita J Anders[3], PhD, Tania Fátima Salvini[2], PhD, Alexandre Rodrigues Leite Oliveira[4], PhD, Fernanda Maria Faturi[2], PhD, Thiago Luiz Russo[1], PhD.

Affiliations:

[1]Laboratory of Neurological Physiotherapy Research, Physical Therapy Department, Federal University of São Carlos (UFSCar), São Carlos, SP, zip code: 13565-905, Brazil (DGB, ACT, CCA, TSM, LGF, TLR).

[2]Skeletal Muscle Plasticity Unit, Physical Therapy Department, Federal University of São Carlos (UFSCar), São Carlos, SP, zip code: 13565-905, Brazil (DGB, TFS, FMT).

[3]Department of Anatomy, Physiology and Genetics, Uniformed Services University of the Health Sciences, Bethesda, MD 20814, USA (JJA).

[4]Department of Anatomy, Cell Biology, Physiology and Biophysics-Institute of Biology, University of Campinas (UNICAMP), Campinas, SP, zip code: 13083-865 Brazil (ALRO).

Running title: Laser therapy and peripheral nerve injury

Corresponding author: Prof. Thiago Luiz Russo, Departamento de Fisioterapia, Universidade Federal de São Carlos (UFSCar), Rodovia Washington Luís km 235, C.P. 676 – CEP: 13565-905 São Carlos, SP, Brazil; Phone: 00 55 16 33518345 FAX: 00 55 16 33612081; E-mail: thiagoluizrusso@gmail.com

ABSTRACT

Background and Objectives: Functional recovery after peripheral nerve injuries (PNI) remains a challenge for rehabilitation specialists. There is convincing evidence that photobiomodulation (PBM) supports post-traumatic peripheral nerve repair and prevents muscle atrophy. However, the mechanisms responsible for these positive outcomes are not fully understood. The aim of this study was to evaluate the temporal effects of a PBM protocol on excitability, morphology and expression and content of neurotrophins (BDNF and NT-4), matrix metalloproteinases (MMP-2 and MMP-9) and their inhibitors (TIMP-1) in rat nerves and muscles after crush injury. **Materials and Methods:** The irradiation parameters were: continuous wave, wavelength: 660 nm, power: 40 mW, energy density on the skin surface: 60J/cm^2, energy per point: 24 J, treatment time: 1 minute per point at two points. Evaluations were performed at 7, 15 and 21 days post-PNI. **Results:** PBM normalized neuromuscular excitability at 21 days post-injury. MMP-2 expression and activity increased at 7 days post-injury in irradiated nerves with a concomitant decrease in MMP-9 expression, leading to a decrease in its activity at 15 days post-injury. BDNF expression was also decreased in the nerve at 21 days post-injury. Regarding denervated muscle, MMP-2 activity and BDNF and NT-4 expression increased at 15 days post-injury in the irradiated groups. **Conclusions:** PBM modulates and accelerates the expression of genes related to nerve repair and muscle re-innervation.

Key-words: Laser therapy, Physiotherapy, Neurological rehabilitation, Peripheral Nerve Injury, Peripheral Nervous System.

INTRODUCTION

Peripheral nerve injuries (PNIs) are common incapacitating clinical occurrences that lead to functional loss (Khuong & Midha, 2012). In the United States of America, about 50 thousand people experience PNIs yearly (Milesi, 2000; Evans, 2001). A Brazilian study showed that 45% of all PNIs were axonotmesis (Kouyoumdjian, 2006).

Wallerian degeneration which occurs in axonotmesis, is a process of nerve tissue degeneration and denervation that in some cases is followed by nerve regeneration and reinnervation of its target tissue (Lundborg, 2005). After Wallerian degeneration, restoration of neuromuscular function occurs through reorganization of the extracellular matrix (ECM) of the affected nerve and muscle. This reorganization of the ECM involves a complex, well-orchestrated process of protein degradation and synthesis that allows the axonal growth cone to re-innervate the denervated muscle fibers and restore movement. It is important to elucidate ECM remodeling to understand peripheral nerve injury and repair (Platt et al., 2003).

A proteolytic zinc-dependent family enzyme named matrix metalloproteinases (MMPs) plays an important role in degradation and reorganization of ECM (Schoser & Blottner, 1999; Ahtikoski et al., 2004; Demestre et al., 2005; Russo et al., 2008). Among the MMPs, MMP-2 (gelatinase A) and MMP-9 (gelatinase B), are key enzymes in the process of ECM remodeling in nerve and skeletal muscle that occurs in responses to injury (Carmeli et al., 2004). Both are known to degrade the non-fibrillar form of type IV collagen and to denature interstitial collagens (Ahtikoski et al., 2004). Studies suggest that, in the nerve, MMP-2 and MMP-9 are involved in axonal growth facilitation after crush injury (Platt et al., 2003; Heine et al., 2004).

Alterations in the pattern of MMPs activity can be beneficial to neuromuscular recovery. However the activity of the MMPs must be stringently controlled to avoid excessive degradation of ECM and, consequently, tissue damage. MMPs are selectively regulated by TIMP-1 (Tissue Inhibitor of MMP). Concomitant increases of MMPs and TIMP-1 activities were observed after PNI suggesting that, during nerve repair, TIMP-1 controls MMPs' activity, therefore protecting basal membrane from uncontrolled degradation which would be harmful to axonal regrowth (La Fleur et al., 1996).

Other factors that also regulate the process of neuromuscular recovery after PNI are the neurotrophins or neurotrophic factors (Omura et al., 2005). They are a family of polypeptides that control the neuronal proliferation, survival, differentiation and

regeneration in the central and peripheral nervous systems, Neurotrophins can also be expressed, for example, in Schwann cells and muscle fibers (Sendtner et al., 2000; Omura et al., 2005). Brain Derived Neurotrophic Factor (BDNF) and neutrofina-4 (NT-4) stand out in this family (Sendtner et al., 2000). BDNF and NT-4 expression varies in muscle and nerve according to the type of nerve injury and the time of injury. It is possible to consider that they could be prognostic markers of neural regeneration. A significant increase of BDNF and NT-4 could act in the process of axonal myelination and neuromuscular junction establishment, respectively (Omura et al., 2000).

Photobiomodulation (PBM) also known as low level light therapy has been used to stimulate the repair of peripheral nerves in animals (Gigo-Benato et al., 2010; Medalha et al., 2012) and human beings (Rochkind et al., 2009b). Our group has been investigating the effects of PBM at the molecular level. Recently using the neuromuscular recovery after a nerve crush injury in rats as our bioassay, we characterized a dose-response curve for two different wavelengths (660 and 803 nm) at different energy densities (10, 60 and 120 J/cm²) (need reference add here and in ref list). The parameters that most effectively supported neuromuscular regeneration were 660 nm wavelength light at an energy density of 60 J/cm². Those laser parameters were used in a recent study in which we reported that PBM increased MMP activity and TNFα protein expression during the acute phase of crush injury of the rat sciatic nerve (add LSM 45: 246-252, 2013 here and in references) However, the temporal pattern of MMPs activity response after laser irradiation in nerve and muscle in the ECM restructuration process was not addressed. T

The hypothesis for the present study is that PBM accelerates neuromuscular recovery, by acting preferentially on neuronal growth markers, such as MMPs and neurotrophins, in acute and sub-acute stages of injury. Thus, the objective of this study was to evaluate the temporal effects of PBM protocol on neuromuscular excitability and morphology, and on the expression of BDNF and NT4, matrix metalloproteinases (MMP-2 and MMP-9) and their inhibitor (TIMP-1) in nerves and muscles after axonotmesis in rats.

MATERIALS AND METHODS

Animals and Experimental Groups

Seventy male Wistar albino rats (Rattus norvegicus), 3 months-old, were used in this study. The animals were maintained in individual cages, with water and food *ad libitum*. The experiment was conducted according international standards of ethics in animal experimentation and was approved by the Ethics and Animal Research Committee of the institution (Process 065/2010).

Ten rats were randomly assigned to one control group and 6 experimental groups:

Normal Group (N): the rats were not injured or submitted to laser irradiation, control;

Peripheral Nerve Injury Group with LLLT simulated 7 days (PNI 7d): rats underwent nerve injury and laser simulation for 5 consecutive days (laser device off);

Peripheral Nerve Injury Group with LLLT 660 nm + 60 J/cm² 7 days (PNI+LLLT7d): rats underwent nerve injury and laser irradiation for 5 consecutive days;

Peripheral Nerve Injury Group with LLLT simulated 15 days (PNI 15d): rats underwent nerve injury and 10 sessions of simulated laser therapy (laser device off);

Peripheral Nerve injury Group with LLLT 660 nm + 60 J/cm² 15 days (PNI+LLLT15d): rats underwent nerve injury and laser irradiated for 10 consecutive days;

Peripheral Nerve Injury Group with LLLT simulated 21 days (PNI 21d): rats underwent nerve injury and laser simulation for 10 consecutive days (laser device off);

Peripheral Nerve Injury Group with LLLT 660 nm + 60 J/cm² 21 days (PNI+LLLT21d): rats underwent nerve injury and laser irradiation for 10 consecutive days. PNI 7d and PNI+LLLT 7d groups were euthanized 7 days after injury, PNI 15d and PNI+LLLT15d at 15 days post-injury, and N, PNI 21d and PNI+LLLT 21d at 21 days post-injury.

Axonotmesis Procedures

Animals were anesthetized with an intraperitoneal injection of a premixed solution containing ketamine (95 mg/kg) and xylazine (12 mg/kg). The skin was shaved and cleaned with 10% povidone iodine. A 2-cm long incision was made on the skin through a gluteal approach, and the right sciatic nerve was exposed. A non-serrated

clamp, exerting a force of 54N, was used for a period of 30 seconds, 10 mm above the bifurcation, to achieve good reproducibility of the axonotmetic lesion. The nerves were kept moist with sterile saline solution throughout the surgical intervention. After surgery, animals were housed in single cages and fed rat chow and water ad libitum (Beer et al., 2001; Varejão, 2004).

Laser Irradiation Protocol

A gallium–aluminum–arsenide laser device (TWIN LASER; MM Optics, São Carlos, SP, Brazil) was used with the following parameters: continuous wave, wavelength: 660 nm, power: 40 mW, spot area: 4 mm^2, energy density at the point of entry: 60 J/cm^2 and energy per point: 24 J, treatment time: 1 minute per point. After the skin was shaved at the site of surgery (recognizable by the surgical scar), laser irradiation was applied transcutaneously to two points along the sciatic nerve, one above and one below the scar site, with a distance of 2 cm between them. Group PNI+LLLT7d was irradiated on 5 consecutive days while groups PNI+LLLT15d, and PNI+LLLT21d were irradiated on 10 consecutive days. Groups PNI7d, PNI15d, and PNI21d received laser simulation of either 5 or 10 consecutive days. The rats were gently held and not anesthetized during irradiation. Laser irradiation did not produce any painful sensation or distress to the animals

Functional Evaluation

The assessment of nerve function recovery was assessed by calculating the sciatic functional index (SFI) as described by Bain et al (1989). The animals were tested in a confined corridor 42 cm long and 8.2 cm wide, with a dark shelter at the end. The corridor was lined with white paper, and ink was applied to the hind feet of the rats with a sponge. The rats were then allowed to walk down the corridor recording their footprints on the paper. Three measurements were taken from the footprints: (1) the print length (PL), that is, the distance from the heel to the third toe; (2) the toe spread (TS), that is, distance from the first to the fifth toe; and (3) the inter-mediary toe spread (ITS), that is, distance from the second to the fourth toe. All three measurements were taken from the experimental (E) and normal (N) sides. The SFI was calculated according to the following equation: SFI = -38.3 x [(EPL-NPL)/NPL] + 109.5 x [(ETS-NTS)/NTS] + 13.3 x [(EITS-NITS)/NITS] – 8.8. The functional evaluation was done prior to injury and at days 1, 6, 14 and 20 post-injury. All groups were analyzed.

Neuromuscular Excitability Evaluation

To monitor the neuromuscular regeneration process, electrical measurements of excitability were performed, according to previous studies (Russo et al., 2010). Briefly, an electro-stimulation device was used (NeMESys 941, Quark, Brasil).

The lumbar skin and skin above the tibialis anterior (TA) muscle were shaved and cleaned for electrode placement. A layer of conductive gel was applied between electrode and skin. Two electrodes were used: one ground electrode (circular self – adhesive electrode 5 cm diameter) was positioned on the back of the animal. The second electrode/active (metal electrode 3 mm diameter) was used to stimulate the TA muscle. During the evaluation procedures, the active electrode was fixed in position to avoid changes in pressure and angle between electrode and skin.

The excitability was evaluated by measures of rheobase, chronaxie and accommodation prior to injury and on days 1, 6, 14 and 20 days post-injury. All groups were evaluated. The rheobase, considered as the minimum amplitude required to twitch, was obtained using the rectangular pulse with pulse duration (T) 1,0 s and interval between pulses (R) 2.0 s. The chronaxie was characterized as the shortest possible pulse duration that resulted in muscle twitch. Therefore, it measured the speed of neuromuscular response to an electrical pulse. The same rectangular pulse was used with R 2.0 s and amplitude equal to twice the rheobase value obtained previously. Accommodation, defined as the tissues capacity to non-response to electrical stimulation of small increases, arose from a current exponential having T 1.0 and R 2.0 s. The muscles were considered denervated when chronaxie values were equal to or smaller than 1 ms (Gigo-Benato et al., 2010; Russo et al., 2010). The rats were anesthetized during this analysis.

Muscle evaluation

The right TA muscle was dissected, removed and divided into two transectional portions from the muscle belly. The lower portion was fixed and frozen in isopentane pre-cooled in liquid nitrogen and was used for histologic and morphometric analysis of muscle fibers. The upper portion was again divided perpendicularly, frozen in liquid nitrogen, and used for protein analysis and gene expression. All muscles were stored in a freezer at -86ºC.

For morphological and morphometric analyses, serial histological sections (10 mm) were cut at the middle portion of the muscle using a cryostat microtome at -25ºC.

These sections were stained with toluidine blue (TB) for analysis of morphology and also for measures of cross-sectional area of muscle fibers. Two hundred muscle fibers were randomly chosen for each muscle, and were measured from the image obtained from central region of the muscle belly.

MMPs activity analysis

MMPs activity was evaluated through zymography. Muscle and nerve fragments were performed as previously described (Russo et al., 2008). Molecular mass of gelatinolytic activities of each band was determined by comparison to the reference protein molecular weight marker (PageRuler Prestained Protein Ladder; Fermentas Life Sciences, Burlington, Ontário, Canada). Activity bands were identified according to their molecular weights (72 kDa: pro-MMP-2; 64 kDa: intermediate MMP-2; 57 kDa: active MMP-2; 92 kDa: pro-MMP-9; 81 kDa: active MMP-9). Densitometric quantitative analysis of total protein in the zymography was performed using GeneTools v3.06 software (Syngene, Cambridge, UK).

Extraction of total RNA

Extraction of total RNA from each animal (nerve and muscle) was obtained using Trizol reagent (Gibco), following manufacturer's recommendations. The optical density of samples was determined by spectrophotometry, with wavelength of 260 nm. To evaluate isolated RNA quality, the ratio between the absorbances at 260 and 280 nm (ratio $\geq$ 1.8) was determined. The quality of the material was also evaluated by electrophoresis of samples (2 μg of total RNA) in formamide-agarose denaturing gel (1%) in MOPS buffer (40 mM morpholino propanesulfonic acid). Subsequently, gels were stained with ethidium bromide.

RT-PCR (Reverse Transcription - Polymerase Chain Reaction)

After RNA isolation, reverse transcription was performed using one microgram of total RNA. The reaction was performed with different volumes of total RNA, 200 u of reverse transcriptase, 0,8 mM dNTPs; 1 mM $MgCl_2$; 0,02 ug/ul primer oligo dT; 4 mM of DTT. Reverse transcription was performed in a thermo cycler (70ºC for 10 min, 42ºC for 60 min and 94ºC for 10 min). The integrity of RT product (cDNAs) was confirmed through non-denaturing agarose gel, stained with ethidium bromide.

Primers

Oligonucleotides (primers) for real time PCR of GAPDH, MMP-2, MMP-9, TIMP-1, BDNF and NT-4 are described in Table 1.

Table 1. Primers Sequence Used to Real-Time RT-PCR

	Forward	Reverse
GAPDH	GATGCTGGTGCTGAGTATGTCG	GTGGTGCAGGATGCATTGCTGA
MMP-2	CTGGGTTTACCCCCTGATGTCC	AACCGGGGTCCATTTTCTTCTTT
MMP-9	GGATGTTTTTGATGCCATTGCTG	CCACGTGCGGGCAATAAGAAAG
TIMP-1	ATAGTGCTGGCTGTGGGGTGTG	TGATCGCTCTGGTAGCCCTTCTC
BDNF	AGCCTCCTCTGCTCTTTCTGCTGGA	CTTTTGTCTATGCCCCTGCAGCCTT
NT4	CCCTGCGTCAGTACTTCTTCGAGAC	CTGGACGTCAGGCACGGCCTGTTC

MMP-2, MMP-9, TIMP-1, and GAPDH were designed using Primer Express software (Applied Biosystems, Foster City, CA). BDNF and NT-4 sequences were obtained from Du et al, 2010 and Zermeño et al., 2009, respectively.

Real time PCR

Amplified RNA levels of the experimental and control groups were analyzed simultaneously, and the reactions were performed in duplicate in a Lightcycler thermo cycler (Rotor Gene 3000, Cobertt Research, San Francisco, USA). PCR amplifications were performed using 10-80 ng/ul of cDNA added to a reaction containing 25 ul of SYBR Green PCR master mix and 50-900 nM of primers (sense and anti-sense) in a solution with 55 ul of total volume, divided into 2 tubes (duplicate). Cycling conditions were performed following each primer standard. After PCR reaction, it was possible to determine the beginning of exponential amplifying phase (Ct, *cycle threshold*) of each sample that was used as data for gene expression analysis. GAPDH was considered as *housekeeping* gene.

Western blot

A hundred milligrams of tissue were homogenized in lysis buffer (Ripa buffer: 10 mM Tris-HCl, pH 7,4; 150 mM NaCl; 1% Nonideto P-40; 1% sodium deoxycholate; 0,1% SDS; 10% glycerol) with protease inhibitors (10 mM sodium pyrophosphate; 10 mM NaF; 1 mM SoV_4; 2 mM PMSF; 10 µg/ml of leupeptin, tripsin, aprotinin and

antipapain inhibitors). Samples were shaken for 30 minutes at 4°C and then centrifuged for 30 minutes also at 4°C. Total proteins were quantified by Bradford method with spectrophotometer at 550 nm and compared to a concentration curve of BCA. Equal amounts of protein were separated in 12% sodium dodecyl sulfate polyacrylamide gel electrophoresis (SDS – PAGE). A pre-colored pattern was used to determine the molecular weight proteins (Kalidoscope Standards Prestained, Bio-Rad, São Paulo, SP, Brazil). Then proteins were transferred to a nitrocellulose membrane by electrophoresis (25 mA for 12 hours). The membranes were stained with Red Ponceau to confirm run quality and protein presence. For antibodies incubating, membranes passed through the following steps: they were rinsed in TBST three times of 10 minutes each; rinsed for 1 hour in 5% nonfat dried milk dissolved in TBST. The membranes were incubated overnight at 4ºC, with primary antibody in 1 ml of TBST. The primary antibodies used were BDNF (Santa Cruz, sc-546, rabbit origin, polyclonal, 1:100) and NT-4 (Chemicon, AB1781, rabbit origin, polyclonal, 1:200). After that, membranes were rinsed three times in TBST for 10 minutes each, and incubated with secondary antibody (IgG, horseradish peroxidase linked whole antibody, 1:7000, nonfat dried milk 0.1% in TBST). In the end, membranes were rinsed three times in TBST. Detection of the labeled protein was done using enhanced chemiluminescence system (High performance chemiluminescence film, Amersham).

Statistic Data Analysis

Shapiro-Wilk and Levene's tests were applied to evaluate the data normality and homogeneity, respectively. One-way ANOVA was used to identify differences amongst groups. When differences were observed, Tukey test was performed. Kruskal Wallis followed by Newman-Keulls was used to evaluate non-parametric data. For all tests, the significance level was set at 5%.

RESULTS

Functional Evaluation

In the first day after injury, there was a significant decrease in SFI values of PNI 21d and PNI+LLLT 21d groups compared to the pre-injury value ($p<0,05$; Fig. 1). This reduction persisted until the 14th day ($p<0,05$ compared to pre-injury; Fig.1), with difference only in 1st day post-injury between PNI 21d and PNI+LLLT21d groups ($p<0,05$). At other moments, there is no difference between PNI 21d and PNI+LLLT 21d groups ($p<0,05$; Fig.1). Normal values of SFI were recovered in 20 days after-injury, in both groups ($p<0.05$, when PNI 21d and PNI+LLLT 21d were compared to pre-injury; Fig. 1).

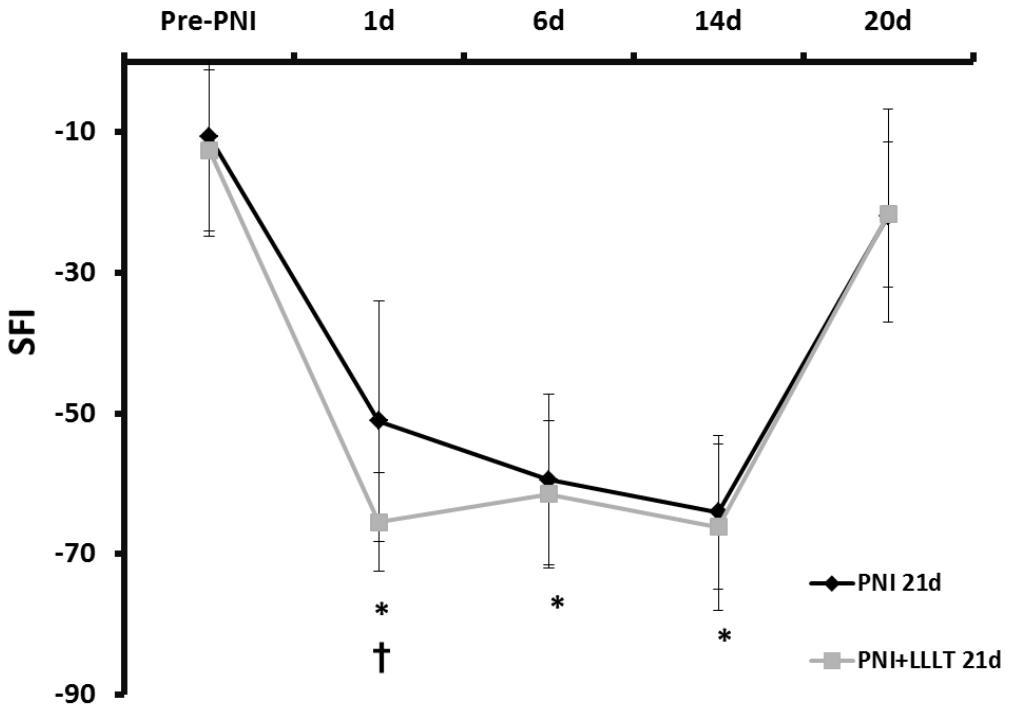

Neuromuscular excitability

The neuromuscular excitability was evaluated by measures of rheobase, chronaxie and accommodation. Figure 2 presents the data collected at 20 days post-injury. Regarding the values of rheobase (Fig. 2A), there was a decrease in rheobase from the 6th day post-injury in PNI 21d and PNI+LLLT 21d groups compared to normal values, obtained pre-injury ($p<0.05$). This decrease was maintained until the 14th day. On the 20th day, a recovery of rheobase values occured with differences between PNI 21d and PNI+LLLT 21d groups ($p=0.005$; Fig. 2A), and the group irradiated with laser

recovered its normal pre-injury values ($p>0.05$), whereas PNI 21d presents higher than normal values ($p<0.05$; Fig. 2A).

After nerve injury, there was an increase in chronaxie values from the 6th day in PNI 21d and PNI+LLLT 21d groups, compared to pre-injury values ($p<0,05$; Fig 2B). This increase persisted until day 20 post-injury in PNI 21d group compared to pre-injury ($p<0.05$). PNI+LLLT 21d group, had increased values at day 14 post-injury ($p<0.05$) and returned to pre-injury values at 20 days post-injury ($p>0,05$; Fig 2B).

Regarding accommodation, a significant reduction was observed in PNI 21d and PNI+LLLT 21d groups only at day 14 post-injury compared to pre-injury meausrements ($p<0.05$; Fig 2C). On day 20 post-injury, the PNI+LLLT 21d group returned to normal values, whereas PNI 21d had higher values than normal ($p=0.03$; Fig 2C).

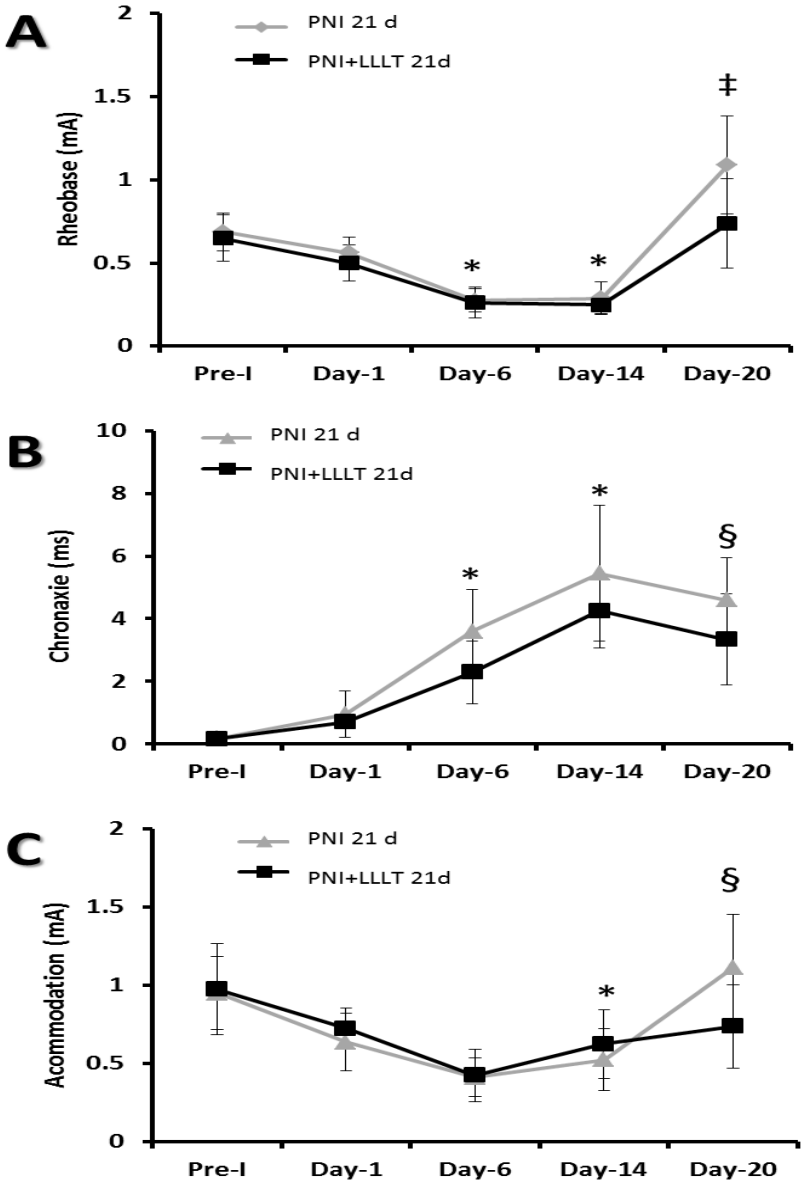

Muscular and peripheral nerve weight

There was a decrease in TA muscle weight at 7 days post-injury if compared to N group (0.67 ± 0.05g; p<0,0001), but without difference between the groups irradiated (PNI+LLLT 7d: 0,45 ± 0,05g) or non-irradiated with laser (PNI 7d: 0,47 ± 0,08g; p=0,2). The loss in muscle weight was maximal at 15 days post-injury and remained stable at 21 days after PNI, compared to N (≈ 50% of reduction) and to PNI 7d and PNI+LLLT 7d groups (≈ 30% of reduction, p<0,0001). No difference was observed between groups PNI and PNI+LLLT 15 or 21 days (0,32 ± 0,02g; p>0,05).

There was no difference found in the sciatic nerve weight between the groups (0,09 ± 0,01g; p>0,05).

Cross-sectional area of muscle fibers and nerve fibers components

A maximal atrophy of 23.9% (average) compared to N was found at day 7 post-PNI in denervated muscle fibers, which remained until 21th day of PNI without difference between injured groups (p>0,05). Regarding the cross-sectional areas of nervous fiber, myelin sheath and axon, at 21 days post-injury, their values were below normal (p<0,05), and there was no difference between PNI 21d and PNI+LLLT 21d groups (p=0,74).

MMPs gene expression and activity in nerve and muscle

Figure 3 presents MMP-2 (Fig. 3A and B), TIMP-1 (Fig.3C and D) and MMP-9 (Fig.3E and F) gene expression, in nerves (Fig. 3A, C and E) and muscles (Fig. 3B, D and F) in different experimental groups. All data were normalized for the expression of the constitutive gene GAPDH and also for the normal group.

MMP-2, TIMP-1 and MMP-9 gene expression in nerve (Fig. 3A, C and E):

MMP-2 expression (Fig 3A), increased in PNI7d, PNI+LLLT7d, PNI 15d and PNI+LLLT21d groups compared to N (p<0,05) and also to PNI+LLLT15d and PNI 21d (p<0.05; Fig. 3A). This increase was greater in the PNI+LLLT7d group than in others (p<0.05; Fig 3A). A similar pattern of expression was observed in TIMP-1 (Fig 3C) with an increase in expression found in PNI 7d, PNI+LLLT 7d, PNI15d and PNI+LLLT21d groups had their expression increased compared to N (p<0.05) and also to PNI+LLLT15d and PNI 21d (p<0.05). Regarding MMP-9 expression (Fig 3E), a

decrease was observed in PNI+LLLT7d related to PNI 7d ($p<0.05$; Fig 2E). No other differences were observed between other groups ($p>0.05$; Fig 2E).

MMP-2, TIMP-1 and MMP-9 gene expression in muscle (Fig. 3B, D and F):

There was an increase in MMP-2 expression in denervated muscles in PNI 7d, PNI 15d and PNI+LLLT 15d compared to N ($p<0,05$; Fig 3B). TIMP-1 increased its expression related to N at 7 and 15 days of injury in groups irradiated or non-irradiated with LLLT ($p<0,05$; Fig 3E), and this increase is more significant in PNI 15d and PNI+LLLT 15d groups ($p<0,05$; Fig 3E) compared to all others. There was no change in MMP-9 expression in different experimental groups ($p>0,05$; Fig. 3F).

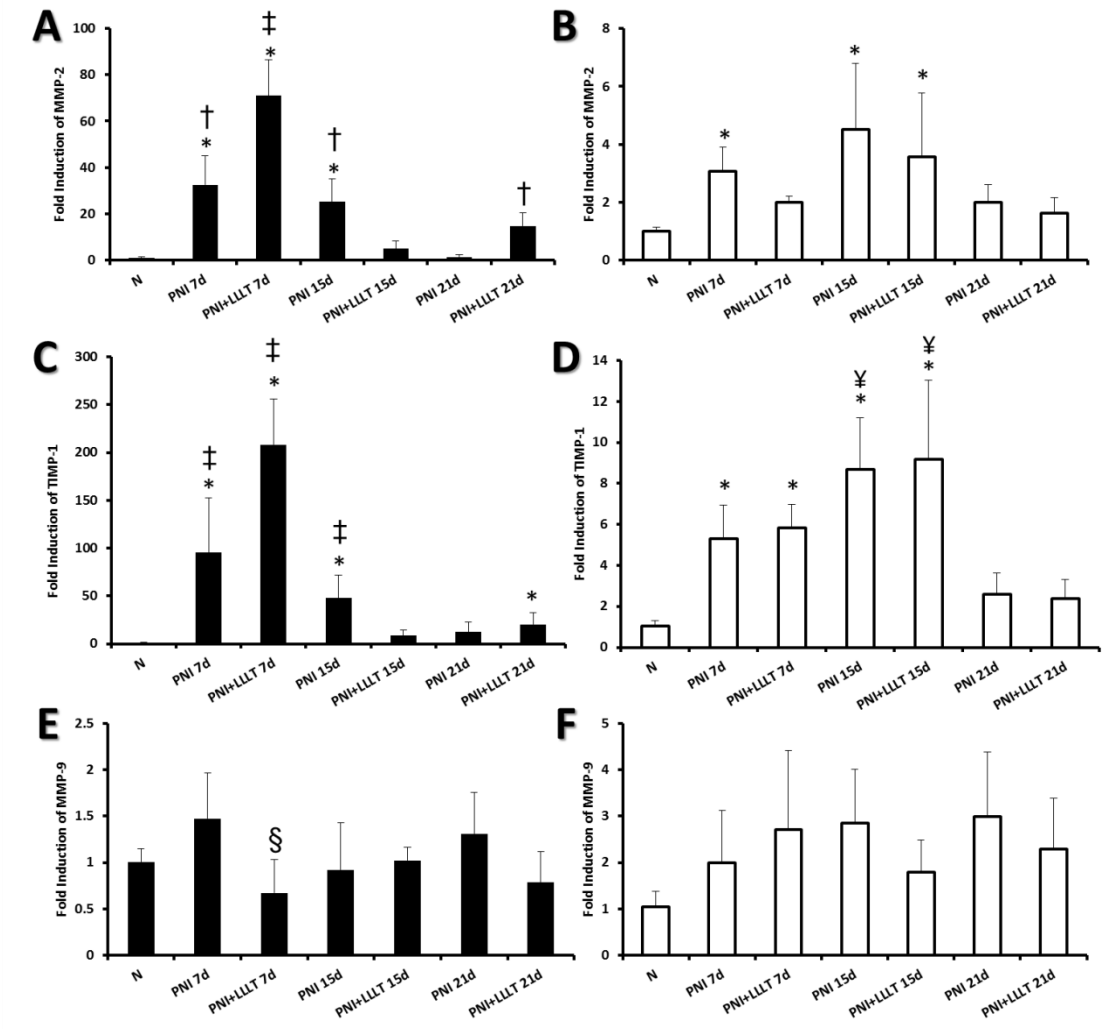

MMPs activity detected by zymography are shown in Figures 4 and 5. MMP-2 was found in nerves and muscles (Fig. 4), while MMP-9 only in nerve (Fig. 5).

Figure 4 shows representative gels of MMP-2 in all groups investigated in nerve (Fig. 4A) and in muscles (Fig. 4C), as well as its respective quantification by densitometry (Fig 4B and D). Three isoforms were identified: 72 KDa: pro-MMP-2; 64 KDa: intermediate MMP-2; and 57 KDa: active MMP-2 (Fig. 4A and C). No difference was observed in density of pro and intermediate MMP-2 isoforms in nerves and muscles of different experimental groups ($p>0.05$; Fig 4B and D). Regarding active isoform in nerves, an increase in its activity is noted in PNI 7d, PNI+LLLT7d, PNI 15d and PNI+LLLT15d groups compared to N ($p<0,05$; Fig 3B). At 21 days, PNI 21 days returned to normal values, while PNI+LLLT21d group remained elevated in relation to N ($p<0,05$; Fig 4B). On the other hand, in muscles, an increase of MMP-2 active isoform activity was observed in PNI+LLLT15d, PNI 21d and PNI+LLLT21d compared to N ($p<0,05$; Fig. 4D).

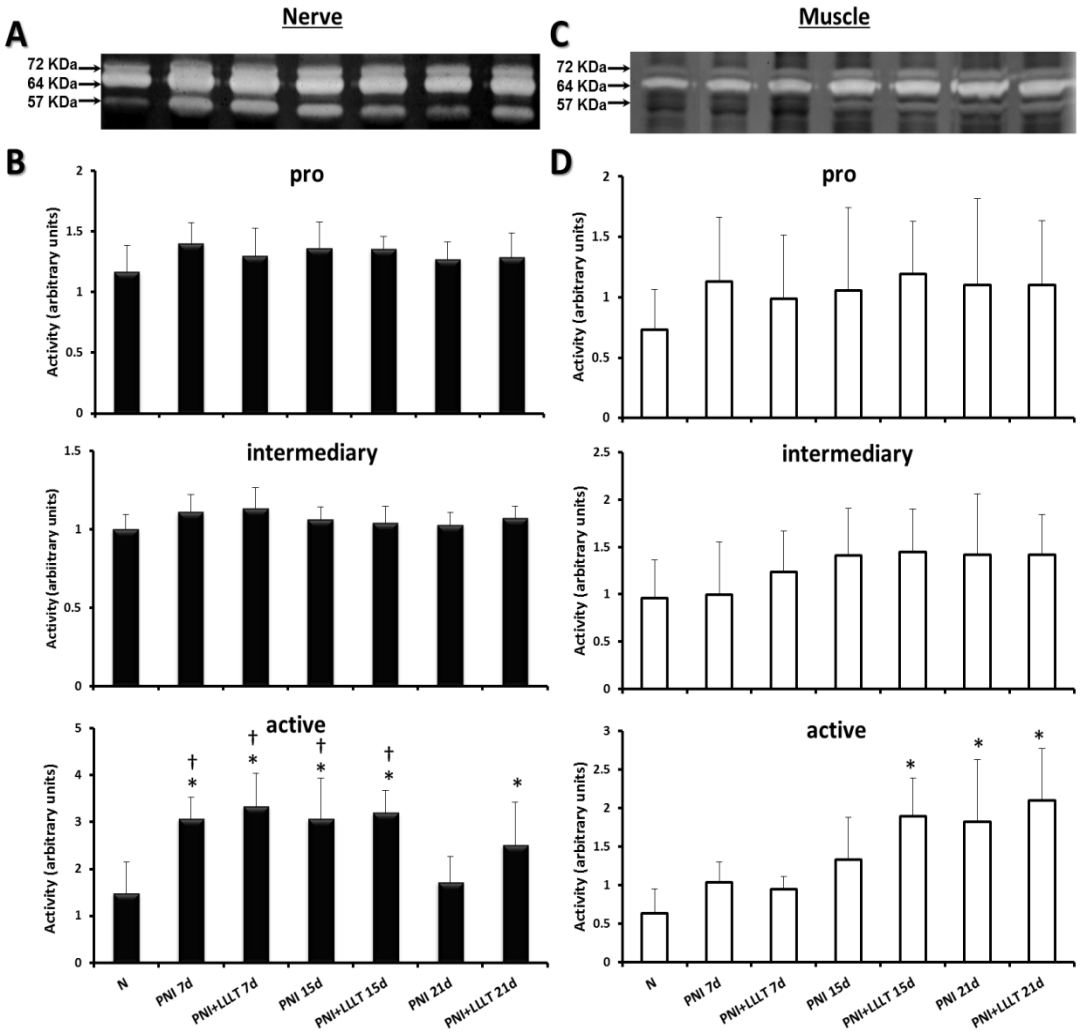

In the nerve, there was no difference observed between the experimental groups in relation to densitometry of pro MMP-9 isoform ($p>0.05$). A decrease in its activity in the PNI+LLLT15d and PNI21d groups occurred compared to the normal group ($p<0.05$; Fig 5B).

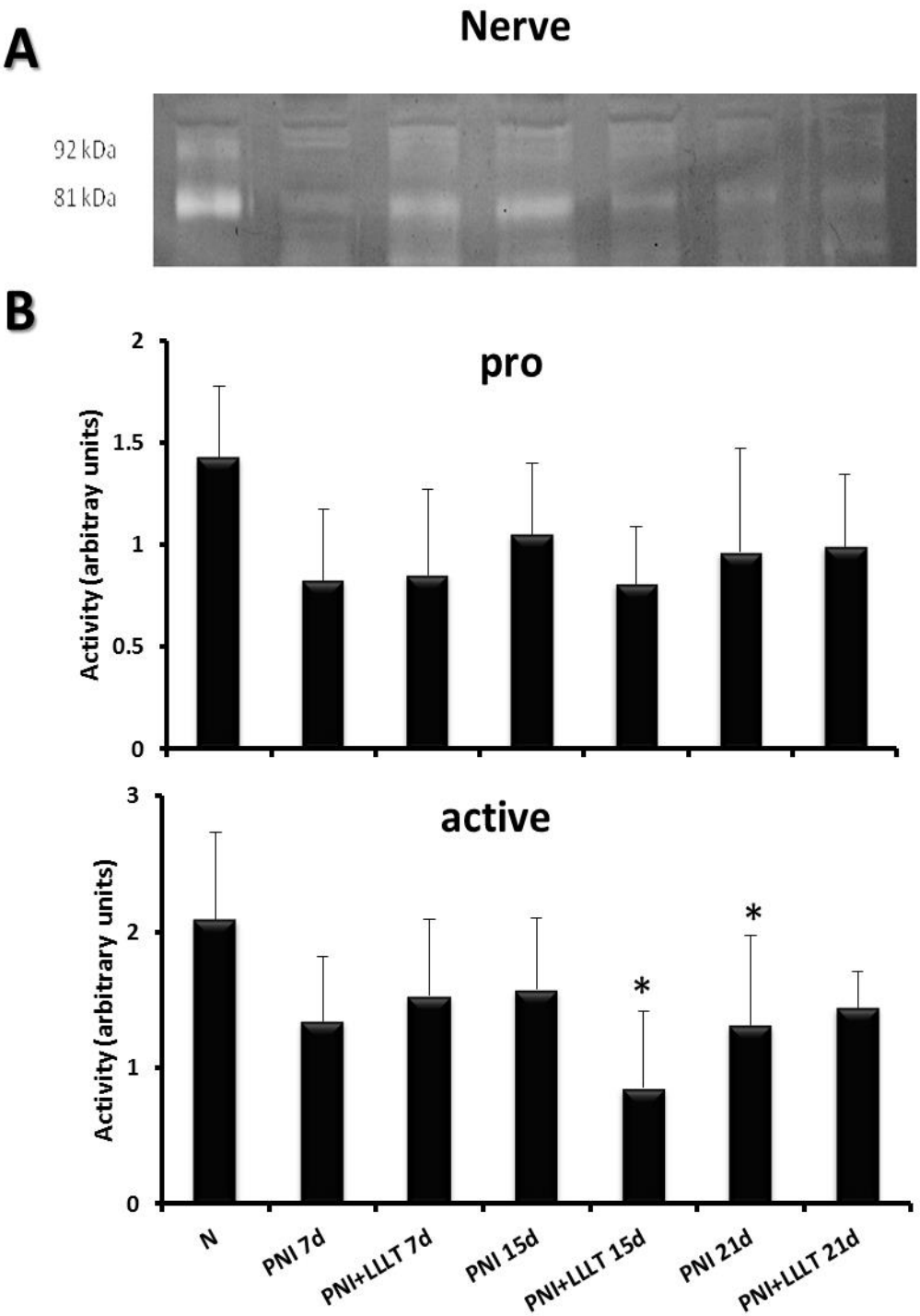

Gene expression and protein content of BDNF and NT-4 in nerves and muscles.

Gene expression of BDNF and NT-4, two important neurotrophic factors, in nerves and muscles, is presented in Figure 6. BDNF gene expression in nerves (Fig. 6A), increased in PNI 7d and PNI+LLLT21d groups compared to N ($p<0.05$; Fig. 6A). PNI7d and PNI+LLLT7d groups showed a significant increase in relation to PNI15d, PNI+LLLT15d and PNI 21d groups ($p<0.05$; Fig. 6A). PNI+LLLT21 had elevated levels compared to all groups ($p<0.05$; Fig.6A). There was no difference in BDNF protein content in nerves (data not shown) between Normal group (Mean = 1.73**)** and all experimental groups (Mean = 4.15). BDNF gene expression in muscles was increased only in PNI+LLLT15d group in relation to N ($p<0,05$; Fig. 6B). Regarding protein content (data not shown), no difference was observed between Normal group (Mean = 0.33) and all experimental groups (Mean = 1,55). Both NT-4 gene expression ($p>0.05$; Fig. 6C) and protein content in nerves (data not shown) remained unaltered (Protein content means: Normal = 1.04; Experimental = 1.07). On the other hand, NT-4 gene expression in muscles was reduced in PNI7d, PNI+LLLT7d and PNI15d groups in relation to all others ($p<0,05$; Fig. 6D). NT-4 protein content in muscle (data not shown) presented no difference between the Normal group (Mean = 1.30) and all experimental groups (Mean = 2,73).

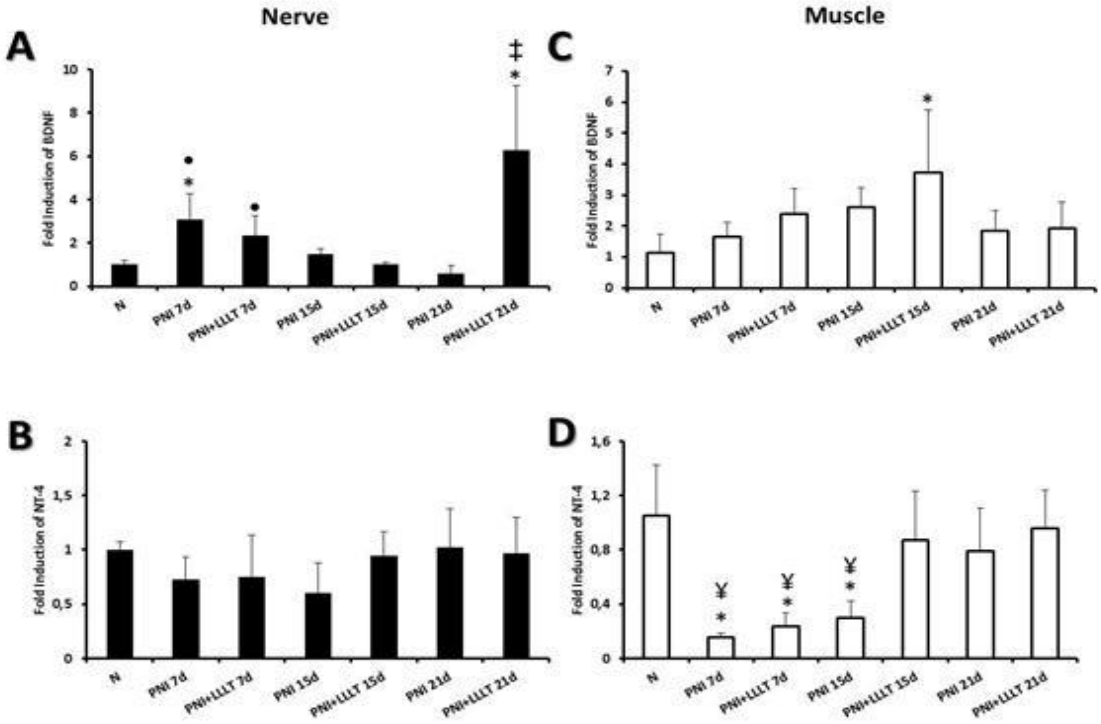

DISCUSSION

The present study showed temporal effects of PBM on modulation of active enzymes related to ECM remodeling and also of neurotrophins in both crushed nerves and denervated muscles. I don't think you can claim this –your data is very confusing and in more cases that not shows no significant difference. These results complemented a previous report (Gigo-Benato et al., 2010) that demonstrated that PBM accelerated neuromuscular recovery after crush nerve injuries. This study characterized a dose-response curve, relating two wavelengths (660 and 803 nm) with different energy densities (10, 60 and 120 J/cm²), therefore, identifying the best parameters of irradiation able to accelerate the neuromuscular recovery after crush nerve injury. Better effects on neuromuscular regeneration were observed using the laser 660 nm with energy density of 60 J/cm² (Gigo-Benato et al., 2010). These parameters were able to recover the cross-sectional area of muscle fibers, nervous fibers and myelin sheaths in animals, 28 days after crushed sciatic nerve. The results of this paper make me question just how effective these parameters were. Why didn't you see the same improvements in this study? This recovery was associated with the increase of MMP-2 activity in nerve and the reduction of MMP-9 and MMP-2 activity in nerves and muscles, respectively. However, it was not clear whether PBM should be started as soon as possible or it could be indicated later, because it was not possible to identify in which moment, over time, the light exerted its effects. In this present study, it is clear that the effects of PBM on the transcriptional level began in the first week post-injury. I don't think that you can claim that this as due to light because the non-laser treated animals also showed the increase at day 7.

The present results showed that on 7th day post-injury, the PBM increased MMP-2 gene expression and decreased MMP-9 expression in nerves. These changes are reflected in the maintenance of increased activity of MMP-2 at 21 days in the group irradiated with laser and a decreased of MMP-9 detected at 15 days. Please check your data carefully. While MMP-2 gene expression increased at day 7 it was not maintained at day 21 due to light it decreased at day 15. For MMP 9 there does not look like a decrease in the pattern at day 15. If your error bars represent the SEM then you can not have a significant difference with overlapped error bars. This pattern is significantly different from those observed in injured non-irradiated groups. Too broad a claim.

It has been previously demonstrated (La Fleur et al., 1996) that, during the initial stages of Wallerian degeneration, the disintegration of cytoskeletal and breakdown of the myelin sheath occur by a coordinated process of MMPs activation. In this study, the authors described that MMP-9 secretion in the early days of nervous injury is important to assist macrophage and neutrophil influxes, and to remove axonal/myelin debris and starting the ECM remodeling. On the other hand, in late stages, reduced MMP-9 activity is required to prevent damage to the ECM.

Alcântara and cols (2013) also presented relevant data about how LLLT can modulate MMP-9 and TNF-α on the first 3 days after nerve crush injury. They showed that LLLT increased the MMP-9 activity in crushed nerves compared to non-irradiated groups, corroborating to previous data that MMP-9 activation and TNF-α are important to improve the healing process on the nervous system during the inflammation process (Rotshenker et al., 2011, Gaudet et al., 2011, La Fleur et al., 1996). All together, these previous reports can contribute to interpret the present ones. In this sense, our findings showed that MMP-9 activity can be accelerated by LLLT in one week when PNI+LLLT 15d is compared to PNI 21d.

Corroborating to findings of the beneficial effect of LLLT on the inhibition of MMP-9 in the final stages of regeneration process, maintenance of MMP-2 activation can also be observed until the 3rd week post-injury. Gantus e cols (2006) showed that MMP-2 is able to degrade ECM compounds that restrain the advance of axonal growth cone, such as chondroitin sulphate proteoglycan (CSPG). Thus, we believe that the maintenance of high levels of MMP-2 at 21 days post-lesion could be related to the degradation of CSPG, stimulating the advancement of axonal growth cone. It is noteworthy that at 21 days post- injury, the levels of MMP-2 returned to baseline in the placebo group (PNI 21d) compared to injured group stimulated with LLLT. Another factor that may have influenced this increased activity in PNI+LLLT 21d is the MMP-2 expression, that remains high in this period.

Furthermore, it should be noted that the increased expression of MMP-2 is followed by an up-regulation of TIMP-1. The literature has shown the important role of TIMP-1 to protect the basement membrane of uncontrolled degradation caused by MMPs after nerve injury (LaFleur et al., 1996; Platt et al., 2003). One hypothesis is that the controlled activity of MMPs by TIMP-1 protects the disorganization of the basement membrane, allowing MMP-2 to guide the growing cone through ECM at the distal nerve stump toward to denervatd muscle fibers (Platt et al., 2003).

Regarding the findings of MMPs expression and activity in denervated muscles, a similar pattern of MMP-2 and TIMP-1 gene expression was noted among experimental groups. However, it is highlighted that the MMP-2 activity was increased in PNI + LLLT 15d group, whilst in non-irradiated animals this increase occurred only at day 21 (PNI 21d). These findings are relevant because it has been described in the literature that MMP-2 releases fibroblast growth factor-basic (bFGF) from ECM. Likely, bFGF is able to stimulate the formation of acetylcholine receptors clusters on muscle sarcolemma, and thus facilitating reinnervation process (Demestre et al., 2005). Furthermore, both MMP-2 and -9 were also previously associated to TGF-β superfamily activation (Yu & Stamenkovic, 2000), which has as member the neurotrophic factor derived glial cell line (GDNF), an important neurotrophin that can act on the survival, proliferation and neuronal differentiation (Wyss-Coray, 2004). Thus, lasertherapy could accelerate the reinnervation of denervated fibers.

Comparing the present data to a previous study (Gigo-Benato et al. 2010), it is possible to describe the temporal regulatory mechanisms of LLLT. It was observed that the increase of MMP-2 activity, in irradiated nerves at 28 days post-PNI (Gigo-Benato et al., 2010), starts already on the 7^{th} day with increases in MMP-2 gene expression, and it remained elevated until the 21^{th} day. These changes in expression could explain the high activity of MMP-2 in nerves after PNI over 28 days (Gigo-Benato et al., 2010). On the other hand, a decrease in MMP-9 expression on day-7 post-injury and a decrease in its activity at day 15 corroborate with the decreased of MMP-9 activity at 28 days (Gigo-Benato et al., 2010). Regarding muscles findings, it seems that the decreased activity of MMP-2 at 28 days, observed by Gigo-Benato et al (2010), is probably due to the increase of its activity as early as 15 days post-injury. All these processes in nerves and muscles seem to be strongly regulated by the expression of TIMP-1.

Regarding the effects of LLLT on expression of neurotrophins, the present study showed that the BDNF expression increases on day-7 post-injury in both irradiated nerves as those simulate. However, at 21 days post-injury the LLLT induced an increased expression of BDNF in peripheral nervous tissue. In relation to muscles, an increase of BDNF expression in PNI + LLLT 15d was detected, although no changes in its protein content was observed. Regarding NT-4 expression, gene expression normal values was detected in PNI + LLLT 15d group, while PNI 15d remained with low values relative to N.

The studies of Garcia et al (2010) and Omura et al (2005) helped in the interpretation of the results of present study. It is already well described in the literature that neurotrophins are related to neural development, maintenance and neuronal maturation of central and peripheral nervous system. Both BDNF and NT-4 exert effects through the interaction with high affinity membrane receptors (TrK) and low affinity ($p75^{NTR}$) (Garcia et al., 2010).

Omura et al (2005) studied messenger RNA expression and BDNF, NT3 and NT4 protein content in nerves submitted to different models of injury, such as neuropraxis, axonotmesis and neurotmesis, as well as in denervated soleus muscles. Analyses were performed 4, 7, 15, and 28 days post injury. In this study, it was observed that BDNF expression increased since the 7^{th} day in denervated soleus muscles. These levels remained elevated until 14^{th} day and returned to normality at 28^{th} day post-injury. Regarding nerves with axonotmesis, BDNF expression increased at day-14 and returned to normal values at 28 days. These findings did not corroborate with ours, which detected an increase in BDNF expression since 7 days in nerves and only at 15 days in TA muscles. Such timing differences can be attributed to different types of muscles investigated and the models of axonotmesis induction. The increase of BDNF in nerves occurs until the process of fibers remyelination has been finished, while in muscle it is attributed to a facilitation of reinervation process of denervated fibers through chemotaxis of neural growth cone. This increase was normalized as soon as functional recovery occurs (Omura et al., 2005). In the present study, it seems that lasertherapy stimulated BDNF expression in PNI+LLLT 21 days group. Similar result was reported in a study that utilized 632.8 nm laser, $10J/cm^2$, post axonotmesis, when the BDNF expression was higher in 15 and 21 days than the other groups non irradiated (Gomes et al., 2012).

Regarding NT-4 expression, an up-regulation in soleus muscles was already described, at 4 and 7 days post-denervation, but no changes in crushed nerves (Omura et al., 2005), corroborating with present study results. In muscles, it was demonstrated that BDNF and NT-4 expression are involved in motor end plate maintenance and also releasing neurotrophins in pre-synaptic membrane contributing to motor neurons survival (Garcia et al., 2010). NT-4 knockout mice showed a large fragmentation of neuromuscular junctions, with post synaptic disorganization of acetylcholine receptors agglomerates and decrease of acetylcholinesterase activity in neuromuscular junction (Belluardo et al., 2001). NT-4 levels decreased fastly post-nerve injury, but then there is

an increase over time (Omura et al., 2005). It seems that lasertherapy was not able to act in this neurotrophin. A similar behavior of expression was observed in another neurotrophin, NT-3, post-lasertherapy (632.8nm, 10J/cm2) in crushed nerve over 7, 14, 21 days of recovery (Gomes et al., 2012).

Concerning functional analysis, a significant reduction in Sciatic Functional Index (SFI) value already in 1st day post-surgery, in both L21d and PNI+LLLT21d groups, clearly showed the functional lost resulting from crushed nerve model. The use of this method of functional analysis is justified through simple application, high dissemination, low cost, besides having good correlation with results obtained from other analysis, which offers us a good view of neuromuscular interaction. However, it seems that SFI is not sensitive enough to detect small differences between groups, because the functional status followed the same pattern in both groups. More accurate analyses, such as cinematic and weight platform (Bervar, 2002; Costa et al., 2009) could be more sensitive to detect discrete functional changes.

Despite of Gigo-Benato et al (2010) detected an increase of myelin sheath and nervous fiber CSA at 28 days in crushed irradiated compared to crushed non-irradiated groups, morphological data from crushed nerves and denervated muscles did not differ each other. Conversely, eletrophysiological data provided an important clinical indicative of neuromuscular recovery. Rheobase and accommodation of PNI+LLLT 21d reached normal values at day-20 indicating normalized excitability. Furthermore, increase in nervous conduction velocity could also be observed by reduced chronaxie values (Russo et al., 2010). Such findings support that, despite of morphological changes had not been detected neither in nerves nor in muscle, electrical changes have already been detected. It seems for the model of axonotmesis, periods before 28 days are important to investigate either molecular adaptation or neuromuscular excitability, but not to morphological changes.

These findings have relevant clinical implications to rehabilitation area. The authors recommend that LLLT application should start at the very beginning phases post-PNI. Even after the ending of therapy, the LLLT´s effects remain until some days after its application, exerting an important regulatory effect, acting in transcriptional and translational levels. In this sense, a next step would be the application of a similar LLLT protocol in human beings to test its efficacy.

The present study shows some limitations, such as the lack of more sensible kinesiological analysis to detect subtle changes in animals' functionality. Besides that,

future studies should consider the tissue location of the proteins here investigated. The evaluation of LLLT effects during acute inflammatory process (≤ 3 days) would help in understanding laser modulatory effects in initial phase of injury.

Ever more, studies have been demonstrated that the laser is a great tool of neuromuscular rehabilitation (Gigo-Benato et al., 2005; Silva-Couto et al., 2012). Nevertheless, due to several problems in normalization of effective protocols to neuromuscular rehabilitation, little progress have been observed to evidence more detailed its mechanisms of action and interaction with nervous and muscle tissues before indicating it to treatment in human beings, ensuring a secure and efficient application. The present study helped to substantiate and to understand the temporal action of laser in neuromuscular regeneration post-axonotmesis, using an efficient protocol of application (Gigo-Benato et al., 2010), found previously by our group, and analyzing specific markers in the process of neuromuscular regeneration, then proving its efficacy and action. Therefore, we can conclude that the present study answers to the initial hypothesis of this study wherein LLLT accelerates neuromuscular recovery, acting preferentially in neuronal growth markers, such as MMPs and neurotrophins, and stimulating neuromuscular excitability recovery in different stages of axonal injury. In this way, it can be indicated to the treatment of peripheral nerve injury post-axonotmesis in humans.

ACKNOWLEDGMENTS

The main support for this research was provided by Fundação de Amparo à Pesquisa do Estado de São Paulo (FAPESP, process 2010/11795-6).

Scientific Initiation scholarship (process number 2010/20291-1)

LEGENDS

Figure 1. Sciatic Functional Index (SFI) in PNI 21d and PNI+LLLT 21d groups. *p<0,05:compared to pre-injury moment; and †p<0,05: compared to PNI 21d. Observe that there is a significant reduction of SFI values already since first day, and it is more evident in PNI+LLLT 21d group. This decrease is maintained until 14th day, without differences between the two groups. Normal SFI values are observed already at 21th.

Figure 2. Neuromuscular excitability throughout 20 days post peripheral nerve injury (PNI). Pre-I: pre injury moment. **A) Rheobasis:** *p<0,05 compared to Pre-I; ‡p<0,05:compared to all other moments and groups. Observe that at 20th day, irradiated group with laser recovers its normal values, while non-irradiated group presents higher values then pre injury. **B) Chronaxie:** *p<0,05 compared to Pre-I; §p<0,05: PNI 21d vs PNI+LLLT 21d. Note that after the increase of chronaxie values, the irradiated group with laser recovers its normal values at 20 days, whereas non-irradiated group remains with an elevated chronaxie. **C) Accommodation:** *p<0,05 compared to Pre-I; §p<0,05: PNI 21d vs PNI+LLLT 21d. The decreasing accommodation values in PNI 21d and PNI+LLLT 21d groups occurs only at 14 days. However, with 20 days the group submitted to laser therapy recovers its normal values, while non-irradiated injured group presented higher values than normal.

Figure 3. MMP-2 (Fig 3A and B), TIMP-1 (Fig 3C and D) and MMP-9 (Fig 3E and F) gene expression in nerves (Fig 3A, C and E) and in muscles (Fig. 3B, D and F) in different experimental groups. A) MMP-2 expression in nerve: *p<0,05 compared to N; †p<0,05 compared to PNI+LLLT 15d and L 21d; and ‡p<0,05 compared to all others experimental groups. B) MMP-2 expression in muscle: *p<0,05 compared to N. C) TIMP-1 expression in nerve: *p<0,05 compared to N; and ‡p<0,05 compared to PNI+LLLT 15d, PNI 21d, PNI+LLLT 21d. D) TIMP-1 in muscle: *p<0,05 compared to N; ¥p<0,05 compared to all other groups. Note that MMP-2 and TIMP-1 expression show a similar pattern. However, in nerves an increase at 7 days occurs in PNI 7d and PNI+LLLT 7d groups, and is more pronounced in irradiated group with laser. At 15 days, PNI+LLLT 15d group shows normal expression values, whereas PNI 15d group

shows an increased expression in relation to N, but lower than the period of 7 days. At 21 days, the expression of PNI+LLLT 21d group increases again, while in PNI 21d it is normal. E) MMP-9 expression in nerve: §p<0,05: compared to PNI 7d. F) MMP-9 expression in muscle. Note a decrease in MMP-9 mRNA levels in nerves of PNI+LLLT 7d group compared to PNI 7d.

Figure 4. MMPs activity in nerves (A and B) and muscles (C and D) in different experimental groups. A and C) Representative gels of MMP-2 activity in nerves (A) and muscles (C), where the following MMP-2 isoforms were localized: 72 KDa: pro-MMP-2; 64 KDa: intermediate MMP-2; and 57 KDa: active MMP-2. B and D) Densitometry of MMP-2 different bands.*p<0,05: compared to N; and †p<0,05: compared to PNI 21d. In nerves, note the activity increase in PNI 7d, PNI+LLLT 7d, PNI 15d and PNI+LLLT 15d groups. At 21 days, PNI 21d recovers normal activity values, whereas irradiated groups with laser (PNI+LLLT 21d) maintain increased in relation to N. In muscles the LLLT increases the activity of MMP-2 active isoform already at 15 days post injury (PNI+LLLT 15d), whereas this increase would occur naturally just at 21 days (PNI 21d).

Figure 5. MMP-9 activity in nerve in different experimental groups. A) Representative gel, where the following isoforms were detected: Pro (92 KDa) and active (81 KDa). *P<0,05 compared to N. Note a decrease in its activity in PNI+LLLT 15d and PNI 21d groups compared to N. LLLT accelerated in one week the decrease of MMP-9 activity. MMP-9 was not detected in muscles.

Figure 6. BDNF (A and C) and NT-4 (B and D) gene expression in nerves (A and B) and muscles (C and D) of different experimental groups. A) BDNF mRNA levels. *p<0,05: compared to N; •p<0,05: compared to PNI 15d, PNI+LLLT 15d, PNI 21d; ‡p<0,05: compared to all other groups. Note the increase of BDNF expression in PNI 7d and PNI+LLLT 21d groups, and that it is more pronounced in the last one. B) NT-4 gene expression in nerves. No significant difference was observed in its expression (p>0,05). C) BDNF gene expression in muscles. *P<0,05 compared to N. D) NT-4

expression. *P<0,05 compared to N. ¥P<0,05 compared to all others groups. Note that LLLT recovers NT-4 normal expression at 15 days.

REFERENCES

ALCÂNTARA CC, GIGO-BENATO D, SALVINI TF, OLIVEIRA AL, ANDERS JJ, RUSSO TL. Effect of low-level laser therapy (LLLT) on acute neural recovery and inflammation-related gene expression after crush injury in rat sciatic nerve. 45(4):246-52, 2013.

AHTIKOSKI, AM TUOMINEN H, KORPELAINEN JT, TAKALA TE, OIKARINEN A. Collagen Synthesis and degradation in polyneuropathy and myopathies. Muscle Nerve. 30 (5):602-82, Nov 2004.

BAIN JR, MACKINNON SE, HUNTER DA. Functional Evaluation of Complete Sciatic, Peroneal, and Posterior Tibial Nerve Lesions in the Rat. Plast Reconstr Surg. 83:129–138, 1989.

BEER GM, STEURER J, MEYER VE . Standardizing Nerve Crushes with a non-Serrated Clamp. J Reconstr Microsurg. 17:531-534, 2001.

BELLUARDO N, WESTERBLAD H, MUDO G, CASABONA A, BRUTON J, CANIGLIA G, PASTORIS O, GRASSI F, IBANEZ CF. Neuromuscular junction disassembly and muscle fatigue in mice lacking neurotrophin-4. Mol Cell Neurosci 18:56–67, 2001.

BERVAR M. An Alternative video footprint analysis to assess functional loss following injury to the rat sciatic nerve. Acta Chir Plast. 44(3):86-9, 2002.

CARMELI E, MOAS M, REZNICK AZ, COLEMAN R. Matrix metalloproteinases and skeletal muscle: a brief review. Muscle Nerve. 29:191–197, 2004.

COSTA LM, SIMÕES MJ, MAURÍCIO AC, VAREJÃO AS. Chapter 7: Methods and protocols in peripheral nerve regeneration experimental research: part IV-kinematic gait analysis to quantify peripheral nerve regeneration in the rat. Int Rev Neurobiol.;87:127-39,2009.

DEMESTRE M, ORTH M, WELLS GM, GEARING A J, HUGHES RA, GREGSON NA. Characterization of matrix metalloproteinases in denervated muscle. Neuropathol Appl Neurobiol. 31:545-555, 2005.

DU C, YANG DM, ZHANG PX, DENG L, JIANG BG. Neurolonal differentiationof PC12 cells induced by sciatic nerve and optic nerve contioned medium. Chinese Med J. 123(3):351-355. 2010.

EHRLICHER A, BETZ T, STUHRMANN B, KOCH D, MILNER V, RAIZEN MG, KAS J. Guiding neuronal growth with light. Proc Natl Acad Sci USA. 99:16024–16028, 2002.

EVANS GR. Peripheral nerve injury: A review and approach to tissue engineered constructs. Anat Rec. 263:396–404, 2001.

GANTUS MAV, NASCIUTTI LE, CRUZ CM, PERSECHINI PM, MARTINEZ AMB. Modulation of extracellular matrix components by metalloproteinases and their tissue

inhibitors during degeneration and regeneration of rat sural nerve. Brain Res. 1122:36–46, 2006.

GARCIA N, TOMÀS M, SANTAFE MM, LANUZA MA, BESALDUCH N, TOMÀS J. Localization of brain-derived neurotrophic fator, neurotrophin-4, tropomyosin-related kinase b receptor, and p75NTR receptor by high-resolution immunohistochemistry on the adult mouse neuromuscular junction. J Perip Nerv Syst;15:40-49, 2010.
GAUDET AD, POPOVICH PG, RAMER MS. Wallerian degeneration: Gaining perspective on inflammatory events after peripheral nerve injury. J Neuroinflam. 2011, 8:110.

GIGO-BENATO D, GEUNA S, ROCHKIND S. Phototherapy for Enhancing Peripheral Nerve repair: a Review of the Literature. Muscle Nerve 31:694-701, 2005.

GIGO-BENATO D, RUSSO TL, TANAKA EH, ASSIS L, SALVINI TF, PARIZOTTO NA. Effects of 660 and 780 nm low-level laser therapy on neuromuscular recovery after crush injury in rat sciatic nerve.Lasers Surg Med. 2010 Nov;42(9):673-82.

GOMES LE, DALMARCO EM, ANDRÉ ES. The brain-derived neurotrophic factor, nerve growth factor, neurotrophin-3, and induced nitric oxide synthase expressions after low-level laser therapy in an axonotmesis experimental model. Photomed Laser Surg. 2012 Nov;30(11):642-7. doi: 10.1089/pho.2012.3242. Epub 2012 Sep 24.

HEINE W, CONANT K, GRIFFIN JW, HÖKE A. Transplanted neural stem cells promote axonal regeneration through chronically denervated peripheral nerves. Exp Neurol. 189(2):231-40, Out 2004.

KHUONG HT, MIDHA R. Advances in Nerve Repair. Current Neurology and Neuroscience Reports, 13:322, 2012.

KOUYOUMDJIAN, J. A. Peripheral Nerve Injuries: A Retrospective Survey of 456 Cases. Muscle Nerve. 34: 785–788, 2006.

LA FLEUR M, UNDERWOOD JL, RAPPOLEE DA, WERB Z. Basementmembrane and repair of injury to peripheral nerve: defining a potential role for macrophages, matrix metalloproteinases, and tissue inhibitor of metalloproteinases-1. J Exp Med. 184:2311–2326, 1996.

LUNDBORG G. Nerve Injury and Repair: Regeneration, Reconstruction, and Cortical Remodeling. 2nd ed. Churchill Livingstone. New York. 2005.

MEDALHA CC, DI GANGI GC, BARBOSA CB, FERNANDES M, AGUIAR O, FALOPPA F, LEITE VM, RENNO ACM. Low-level laser therapy improves repair following complete resection of the sciatic nerve in rats. Lasers Med Sci 27:629-635, 2012.

MILLESI H. Techniques for Nerve Grafting. Hand Clinics 16: 73-91, 2000

OMURA T, SANO M, OMURA K, HASEGAWA T, et al. Different expressions of BDNF, NT3, and NT4 in muscle and nerve after various types of peripheral nerve injuries. J Perip Nerv Sys. 2005; 10:293-300.

PLATT CA, KREKOSKI RV, WARD DR, EDWARDS J, GAVRILOVIC. Extracellular Matrix and Matrix Metalloproteinases in Sciatic Nerve. Journal of Neuroscience Research. 74:417–429, 2003.

ROCHKIND S, EL-ANI D, NEVO Z, SHAHAR A. Increase of Neuronal Sprouting and Migration Using 780nm Laser Phototherapy as Procedure for Cell Therapy. Lasers in Surgery and Medicine .41:277–281, 2009. a

ROCHKIND S, GEUNA S, SHAINBERG A. Chapter 25 phototherapy in peripheral nerve injury effects on muscle preservation and nerve regeneration. Int Rev Neurobiol. 87:445-64, 2009.b

ROTSHENKER S. Wallerian degeneration: the innate-immune response to traumatic nerve injury. J Neuroinflam 2011, 8:109.

RUSSO TL, PEVIANI SM, DURIGAN JL, SALVINI TF. Electrical stimulation increases matrix metalloproteinase-2 gene expression but does not change its activity in denervated rat muscle. Muscle Nerve. 37(5):593-600, 2008.

RUSSO TL, PEVIANI SM, DURIGAN JL, GIGO-BENATO D, DELFINO GB, SALVINI TF. Stretching and electrical stimulation reduce the accumulation of MyoD, myostatin and atrogin-1 in denervated rat skeletal muscle. J Muscle Res Cell Motil. 31:45-57, 2010.

SCHOSER BG, BLOTTNER D. Matrix metalloproteinases MMP-2, MMP-7 and MMP-9 in denervated human muscle. Neuroreport. 10:2795-2797, 1999.

SENDTNER M, PEI G, BECK M, SCHWEIZER U, WIESE S. Developmental motoneuron cell death and neurotrophic factors. Cell Tissue Res. 2000 301:71-84.

SILVA-COUTO MA, GIGO-BENATO D, TIM CR, PARIZOTTO NA, SALVINI TF, RUSSO TL. Effects of low-level laser therapy after nerve reconstruction in rat denervated soleus muscle adaptation. Rev bras fisioter. 2012 jul-aug;16(4):320-7. Epub 2012 jul 17.

VAREJÃO A S, CABRITA A M, MEEK M F, BULAS-CRUZ J, MELO-PINTO P, RAIMONDO S, GEUNA S, GIACOBINI-ROBECCHI MG. Functional and Morphological Assessment of a Standardized Rat Sciatic Nerve Crush Injury with a non-Serrated Clamp. J Neurotrauma. 21:1652-1670, 2004.

WYSS-CORAY T. Transforming Growth Factor-β Signaling Pathway as a Therapeutic Target in Neurodegeneration. J Mol Neurosc. 24:149-153, 2004.

YU Q, STAMENKOVIC I. Cell surface-localized matrix metalloproteinase-9 proteolytically activates TGF-β and promotes tumor invasion and angiogenesis. Genes Dev. 14:163-176, 2000.

ZERMEÑO V, SPINDOLA S, MENDOZA, HERNÁNDEZ-ECHEAGARAY E. Differential expression of neurotrophins in postnatal C57BL/6 mice striatum. Int J Biol Sci. 5;118-120, 2009.